AD_____

Award Number: W81XWH-04-1-0534

TITLE: Identification of Potential Therapeutic Mechanisms for HIP1 Inhibition in Breast Cancer

PRINCIPAL INVESTIGATOR: Theodora S. Ross M.D., Ph.D.

CONTRACTING ORGANIZATION: University of Michigan
Ann Arbor, MI 48109

REPORT DATE: May 2006

TYPE OF REPORT: Annual

PREPARED FOR: U.S. Army Medical Research and Materiel Command
Fort Detrick, Maryland 21702-5012

REPORT DOCUMENTATION PAGE

Form Approved
OMB No. 0704-0188

1. REPORT DATE	2. REPORT TYPE	3. DATES COVERED
01-05-2006	Annual	14 Apr 2005 – 13 Apr 2006

4. TITLE AND SUBTITLE

Identification of Potential Therapeutic Mechanisms for HIP1 Inhibition in Breast Cancer

5a. CONTRACT NUMBER

5b. GRANT NUMBER
W81XWH-04-1-0534

5c. PROGRAM ELEMENT NUMBER

6. AUTHOR(S)

Theodora S. Ross M.D., Ph.D.

5d. PROJECT NUMBER

5e. TASK NUMBER

5f. WORK UNIT NUMBER

7. PERFORMING ORGANIZATION NAME(S) AND ADDRESS(ES)

University of Michigan
Ann Arbor, MI 48109

8. PERFORMING ORGANIZATION REPORT NUMBER

9. SPONSORING / MONITORING AGENCY NAME(S) AND ADDRESS(ES)
U.S. Army Medical Research and Materiel Command
Fort Detrick, Maryland 21702-5012

10. SPONSOR/MONITOR'S ACRONYM(S)

11. SPONSOR/MONITOR'S REPORT NUMBER(S)

12. DISTRIBUTION / AVAILABILITY STATEMENT
Approved for Public Release; Distribution Unlimited

13. SUPPLEMENTARY NOTES
Original contains colored plates: ALL DTIC reproductions will be in black and white.

14. ABSTRACT The first hypothesis we are testing is that HIP1 expression is necessary for breast tumorigenesis. We have successfully generated a cohort of breast cancer prone mice (MMTV-Myc) that are deficient (n=20) or replete for HIP1 (n=20). The ongoing experiments show that HIP1 deficiency inhibits the formation of breast tumors. This result is similar to our work that demonstrated that HIP1 is necessary for prostate tumorigenesis (Bradley et al., 2005 Ca Res). These HIP1 deficient/MMTV-Myc experiments have taken an interesting turn this year. Essentially, we have analyzed the rare tumors that develop in the MMTV-Myc/Hip1 knockout mice and found that cells derived from these tumors (but not the normal tissues from the same mouse) express a "mutant" form of HIP1. We think that this is a way for the cells to adapt to the original targeted loss of function mutation in the Hip1 gene. These data indicate that the expression of HIP1 is completely necessary for the survival of Myc-induced breast cancers. Our plan is to identify the sequence of the "mutant" forms in hopes of discovering areas of the HIP1 sequence to target for small molecule inhibition. The second hypothesis we have been testing is that dysregulation of endocytosis of EGFR by HIP1 is a mechanism by which HIP1 promotes breast cancer evolution. Indeed, we have found that HIP1 overexpression inhibits the degradation the EGFR (Hyun et al., 2004 J Biol Chem). Showing that HIP1 is necessary for breast cancer progression and modulates key growth factor receptors involved in breast cancer, fuels the idea that HIP1 inhibition has excellent therapeutic potential. We will continue to explore the activityofdistinctregionsofHIP1todiscoverinhibitorsforuseinthetreatmentofbreastcancer.

15. SUBJECT TERMS
HIP1 Myc endocytosis EGFR

16. SECURITY CLASSIFICATION OF:				18. NUMBER OF PAGES	19a. NAME OF RESPONSIBLE PERSON
a. REPORT	b. ABSTRACT	c. THIS PAGE			USAMRMC
U	U	U	UU	43	19b. TELEPHONE NUMBER *(include area code)*

Table of Contents

INTRODUCTION: Huntingtin Interacting Protein 1 (HIP1) is a clathrin and inositol lipid binding protein that may be involved in neurodegeneration by virtue of its interaction with huntingtin, the protein mutated in Huntington's disease. It is also associated with leukemia by discovery of the oncogenic HIP1/PDGFβR fusion protein that resulted from a t(5;7) chromosomal translocation in a patient with chronic myelomonocytic leukemia. We think HIP1 is involved in breast tumorigenesis for the following reasons. First, HIP1 is over-expressed in primary breast tumors (*1*). Second, expression of a dominant negative mutant of HIP1 (*2*) or genetic deletion of HIP1 leads to apoptosis of normal as well as tumor tissue suggesting that expression of HIP1 may be necessary for cellular survival of many cell types (*3,4*). Third, over-expression of HIP1 in NIH/3T3 cells leads to transformation (*1*). Finally, recently we have found that cells cultured from HIP1 deficient breast tumors express a mutant form of HIP1 suggesting that there are HIP1 sequences that are completely necessary for breast tumor survival. The purpose of this IDEA grant is to explore the role of HIP1 in breast cancer by determining its necessity in breast tumorigenesis and test for the effects of HIP1 overexpression on the signaling from key growth factor receptors that are known to function in the pathophysiology of breast cancer.

BODY: The first hypothesis we proposed to the DOD was that HIP1 expression is necessary for breast cancer evolution. To test this we generated a cohort of breast cancer prone transgenic mice (MMTV-*Myc*) that are deficient (n=20) or replete for HIP1 (n=20). HIP1 deficient adult mice are relatively healthy allowing for such experiments. Our preliminary data from last year indicated that HIP1 deficiency inhibited the progression rather than the incidence of breast tumors in this mouse model. This result was similar to our recently published work showing that HIP1 is necessary for the progression of prostate cancer (Figure 1 of appended manuscript #2; (*5*)). These MMTV-*Myc* experiments are ongoing. In an effort to understand how tumors grew differently in the presence or absence of HIP1 we cultured cells derived from the HIP1 deficient mice. To our surprise, in all cases we found that a mutant form of HIP1 was expressed at high levels in cells derived from the HIP1 deficient knockout/MMTV-myc mouse breast tumors. Our current focus is to understand the primary sequence of this mutant form, how it is generated and what protein domains are altered as a result of this mutant form. We expect to have a publication of high impact on this topic by the end of this year.

The second hypothesis we proposed to the DOD was that dysregulation of endocytosis of growth factor receptors by HIP1 is a mechanism by which HIP1 promotes breast cancer evolution. Indeed, we have found that HIP1 overexpression inhibits the degradation the EGFR and the estrogen receptor (appended manuscripts #1 and #3; (*6*)). To determine if the deficiency of HIP1 leads to increased degradation of the EGFR we have analyzed tissues from mice with deficiency of HIP1 and/or HIP1r. The double deficient mice are remarkable in that they suffer severe degenerative or premature "aging" phenotypes that include a shortened lifespan, progressive wasting and vertebral column defects. Despite HIP1 and HIP1r's ability to stabilize growth factor receptors and interact with the endocytic machinery, we have not yet found double HIP1/HIPr deficient tissues with diminished receptor tyrosine kinases signal transduction or defects in endocytosis. The upcoming year will involve evaluating these mice for PtdIns 3-kinase, endocytic and actin pathway abnormalities. Showing that HIP1 is necessary for breast cancer progression and modulates key growth factor receptors, continues to fuel the idea that HIP1 inhibition has excellent therapeutic potential. We will continue to the quest to discover the activity of HIP1 using loss-of-function and gain-of-function

experiments as well as conduct a search for regions of HIP1 that may be useful to target in the treatment of breast cancer.

KEY RESEARCH ACCOMPLISHMENTS:

1. We have generated a cohort of breast cancer prone MMTV-*Myc* mice that are deficient for HIP1 to test for its role in breast cancer initiation, maintenance or evolution. We have discovered that HIP1 is mutant in breast tumors that do develop in these mice and this hopefully will lead to a very nice **publication this year (2006).**

2. We have discovered that HIP1 and its only known mammalian relative, HIP1r, prolong the half-life of the EGFR when overexpressed. This has lead to the publication of appendix manuscript #2.

3. We have generated 8 different HIP1/HIP1r deficient fibroblasts and are in the process of analyzing them for actin abnormalities, growth and survival properties, altered growth factor receptor stability and ability to be transformed by key oncogenes (RasV12, Myc, HER2)**. We expect to publish our findings on this by 2007.**

REPORTABLE OUTCOMES: Four manuscripts have been published over the last two years that are relevant to this proposal and are found in the appendix.

CONCLUSIONS: My laboratory is interested in the mechanisms that transform normal cells into cancer cells. We have recently identified a novel HIP1 mediated mechanism whereby alterations in endocytosis cause cancer by simultaneously increasing signaling through multiple mitogenic and survival pathways in parallel. This was the basis for our proposal to study this pathway in breast cancer. Using DOD funds we have succeeded in generating a mouse model that indicates that HIP1 is completely necessary for Myc-induced breast tumorigenesis *in vivo*. In collaboration with Ian Mills we have identified HIP1 as a nuclear hormone (AR, ER, GR) transcriptional coregulator (*7*). We have also discovered that HIP1 alters growth factor receptor stability by inhibiting its degradation at a stage that is not the uptake phase of endocytosis but is instead localized to the early signaling endosomes (*8*). The latter discovery is surprising to us as we had hypothesized that HIP1 affected the density of surface receptors as a mechanism for cancer cell survival (*1*). Our future work on this topic will involve analysis of the loss of HIP1 function on the ability of MEFs to be transformed, analysis of the sequence of the mutant form of HIP1 discovered in tumors from HIP1 "deficient" MMTV-*Myc* transgenic mice, obtain a better understanding of endosome signaling versus surface receptor signaling in transformation of normal cells to cancer cells and ultimately develop a screen for HIP1 inhibitors based on analysis of natural mutations of HIP1 in tumor cells.

REFERENCES:

(*1*) Rao DS, Bradley SV, P.D. K, T.S. H, Saint-dic D., K.I. O-W, et al. Altered Receptor Trafficking in Huntingtin Interacting Protein 1-Transformed Cells. Cancer Cell 2003;3:471-82.

(*2*) Rao DS, Hyun TS, Kumar PD, Mizukami IF, Rubin MA, Lucas PC, et al. Huntingtin-interacting protein 1 is overexpressed in prostate and colon cancer and is critical for cellular survival. J Clin Invest 2002;110:351-60.

(*3*) Rao DS, Chang JC, Kumar PD, Mizukami I, Smithson GM, Bradley SV, et al. Huntingtin interacting protein 1 Is a clathrin coat binding protein required for differentiation of late spermatogenic progenitors. Mol Cell Biol 2001;21:7796-806.
(*4*) Oravecz-Wilson KI, Kiel MJ, Li L, Rao DS, Saint-Dic D, Kumar PD, et al. Huntingtin Interacting Protein 1 mutations lead to abnormal hematopoiesis, spinal defects and cataracts. Hum Mol Genet 2004;13:851-67.
(*5*) Bradley SV, Oravecz-Wilson KI, Bougeard G, Mizukami I, Li L, Munaco AJ, et al. Serum antibodies to huntingtin interacting protein-1: a new blood test for prostate cancer. Cancer Res 2005;65:4126-33.
(*6*) Hyun TS, Rao DS, Saint-Dic D, Michael LE, Kumar PD, Bradley SV, et al. HIP1 and HIP1r stabilize receptor tyrosine kinases and bind 3-phosphoinositides via epsin N-terminal homology domains. J Biol Chem 2004;279:14294-306.
(*7*) Mills IG, Gaughan L, Robson C, Ross T, McCracken S, Kelly J, et al. Huntingtin interacting protein 1 modulates the transcriptional activity of nuclear hormone receptors. J Cell Biol 2005;170:191-200.
(*8*) Hyun TS, Ross TS. HIP1: trafficking roles and regulation of tumorigenesis. Trends Mol Med 2004;10:194-9.

APPENDICES:

1. Appendix manuscript #1: Mills IG et al., *Interacting Protein 1 (HIP1) modulates the transcriptional activity of nuclear hormone receptors*. J. Cell Biol. 2005; 170 (2): 191-200.

2. Appendix manuscript #2: Bradley, S.V., et al., *Humoral Immune Response to HIP1: a novel blood test for prostate cancer*. Cancer Res, 2005; 65: (10): 4126-4133.

3. Appendix manuscript #3: Hyun, T.S., et al., *HIP1 and HIP1r stabilize receptor tyrosine kinases and bind 3-phosphoinositides via epsin N-terminal homology domains.* J Biol Chem, 2004. **279**(14): p. 14294-306.

4. Appendix manuscript #4: Hyun, T.S. and T.S. Ross, *HIP1: trafficking roles and regulation of tumorigenesis.* Trends Mol Med, 2004. **10**(4): p. 194-9.

Huntingtin interacting protein 1 modulates the transcriptional activity of nuclear hormone receptors

Ian G. Mills,[1] Luke Gaughan,[2] Craig Robson,[2] Theodora Ross,[3] Stuart McCracken,[2] John Kelly,[1] and David E. Neal[1]

[1]Cancer Research UK Uro-Oncology Research Group, Department of Oncology, University of Cambridge, Hutchison/Medical Research Council Cancer Research Centre, Cambridge CB2 2XZ, England, UK
[2]Prostate Research Group, Northern Institute for Cancer Research, University of Newcastle upon Tyne, Medical School, Newcastle upon Tyne NE2 4HH, England, UK
[3]Department of Internal Medicine and Graduate Program in Cellular and Molecular Biology, University of Michigan Medical School, Ann Arbor, MI 48109

Internalization of activated receptors regulates signaling, and endocytic adaptor proteins are well-characterized in clathrin-mediated uptake. One of these adaptor proteins, huntingtin interacting protein 1 (HIP1), induces cellular transformation and is overexpressed in some prostate cancers. We have discovered that HIP1 associates with the androgen receptor through a central coiled coil domain and is recruited to DNA response elements upon androgen stimulation. HIP1 is a novel androgen receptor regulator, significantly repressing transcription when knocked down using a silencing RNA approach and activating transcription when overexpressed. We have also identified a functional nuclear localization signal at the COOH terminus of HIP1, which contributes to the nuclear translocation of the protein. In conclusion, we have discovered that HIP1 is a nucleocytoplasmic protein capable of associating with membranes and DNA response elements and regulating transcription.

Introduction

Endocytosis is important for receptor internalization, nutrient uptake, antigen presentation, pathogen internalization, and maintenance of plasma membrane surface area. Endocytosis occurs via several distinct pathways and requires coordinated interactions between a variety of molecules at the membrane and cell cortex. In yeast, a functional connection between the actin cytoskeleton and endocytosis has been firmly established (Geli and Riezman, 1998). Mutations in actin and in several actin-binding proteins inhibit both receptor-mediated and fluid-phase endocytosis (Kubler and Riezman, 1993; Munn et al., 1995).

To gain insights into the roles of actin in endocytosis, it was important to identify actin-binding proteins with a functional involvement in endocytosis. Sla2p was one of the first to be identified in a synthetic lethal screen in yeast against a null allele of *ABP1*, a gene encoding an actin-binding protein implicated in cytoskeletal regulation, endocytosis, and cAMP signaling. Sla2p is a peripheral membrane protein that contains a novel NH_2-terminal domain, three putative coiled coil domains, a putative leucine zipper, and a COOH-terminal talin-like domain (Holtzman et al., 1993; Wesp et al., 1997). Sla2p binds to F-actin in vitro through the talin-like domain and partially colocalizes with F-actin in cortical patches (McCann and Craig, 1997; Yang et al., 1999).

Homologues of Sla2p have since been identified in nematodes (*ZK370.3*) and humans (HIP1 and HIP1R). Huntingtin interacting protein 1 (HIP1) is predominantly expressed in brain and was first identified in a yeast two-hybrid screen for interacting partners of huntingtin (Kalchman et al., 1997; Wanker et al., 1997). Huntington's disease is an inherited neurodegenerative disorder caused by expansion of the codon CAG in the huntingtin gene, which leads to expression of a polyglutamine tract in the protein (Reddy et al., 1999). The affinity of the huntingtin protein–HIP1 interaction is inversely correlated to the polyglutamine repeat length (Kalchman et al., 1997). HIP1 is a 116-kD AP180 NH_2-terminal homology (ANTH) domain–containing protein capable of binding to phosphatidylinositol lipids and recruiting clathrin via a short peptide motif of the LLMDMD type in the vicinity of a central coiled coil domain (Mishra et al., 2001; Hyun et al., 2004). Consequently, much of the functional work on the HIP1 family has focused on its ability to modulate actin dynamics in clathrin-mediated endocytosis.

However, HIP1 was recently found to be overexpressed in a subset of cancers of the prostate and colorectum (Rao et al., 2002). Prostate cancer is a disease, which in its advanced form is associated with changes in the transcriptional response and expression of a polyglutamine repeat–containing transcription

I.G. Mills and L. Gaughan contributed equally to this paper.

Correspondence to I.G. Mills: igm23@cam.ac.uk

Abbreviations used in this paper: ANTH, AP180 NH_2-terminal homology; AR, androgen receptor; ARE, androgen response element; ChIP, chromatin immunoprecipitation; HIP1, huntingtin interacting protein 1; PSA, prostate-specific antigen; siRNA, silencing RNA.

The online version of this article includes supplemental material.

The Journal of Cell Biology, Vol. 170, No. 2, July 18, 2005 191–200
http://www.jcb.org/cgi/doi/10.1083/jcb.200503106

Supplemental Material can be found at:
http://www.jcb.org/cgi/content/full/jcb.200503106/DC1

factor, the androgen receptor (AR; Chen et al., 2004). The AR is a member of the nuclear hormone receptor superfamily of transcription factors. The AR consists of an NH_2-terminal domain containing polyglutamine and polyglycine repeats, which interacts with a series of transcriptional coregulators; a zinc finger DNA-binding domain; a hinge region encompassing nuclear localization signals; an acetylation site; and a COOH-terminal ligand-binding domain. The nuclear translocation of this transcription factor is dependent on the binding of androgen by the COOH-terminal ligand-binding domain. An actin-binding protein, filamin, was recently shown to interact with the receptor and to be required for translocation (Ozanne et al., 2000).

A subset of endocytic adaptor proteins including Eps15 and Epsin1 have been reported to undergo nucleocytoplasmic shuttling on the basis that their steady-state distribution becomes nuclear upon treating cells with an antifungal antibiotic, Leptomycin B, which inhibits nuclear export (Hyman et al., 2000; Vecchi et al., 2001). A strong argument against a nuclear distribution of these proteins is the absence of a nuclear subfraction under untreated conditions, although this can be explained by a high rate of nuclear export. A potential nuclear function for Eps15 and CALM was reported to be the regulation of transcription on the basis of their modulatory effects using a GAL4-based transactivation assay (Vecchi et al., 2001).

In this study, we have examined the effects of androgen treatment on the subcellular distribution of HIP1 and the effects of this protein on AR-mediated transcription. We have uncovered a functional association of HIP1 with androgen response elements (AREs), providing the first direct evidence for transcriptional modulation of hormone-responsive genes by an endocytic adaptor.

Results

HIP1 is both nuclear and cytosolic

A characteristic of prostatic tissue is a transcriptional response to androgen, which is mediated by the AR. We used an AR expressing prostate cancer cell line LNCaP to examine by subcellular fractionation changes in the distribution of the endogenous AR and HIP1 in response to treatment with a synthetic androgen, Mibolerone. Treating LNCaP cells with Mibolerone resulted in a 70% increase in nuclear AR but also resulted in a nuclear redistribution of HIP1 of up to 50% (Fig. 1 C). In contrast, clathrin, a binding partner of HIP1, remained entirely cytosolic (Fig. 1 A). This nuclear translocation was observed using confocal microscopy after Mibolerone treatment (Fig. 1 B). Translocation of endogenous AR and HIP1 was also induced by treating LNCaP cells with the physiological androgen dihydrotestosterone (unpublished data).

HIP1 associates with the AR

HIP1 was first identified as an interacting partner of a polyglutamine repeat–containing protein, huntingtin, in a yeast two-hybrid screen with a binding affinity inversely proportional to the size of the polyglutamine tract (Wanker et al., 1997). We tested whether HIP1 also interacts with the AR, also a polyglutamine repeat–containing protein, using immunoprecipitation.

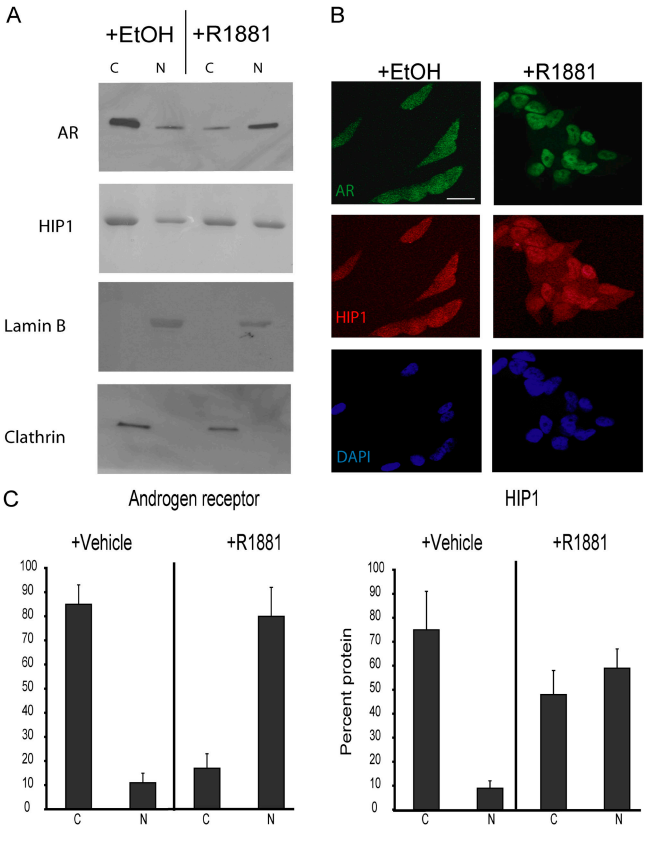

Figure 1. **HIP1 is found in a nuclear subcellular fraction.** (A) LNCaP cells were fractionated after Mibolerone or vehicle treatment. Nuclear (N) and cytosolic (C) fractions were resolved by SDS-PAGE (50 μg per lane), transferred to nitrocellulose, and blotted for the AR, HIP1, lamin B, and clathrin, illustrated here with representative blots. (B) LNCaP cells were grown in steroid-depleted media for 48 h and then treated with 10 nM Mibolerone or ethanol. HIP1 was detected using mouse mAb and the AR was detected using a rabbit polyclonal antibody. The nuclei were stained with DAPI. Bar, 70 μm. (C) The degree of translocation of the AR and HIP1 was quantitated by densitometric analysis of the blots. Data shown represent the means of five independent experiments ± SD.

Endogenous AR and HIP1 were coimmunoprecipitated from the LNCaP cell line (Fig. 2 A). This has been confirmed independently by band identification using mass spectroscopy (unpublished data). We have also confirmed this interaction using transfected COS7 cells in a mammalian two-hybrid screen with the AR coactivator Tip60 as a positive control (Brady et al., 1999; unpublished data).

We used a GAL4-based transactivation assay in an attempt to identify domains of HIP1 with potential nuclear functions (Fig. 2 B). Expression constructs encoding the GAL4 DNA-binding domain fused to full-length HIP1, a construct bearing the FxDxF/coiled coil and I/LWEQ domains (ΔANTH), and a construct consisting of the COOH-terminal I/LWEQ domain alone were cotransfected along with a reporter plasmid encoding the luciferase gene under the transcriptional control of a GAL4-responsive promoter into AR-null COS7 cells. GAL4-HIP1 and GAL4-ΔANTH produced a three- to fourfold transactivation over the basal value produced by GAL4 alone (Fig. 2 B). Although the degree of transactivation was lower than that produced by E2F1, an established trans-

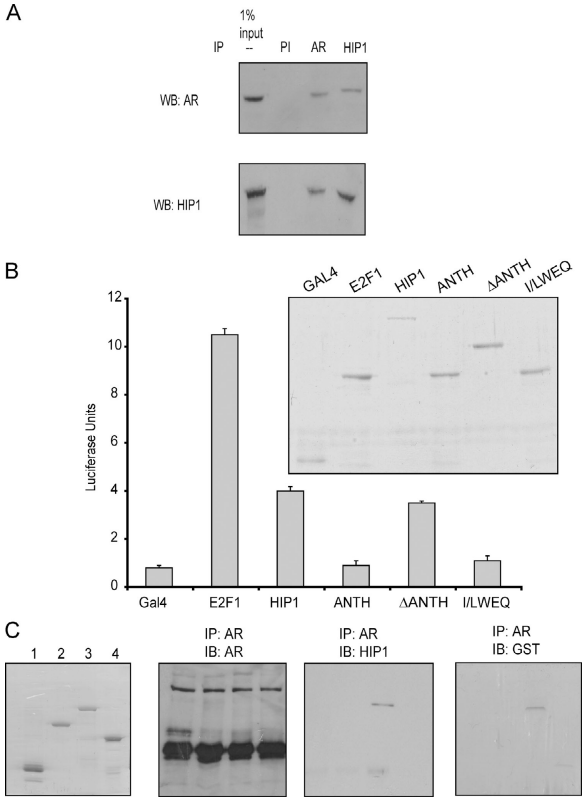

Figure 2. **Association between HIP1 and the AR.** (A) LNCaP cells were transiently transfected with 2 μg pcDNA3-AR and pcDNA3-Myc-HIP1 per 90-mm dish. Cell lysates were immunoprecipitated with an anti-AR antibody and immunoblotted with an anti-AR polyclonal antibody and an anti-HIP1 mAb. (B) HIP1 acts as a transcriptional regulator in GAL4-based assays. COS-7 cells were cotransfected with a GAL4-regulated luciferase reporter construct, and chimeric constructs encompassing the GAL4 DNA-binding domain fused to HIP1 and the following domains: ANTH (encompassing aa 1–310), ΔANTH (encompassing aa 320–1037), and I/LWEQ (encompassing aa 800–1037). Luciferase activity was measured 48 h after transfection on equal amounts of total cellular lysates that expressed comparable levels of the various GAL4 fusion proteins as assessed by anti-GAL4 immunoblot (inset). Graphed data represent the means of three independent experiments with error bars for the SD. (C) COS7 cells were transfected with 2 μg pcDNA3-AR per 9-cm dish. Lysates were prepared and the AR was immunoprecipitated from 300 μg of lysate supplemented with 10 μg of recombinant proteins. The left panel is a Coomassie-stained gel illustrating the equivalent loading of GST (lane 1), GST-ANTH domain (lane 2), GST-FxDxF/coiled coil domain encompassing aa 320–800 (lane 3), and GST-I/LWEQ domain (lane 4). Immunoprecipitates were blotted for AR, HIP1, and GST as indicated.

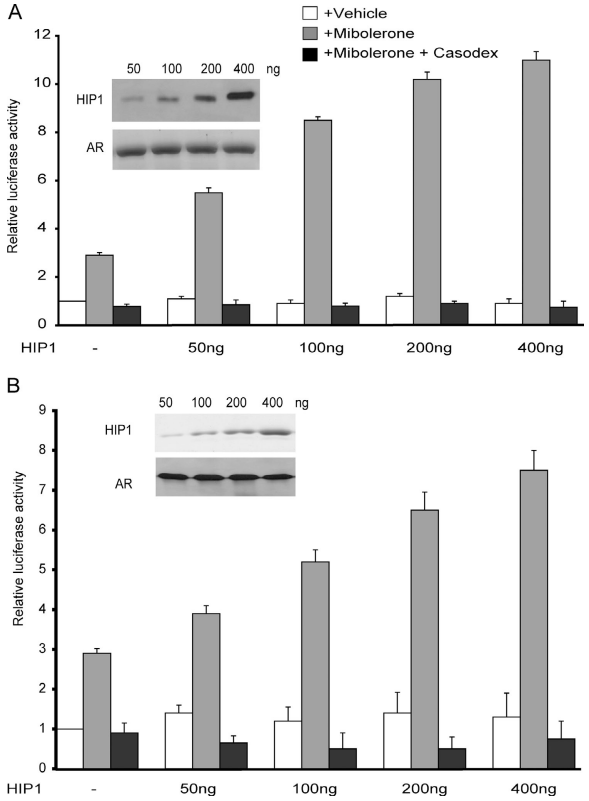

Figure 3. **HIP1 is a transcriptional coregulator for the AR.** (A) COS7 cells were transfected with 50 ng pcDNA3-AR plus increasing quantities of pcDNA3-HIP1 (0, 50, 100, 200, and 400 ng) together with 100 ng of a pPSA luciferase reporter construct (pPSALuc). Cells were treated with10 nM Mibolerone ± 1 μM bicalutamide (Casodex) for 48 h and luciferase activity was normalized for transfection efficiency as determined by β-galactosidase assays and expressed relative to vehicle-treated singly transfected AR-positive cells. Data shown represent the means of three independent experiments ± SD. (insets) Lysates were prepared and run at 50 μg per lane before blotting for HIP1 and AR. (B) COS7 cells were transfected with 50 ng pcDNA3-AR plus increasing quantities of pcDNA3-HIP1 (0, 50, 100, 200, and 400 ng) together with 100 ng of a minimal ARE luciferase reporter construct ($pARE_4$-Luc). After 48 h, cells were lysed and luciferase assays were performed as described. Data shown represent the means of three independent experiments ± SD.

activator, it was statistically significant and at a similar level to that observed for endocytic proteins previously reported to undergo nucleocytoplasmic shuttling (Vecchi et al., 2001).

We attempted to narrow down the binding site for the AR in HIP1 by expressing and purifying GST-tagged domain constructs of HIP1 encompassing the coiled coil domain, the coiled coil/DxF region, and the COOH-terminal I/LWEQ domain from *Escherichia coli*. We then incubated these recombinant domains with lysate extracted from COS7 cells transfected with the AR and, after immunoprecipitation with a polyclonal AR antibody, blotted for the AR, GST, and HIP1. Equal quantities of the AR were immunoprecipitated in the conditions used. A HIP1 blot detected an association with the FxDxF/coiled coil domain and this was confirmed using an antibody raised against GST (Fig. 2 C). From these data we conclude that HIP1 and the AR associate, and that this association requires the central FxDxF/coiled coil domain of HIP1.

HIP1 is a transcriptional regulator of hormone receptors

We investigated the effects of ectopic HIP1 expression on the transcriptional activity of the AR using a luciferase reporter construct driven by a prostate-specific antigen (PSA) promoter, pPSALuc. COS7 cells were cotransfected with the AR and increasing quantities of HIP1. The transcriptional response to androgen stimulation was enhanced in a dose-dependent manner with a maximal fourfold enhancement above the stimulatory level achieved in the absence of HIP1 (Fig. 3 A). Coactivation was selectively blocked with an anti-androgen, bicalutamide (Casodex; Fig. 3 A). HIP1-dependent coactivation is therefore unlikely to be a cross talk effect occurring through AR-independent

signaling. Coactivation was also observed when a minimal ARE reporter construct was used, further arguing against surrogate effects on the activities of other transcription factors (Fig. 3 B).

To determine whether the effects on AR-mediated transcription reflected an association between HIP1 and AREs, or were less direct, chromatin immunoprecipitations (ChIP) were undertaken using antibodies against HIP1 and the AR. Sequences corresponding to the proximal (AREI) and distal (AREIII) AREs were amplified by PCR (Fig. 4 A). ChIP assays were performed over 4 h after treatment of LNCaP cells with Mibolerone. A temporal recruitment of HIP1 and the AR to both AREI and AREIII was observed, though the temporal recruitment of HIP1 differed somewhat from that of the AR (Fig. 4 B). HIP1 was recruited within 1 h of Mibolerone treatment to AREI at levels that were sustained over the 4-h treatment period in contrast to the biphasic recruitment of the AR, which peaked at 1 and 4 h maxima. Recruitment of the AR to AREIII was also biphasic, resembling the pattern of recruitment to AREI (Fig. 4 B). In contrast, the recruitment of HIP1 to AREIII was monophasic with maximal recruitment detectable 1 h after stimulation with Mibolerone. In a reChIP assay, immunoprecipitated chromatin extracts were blotted for HIP1 and the AR after 2 h of treatment with Mibolerone. HIP1 and the AR were reciprocally immunoprecipitated and associated with AREI but not with a non-ARE–containing region of the PSA promoter (AREX; Fig. 4 C).

Synchronous AR binding is not a requisite for the association of HIP1 with AREs, and HIP1 may therefore potentially associate with other promoters/response elements and regulate the transcriptional activity of other nuclear hormone nuclear receptors. Indeed, cotransfection of HIP1 with α and β isoforms of the estrogen receptor enhanced their transcriptional response to estradiol treatment. The coactivation effect of HIP1 was appreciably greater than that of one of the best-characterized estrogen receptor coactivators, p300 (Fig. S1, A and B, available at http://www.jcb.org/cgi/content/full/jcb.200503106/DC1; Hanstein et al., 1996). Furthermore, increasing quantities of HIP1 cotransfected into COS-7 cells along with the glucocorticoid receptor produced progressive transcriptional coactivation of this receptor (Fig. S1 C). Interestingly, when HIP1 is cotransfected into COS7 cells along with a fusion of GAL4 with the ligand-binding domain (GAL4-LBD) of the glucocorticoid receptor, no additional transcriptional enhancement is observed (Fig. S1 D). This implies that the effects of HIP1 on other nuclear hormone receptors may depend on the NH_2-terminal domains of these proteins. HIP1 therefore affects the transcriptional activity of other members of the nuclear hormone receptor family and this is characteristic of many AR coregulators.

HIP1 levels affect the rate of AR degradation

We examined whether endogenous HIP1 was also required to sustain AR transcriptional activity by taking a silencing RNA (siRNA) approach to knockdown HIP1 in LNCaP cells (Fig. 5 A). HIP1 levels were reduced by 70–80% using this approach, as were levels of PSA, an androgen-responsive gene product for which AR activity is required. Protein levels of the

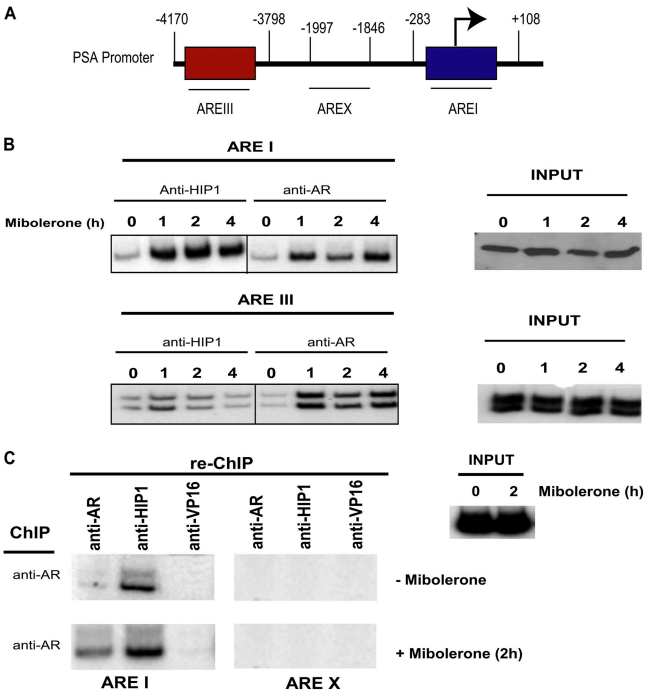

Figure 4. **HIP1 associates with ARE.** (A) Schematic diagram of the PSA promoter and ChIP assay with the length of PCR products denoted by a black bar. (B) ChIP was performed in LNCaP cells using both HIP1 and AR antibodies over a 4-h androgen time course. PCR was performed for AREs I and III. (C) ReChIP assays were performed in LNCaP cells by reprobing AR immunocomplexes with AR and HIP1 antibodies after 2-h androgen treatment. AR-HIP1 association was analyzed at ARE I and a non-ARE–containing portion of the PSA promoter (AREX).

AR were also reduced and quantitative reverse transcriptase PCR for HIP1, HIP1R, AR, and PSA was used to determine whether the reduction in the protein levels was reflected at the mRNA level. HIP1 mRNA was significantly reduced as predicted from the siRNA targeting of this protein, as were the mRNA levels of PSA, which reflects both the decreased level of AR in the treated cells and perhaps reduced transcriptional activity although it was not possible to differentiate between these two factors (Fig. 5 B). Strikingly, the mRNA levels of the AR itself were unaffected, and this implied that the reduction in the protein levels of the AR reflected an effect on protein rather than mRNA turnover. We explored this further by repeating the siRNA experiment and at 36 h after treatment inhibiting new protein synthesis by treating the cells with cycloheximide. Lysates were then prepared at two hourly time points after the application of the cycloheximide block and blotted for the AR, HIP1, and β-tubulin. The half-life of the AR was found to be reduced threefold in cells treated with siRNA-targeting HIP1 versus control siRNA (Fig. 5 C). HIP1 therefore reduces the rate of AR degradation. It is not currently known what the mechanism for AR degradation may be. There is evidence that the AR is ubiquitinated and that this enhances its transcriptional activity, whereas treatment with proteasomal inhibitors reduces the rate of AR dissociation from the AREs and AR-mediated transcription (Beitel et al., 2002; Burgdorf et al., 2004). However, treatment of cells with MG132, a proteasomal inhibitor, has not been shown to increase the protein levels of

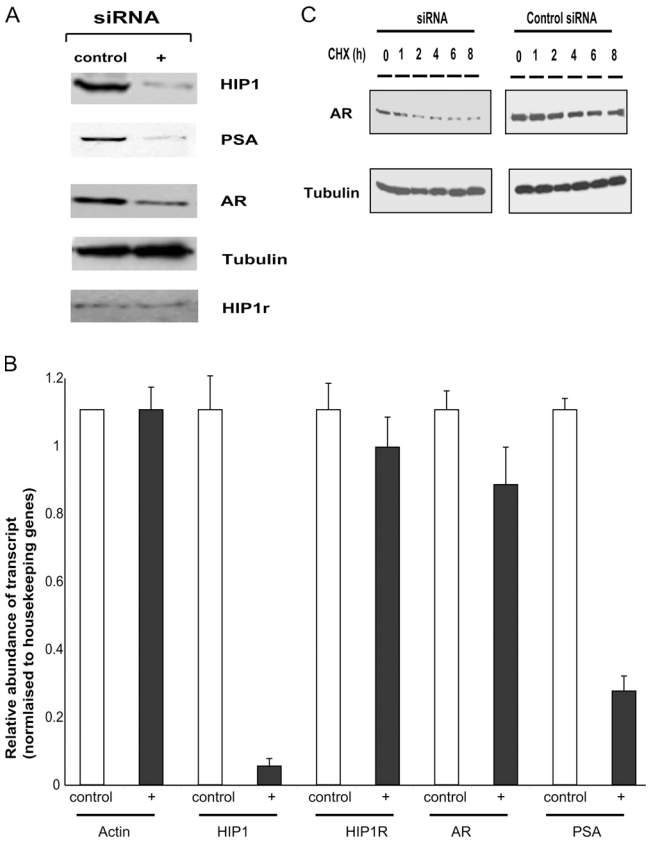

Figure 5. **Silencing HIP1 expression reduces the transcriptional activity and protein levels of the AR.** (A) LNCaP cells were transfected with a combination of HIP1 siRNAs versus a control siRNA. After 48 h, cell lysates were blotted for HIP1, HIP1R, AR, PSA, and tubulin. (B) Relative expression of AR, actin, HIP1, HIP1R, and PSA genes in LNCaP cells analyzed by real-time RT-PCR after transfection with either scrambled control or HIP1 siRNA. The data represent experimental triplicates normalized to actin levels from cells treated with a scrambled control siRNA and the error bars correspond to the SD on this data. (C) LNCaP cells were transfected with HIP1 siRNA or a scrambled control siRNA. After 40 h, cells were treated with cycloheximide (CHX). Cells were lysed during the course of the following 8 h with Western blot analysis of AR levels. Lysates were also probed by Western blotting for tubulin as a loading control.

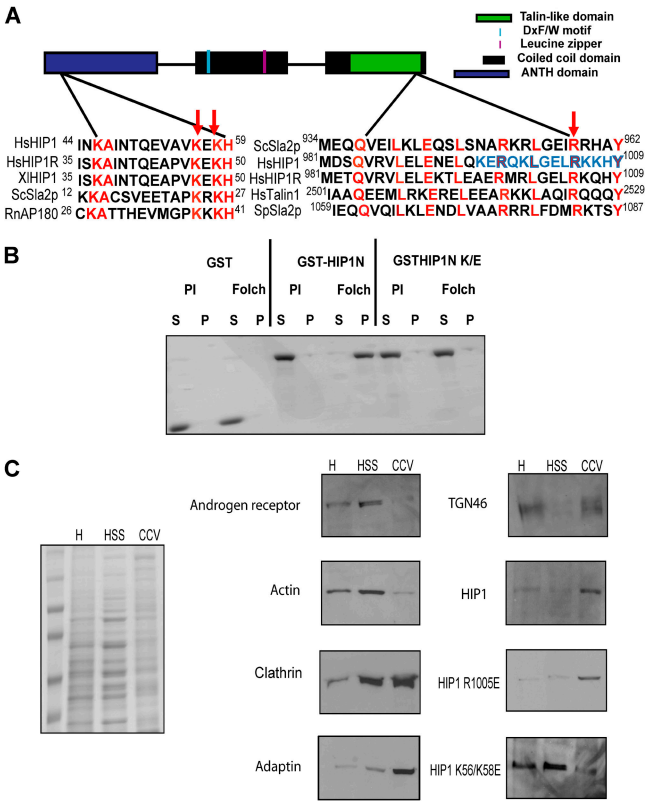

Figure 6. **The effects of the K56E/K58E double mutation on lipid binding by HIP1.** (A) A sequence alignment of the putative α1-to-α2 loop region of HIP1 with that of other ANTH domain proteins based on the crystal structure of the CALM (Altschul et al., 1997; Ford et al., 2001). Note key lipid binding residues (red); sequence identity (red); mutated residues (red arrowheads); and predicted NLS using http://cubic.bioc.columbia.edu/cgi/var/nair/resonline.pl (blue amino acids). Sequence identifications: HsHIP1 (NP_005329), HsHIP1R (NP_003950), Sp putative clathrin coat assembly protein (NP_596345), ScSla2p (NP_014156), Xl Hip1-prov protein (AAH77182), and RnAP180 (CAA48748). *Hs, Homo sapiens; Sc, Saccharomyces cerevisiae; Sp, Schizosaccharomyces pombe; Xl, Xenopus laevis; Rn, Rattus norvegicus.* An I/LWEQ module sequence alignment prepared using CLUSTALW incorporating the predicted fourth α helix of the module is shown (McCann and Craig, 1999). Additional sequence identifiers: HsTalin1 (AAF27330) and SpSla2p (NP_594069). (B) Coomassie-stained gel of a sedimentation assay with phosphatidylinositol (PI) and brain (Folch) liposomes. P, pellet; S, supernatant. Liposomes were incubated with 5 μM of the indicated proteins: GST, GST-HIP1N (aa 1–310), GST-HIP1N K/E (aa 1–310 K56E/K58E). (C) Isolation of an enriched clathrin-coated vesicle fraction from LNCaP cells. LNCaP cells were transfected with pcDNA3 HIP1 R1005E or HIP1 K56E/K58E or vector alone. 48 h posttransfection they were disrupted by homogenization and CCV fractions were isolated using a protocol adapted from Hirst et al. (2004). Coomassie blue–stained gel (left) and Western blots of equal protein loadings of homogenate (H), high speed supernatant (HSS), and CCV fractions from the isolation procedure.

the AR appreciably and so a direct link between AR ubiquitination and AR degradation is yet to be made (Tanner et al., 2004).

Transcriptional regulation by HIP1 is distinct from lipid binding and requires a COOH-terminal NLS

HIP1 has in the past been reported to play a role as an adaptor in clathrin-dependent membrane trafficking of growth factor receptors through the binding of phosphoinositides and clathrin (Hyun et al., 2004). It was therefore important to dissect the transcriptional effects of HIP1 from its other established functions. To do this, mutations were made in the phosphoinositide-binding ANTH domain of HIP1 based on the strong homology with other ANTH domain–containing proteins (Fig. 6 A). The crystal structure of the ANTH domain of clathrin assembly lymphoid myeloid leukemia protein (CALM) in complex with a soluble short-chain (diC_8) L-α-D-*myo*-phosphatidylinositol-4,5-bisphosphate has been resolved and the strong homology with HIP1 therefore enabled us to identify conserved basic residues predicted to lie in the lipid binding pocket (Ford et al., 2001). Two conserved lysine residues were mutated (K56E/K58E) and the effects of these HIP1 mutations were tested using bacterially expressed wild-type and mutant HIP1 ANTH domains (HIP1N; amino acids 1–310) in a liposome sedimentation assay. Mutation of the equivalent conserved residues in *Saccharomyces cerevisiae* Sla2p (Lysines-24 and -26 to alanine) result in the complete ablation of lipid binding (Sun et al., 2005). In our study, neither the wild-type nor the mutant construct bound efficiently to control

liposomes but the wild-type HIP1 ANTH domain bound effectively to liposomes produced from bovine brain lipid extract (Folch lipids; Fig. 6 B). However, the double lysine mutation knocked out lipid binding as predicted.

To determine whether the K56E/K58E mutation affected the subcellular distribution of HIP1, LNCaP cells were transfected with Myc-His HIP1 or the HIP1 K56/K58E double mutant. Enriched clathrin-coated vesicle fractions were prepared and blotted for clathrin, HIP1, and adaptors. The double mutant of HIP1 was significantly de-enriched from the CCV fraction relative to the wild-type protein (Fig. 6 C). The lipid binding mutation may therefore increase the size of the "free" or cytosolic pool of HIP1 available to associate with the AR and/or alternative scaffolds such as DNA response elements and transcription complexes.

The COOH-terminal I/LWEQ domain has regularly spaced, conserved amino acids believed to comprise four α-helices, and in Sla2p and HIP1R this domain binds to F-actin (Engqvist-Goldstein et al., 1999; Legendre-Guillemin et al., 2002). Mutation of a conserved residue, arginine-958, in Sla2p ablates actin binding (McCann and Craig, 1999). Although by sequence alignment this arginine residue (R1005) is also present in HIP1, there is only limited biochemical evidence for an association between a recombinantly expressed I/LWEQ domain fragment and actin (Senetar et al., 2004). Indeed binding is absent if a larger expression construct incorporating an upstream α-helix (USH) is used in the same binding assay. Other groups have also been unable to detect actin binding with expression constructs encompassing the entire talin-like (I/LWEQ) domain (Legendre-Guillemin et al., 2002).

Given this ambiguity and in light of the nuclear role that we have uncovered for HIP1, we undertook algorithmic searches for other motifs within this COOH-terminal domain. We identified a putative NLS at the COOH terminus between amino acids 996 and 1009 resembling the consensus RK]x[RK]x[KR]x[4–6]RKK, which is strikingly absent in other proteins with talin-like domains (Fig. 6 A; Cokol et al., 2000). This implied an alternative role for R1005 in nuclear transport. We therefore mutated this residue to a glutamate and tagged GFP expression vectors with the HIP1 NLS, the mutated NLS, and the equivalent sequence region in HIP1R. Confocal imaging revealed that the GFP-HIP1 construct has an incomplete but clear nuclear colocalization in comparison to GFP-HIP1R (Fig 7, A and B). Subcellular fractionation revealed that this amounted to an approximate doubling in the amount of nuclear GFP when compared with GFP-HIP1R, the R1005E mutant, or GFP alone (Fig. 7, C and D). This indicates that an NLS within HIP1 itself can contribute to nuclear import and predicts an interaction between HIP1 and importins. A large number of imported proteins contain multiple or bipartite NLS motifs, which cumulatively result in high efficiency of import. Given the fact that the AR contains NLS motifs in its hinge region, we cannot rule out the possibility that other NLS-containing proteins may translocate into the nucleus in a complex with HIP1. This would explain why, in COS7 cells cotransfected with HIP1 and the AR, the nuclear translocation of both is androgen-reponsive and more efficient than that of

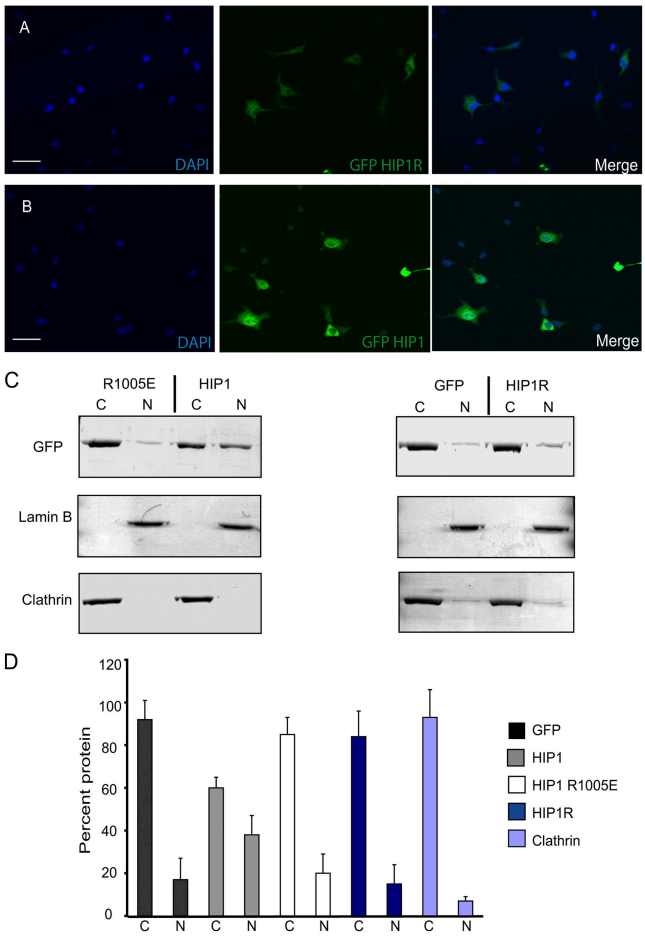

Figure 7. **Characterization of an NLS at the COOH terminus of HIP1.** COS7 cells were transfected with GFP-HIP1R (aa 992–1009; A) or GFP-HIP1NLS (aa 992–1009; B) 48 h before imaging and fixation. Nuclei were stained with DAPI. GFP-HIP1R is predominantly cytosolic, whereas GFP-HIP1 has a nucleocytoplasmic distribution. Bars, 80 μm. (C) COS7 cells were transfected with GFPHIP1, GFPHIP1_R1005E, GFPHIP1R, and GFP alone and were fractionated to give nuclear (N) and cytoplasmic (C) fractions, which were resolved by SDS-PAGE (50 μg per lane) and blotted for GFP, lamin B, and clathrin. (D) The degree of translocation of GFP, GFPHIP1, GFPHIP1_R1005E, GFPHIP1R, and clathrin was quantitated by densitometric analysis. Data shown represent the means of five independent experiments ± SD.

the GFP-tagged minimal NLS (Georget et al., 2002; Saporita et al., 2003).

On the basis of this preliminary characterization of the HIP1 mutants, we predicted that the lipid binding mutant (K56E/K58E) might enhance the ability of HIP1 to coactivate the AR by increasing the available cytosolic pool of HIP1 for nuclear import. We also hypothesized that reducing nuclear import with the R1005E mutation might conversely reduce the transcriptional activity of the AR by having a dominant negative effect on the nuclear import of both HIP1 and, owing to their association, the AR. To test this, we transfected mutant and wild-type HIP1 into COS7 cells and examined the Mibolerone response of the pPSALuc reporter construct. The K56E/K58E HIP1 mutant produced a twofold greater enhancement of transcription than wild-type HIP1 under conditions of androgen stimulation (Fig. 8 A). In contrast, the R1005E mutation repressed transcriptional activ-

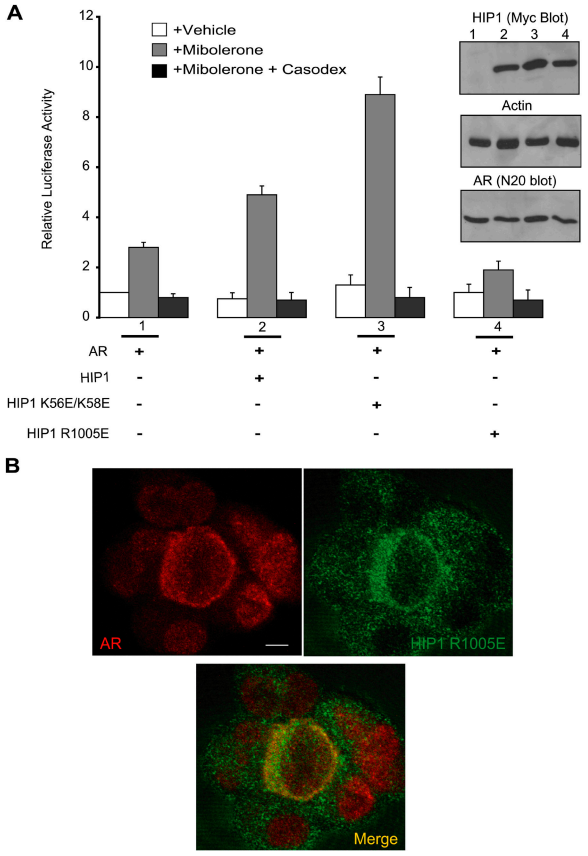

Figure 8. **Effects of lipid binding and NLS mutations on the coregulator functions of HIP1.** (A) COS7 cells were transiently transfected with pcDNA3-HIP1, HIP1 K56E/K58E, or HIP1 R1005E constructs, pcDNA3-AR and the pPSALuc reporter. Luciferase assays were performed after treatment with 10 nM Mibolerone and 1 μM Casodex. Data shown represent the means of three independent experiments ± SD. Lysates were blotted for HIP1 and AR as well as actin as a loading control. (B) HIP1 R1005E was transfected into LNCaP cells undergoing steroid depletion. Cells were treated with 10 nM Mibolerone for 2 h, fixed, and stained for the AR (red) and with a Myc antibody for HIP1 R1005E (green). Bar, 10 μm.

ity by fourfold. Examining androgen-treated cells expressing the R1005E mutant we noted that there was a reduction in the apparent nuclear translocation of the AR in cells coexpressing the AR and the mutant (Fig. 8 B and Fig. S2, available at http://www.jcb.org/cgi/content/full/jcb.200503106/DC1).

Discussion

Nuclear translocation of membrane trafficking proteins

It has previously been proposed that certain endocytic proteins undergoing nucleocytoplasmic shuttling might function as protein scaffolds in the nucleus and exert regulatory effects on transcription (Vecchi et al., 2001). Endocytic proteins first reported to undergo nucleocytoplasmic shuttling were not found to be stimulated to translocate to the nucleus upon treatment with epidermal growth factor or phorbol ester (Vecchi et al., 2001). In contrast, we report here that HIP1 translocates to the nucleus and that this translocation is androgen inducible (Fig. 1). The theme of a direct integration between signal-dependent membrane trafficking events and transcription is a new and emerging one. The only other example of a stimulus-induced nuclear translocation of an endocytic protein is the EGF-dependent translocation of APPL (adaptor protein containing PH domain, PTB domain, and leucine zipper motif) to the nucleus, which complexes with histone deacetylase multiprotein complex to regulate chromatin structure and transcription (Miaczynska et al., 2004). In contrast, HIP1 associates with a transcription factor, the AR, and perhaps other members of the nuclear hormone receptor family to enhance their transcriptional activity.

The overexpression of HIP1 in prostate cancer, as an endocytic protein capable of translocating to the nucleus and coactivating androgen-dependent transcription, is of potential importance in the study of hormonal responses in prostate cancer. A major focus of the prostate cancer field thus far has been on androgen hypersensitivity and kinase-dependent cross talk between growth factor pathways and nuclear hormone receptors rather than adaptor-based cross talk acting on both promoters and membranes (Chen et al., 2004; Culig, 2004). Our work now suggests that HIP1 may be capable of such integration given the association with AREs and the coactivation of AR-mediated transcription (Figs. 3 and 4).

HIP1 as a transcriptional regulator of the AR

It remains to be shown whether the association between HIP1 and the AR and between HIP1 and DNA is indirect or direct. Immunoprecipitation has demonstrated an association between the AR and the FxDxF/coiled coil domain of HIP1 (Fig. 2, A and C). Mammalian two-hybrid assays suggest that the NH_2-terminal domain of the AR is a potential binding site for HIP1 (unpublished data). However, this region also binds other transcriptional coregulators, which could act as a molecular bridge to HIP1, and so more detailed mapping of the interaction site in the AR is required (Metzler et al., 2001; Sampson et al., 2001; Waelter et al., 2001).

The function of the I/LWEQ domain of HIP1 has previously proven difficult to confirm despite strong sequence homology with well-characterized actin-binding proteins (Legendre-Guillemin et al., 2002; Senetar et al., 2004). We have identified an NLS within the COOH-terminal I/LWEQ domain, which promotes the nuclear localization of GFP, and we believe that this distinguishes HIP1 from its actin-binding homologues (Figs. 6 A and 7). This motif may also explain a nuclear pool of HIP1 of variable size observed in transfected and untransfected COS7 cells by others (unpublished data). The NLS, although not strong enough to localize GFP constitutively to the nucleus, suggests that HIP1 may therefore have additional nuclear functions and transcriptional effects that are independent of hormonal stimulation and AR expression.

HIP1 is believed to be recruited from the cytosol to membranes through the binding of phosphoinositides by the ANTH domain. We have demonstrated that the nuclear translocation of HIP1 is an alternative dynamic event using cytosolic HIP1. Ablating lipid binding and therefore membrane recruitment with a double lysine mutation in the ANTH domain increases the transcriptional coactivation of HIP1 (Figs. 6 and 8). The

NLS in HIP1 is also clearly equally important for the coactivator function of HIP1 because the R1005E mutation within this motif converts HIP1 from a coactivator to a potent corepressor (Fig. 8 A). Although this mutant can still bind to the AR (not depicted), the steady-state distribution of AR in R1005E-transfected cells is altered such that the AR appears largely cytosolic in certain cells (Fig. 8 B).

Other groups have in the past reported a requirement for F-actin binding proteins in the nuclear translocation of the AR although HIP1 itself has not been found so far to bind to F-actin other than in vitro in biochemical experiments (Ozanne et al., 2000; Schrantz et al., 2004; Senetar et al., 2004). Our findings imply that the R1005E mutation exerts its influence on AR signaling as a nuclear trafficking mutant by in part interfering with nuclear entry after androgen treatment (Fig. 8 B and Fig. S2).

Previously, it has been reported that the AR shuttles in and out of the nucleus several times after androgen treatment (Tyagi et al., 2000). Given that the NLS in HIP1 is weak and that the AR contains its own NLS motifs in the hinge domain, it is unlikely that the R1005E HIP1 mutant could block the nuclear translocation of the AR. The more plausible explanation must therefore be that the association between HIP1 and the AR occurs to some degree in the cytoplasm and affects the cycling and turnover of the receptor. A role for HIP1 in regulating the degradation or turnover of the AR is implied by the reduction in steady-state AR levels induced by HIP1 siRNA and the increased rate of AR degradation after the imposition of a cycloheximide block (Fig. 5). A link between nuclear translocation of the AR and its degradation was made when lysine mutations in the NLS of AR were shown to delay nuclear entry of the protein in response to ligand and inhibit proteasomal degradation (Thomas et al., 2004). Degradation of native AR by a cytosolic complex incorporating the E3 ubiquitin ligase, Hsc70 interacting protein (CHIP), was recently reported (Thomas et al., 2004). We therefore hypothesize that the R1005E mutant delays AR nuclear translocation in response to ligand, thus making the receptor available to such a complex for degradation and so repressing transcription. However, other factors that may contribute to the striking repressive effect of the R1005E mutant on transcription by the AR include an alteration in the steady-state nucleocytoplasmic distribution of the AR or disruption to the assembly of an active AR transcription complex on promoters.

In conclusion, the field of endocytosis is now developed enough for network theory to be applied to the large inventory of adaptors and their protein–protein and protein–lipid interactions (Praefcke et al., 2004). In contrast, mapping adaptor interactions at a nuclear and promoter level, be it by ChIP-on-ChIP or ChIP display, is only just beginning (Barski and Frenkel, 2004; Praefcke et al., 2004; Wang, 2005). HIP1 is an example of an emerging subset of adaptor proteins capable of nuclear translocation and associating with promoters and transcriptional machinery. It and other adaptors have been linked with cancer progression through correlative changes in expression and, in leukemias, gene fusions. Although their mechanistic contribution to cancer progression remains to be elucidated, a role as transcriptional regulators at promoters may prove as significant as their involvement in membrane trafficking and endocytosis.

Materials and methods

Constructs and protein expression

Derivatives and mutants were subcloned into pGEX4T1 or 4T2, expressed in *E. coli* BL21 cells, and affinity purified before use. HIP1 expression constructs were made with the pcDNA3.1 Myc-His6 expression vector as described previously (Rao et al., 2002). GFP-tagged NLS constructs used primers spanning aa 992–1009 ligated into the BamHI–NotI sites of the NH_2-terminal GFP-tagging vector pQN1-FC3 (Qbiogene), HIP1NLS (GATCCGAATTGCAGGATCCAAGGAGCGTCAAAAACTGGGAGAGCTTCGGAAAAAGCACTACGAGGGC), and HIP1R-NLS (GATCCACGGCTGAGGCTGAACGCATGCGGCTGGGGGAGTTGCGGAAGCAACACTACGTGGGC). The K56E/K58E was made using sense and antisense primers incorporating the appropriate single base changes highlighted in bold: gtggctgta**g**aggaa**g**aacacgccagaacg and cgttctggcgt**ct**tcct**ct**acagccac; and for the R1005E mutant using sense and antisense primers: gggagagctt**ct**caaaaagcac and gtgcttttt**ga**gaagctctccc using two cycling conditions for each construct. Cycling protocol 1: 13 cycles consisting of 94°C for 40 s, 65°C for 30 s, and 70°C for 18 min and followed by a final 67°C extension step lasting 18 min. Cycling protocol 2: 18 cycles consisting of 94°C for 40 s, 62°C for 30 s, and 67°C for 18 min and followed by a final 67°C extension step lasting 15 min. In both cases the template DNA was digested using DpnI, with a 37°C incubation lasting 45 min and a subsequent denaturation step (65°C, 20 min) before transformation into an XL-1 Blue strain of *E. coli*. An NH_2-terminal construct of HIP1 comprising aa 1–310 was PCR subcloned into the EcoRI–NotI sites of pGEX4T2 using a sense (ggaattcatatggatcggatggccagctccatgaag) and an antisense primer (ttttcttttgcggccgctaagggctgatatgttctgacagggctg).

The following expression vectors have previously been described: pcDNA3-AR and TK-GAL4UASLuc, pPSALuc, pGAL4DBD-Erβ, pGAL4DBD-ERα, MMTVLuc, pCMV-β-gal, and $pARE_4$-Luc (Brady et al., 1999; Gaughan et al., 2001; Lu et al., 2001). $pARE_4$-Luc consists of a minimal promoter and was constructed by inserting four synthetic tandem repeats of the ARE primers (5′-TGTACAGGATGTTCTGAATTCCATGTACAGGATGTTCT-3′ and 5′-AGAACATCCTGTACATGAATTCAAGAACATCCTGTACA-3′) in front of an E1b minimal TATA box sequence, followed by a firefly luciferase gene.

RNA interference

HIP1 knockdowns were performed using three siRNA constructs, which were obtained as H1 cassettes (GenScript) and had the following sense sequences: GAACCAAGAUGGAGUACCA (HIP1nts440-459); GCACUACGAGCUUGCUGGU (HIP1nts3021-3039); GGACGAGGCUGGAGAAAGU (HIP1nts510-528). A scrambled siRNA was purchased from QIAGEN and had the sequence UUCUCCGAACGUGUCACGUdTdT. In brief, 250,000 LNCaP cells were plated onto a 24-well plate (Corning) and left for 1 d to grow. On the day of transfection, 1 μg of each oligo either alone or in combination was transfected into individual wells at a ratio of 1 μg of oligo to 6 μl of transfection reagent (RNAifect; QIAGEN) according to the manufacturer's guidelines.

Western blotting

Total cell extracts were prepared by lysing cells for 30 min on ice in lysis buffer containing 50 mM Tris, pH 6.8, 150 mM NaCl, 50 mM sodium glycerophosphate, 10 mM NaF, 1 mM sodium orthovanadate, complete protease inhibitor (Roche), and 1% NP-40. The extracts were cleared by centrifugation for 30 min at 17,000 *g* and then boiled in SDS sample buffer for 10 min. Total cell lysate (20–30 μg) was resolved by SDS-PAGE (10% gel), transferred on to an Immobilon-P membrane (Millipore), and the signal was visualized by ECL (GE Healthcare). Membranes were blotted with antibodies against HIP1 (NOVUS Biologicals), AR (Santa Cruz Biotechnology, Inc.), PSA (Santa Cruz Biotechnology, Inc.), lamin B (Santa Cruz Biotechnology, Inc.), actin (Sigma-Aldrich), clathrin heavy chain (Transduction Laboratories), GFP (CLONTECH Laboratories, Inc.), TGN46 (Serotec), γ-adaptin (Sigma-Aldrich), Myc (Cell Signaling), β-tubulin, and HIP1R (polyclonal: gift from T. Ross, University of Michigan Medical School, Ann Arbor, MI).

Isolation of nuclear and cytosolic fractions from cell lines

Nuclei were isolated from LNCaP cells according to published protocols (Schreiber et al., 1989). Confluent cells from 90-mm dishes were washed twice in ice-cold TBS, and then gently scraped into 800 μl of cold homogenization buffer (10 mM Hepes, pH 7.9, 10 mM KCl, 0.1 mM EDTA, 0.1 mM EGTA, 1 mM DTT, and 0.5 mM PMSF) and allowed to swell on ice for 15 min. Cells were lysed by addition of 50 μl of a 10% solution of

NP-40 followed by 10-s vigorous vortexing. Nuclei were pelleted by centrifugation at 14,000 rpm for 30 s. The cytoplasmic fraction was removed, and nuclei were washed twice in homogenization buffer with NP-40 and resuspended in 200 μl of the same buffer. Nuclei were solubilized by sonication, and protein concentrations of nuclear and cytoplasmic fractions were determined using the BCA protein assay (Pierce Chemical Co.). Equal amounts of protein from all fractions were boiled in 2× Laemmli sample buffer, separated by SDS-PAGE, and transferred to nitrocellulose. Membranes were blotted with antibodies to AR (Santa Cruz Biotechnology, Inc.) and HIP1 (NOVUS Biologicals), as well as anti-lamin B (Santa Cruz Biotechnology, Inc.) and clathrin heavy chain (Transduction Laboratories) that were used as nuclear and loading control probes. Primary antibodies were followed up with appropriate HRP-conjugated secondary antibodies (Dako). Immunoreactive bands were visualized with ECL using SuperSignal substrate (Pierce Chemical Co.). Blots were scanned using a densitometer (model FL-5000; Fuji) and band densities were quantitated using ImageQuant software. Gel and blot images were prepared for the illustrations with the use of Adobe Photoshop software.

CCV isolation

CCVs were isolated from LNCaP cells growing on six to eight 75-cm^2 tissue culture flasks using an adaptation of an existing protocol (Hirst et al., 2004). Protein levels were assayed, and equal protein loadings of the fractions were blotted after SDS-PAGE.

Cell culture and microscopy

COS7 and LNCaP lines were grown in DME and RPMI-1640 media, respectively, supplemented with 10% FBS or charcoal-stripped FBS (Hyclone). Cells were grown in steroid-depleted media for 48 h pretransfection and were then transfected with Fugene according to the manufacturer's protocol. Cells were fixed with 3% PFA, followed by permeabilization with 0.1% saponin. Primary antibodies are listed in the Western blotting section; secondary antibodies were purchased from Molecular Probes. Images were acquired on a confocal microscope (model LSM510 META; Carl Zeiss MicroImaging, Inc.) equipped with the appropriate filters and laser lines. Images were rendered in image browser software (Carl Zeiss MicroImaging, Inc.) before processing for publication using Adobe Photoshop.

RNA extraction and quantitative RT-PCR

Total RNA was extracted from growing LNCaP cells using TRIzol reagent (Invitrogen) according to the manufacturer's instructions. Real-time PCRs were performed using a SYBR Green PCR Master Mix (Applied Biosystems) in an ABI PRISM 7900HT Sequence Detection System (Applied Biosystems) according to the manufacturer's instructions. Cycling conditions were 50°C for 2 min, 95°C for 10 min, 40 cycles of 95°C for 15 s, and 60°C for 1 min. The following primer pairs were used to profile the AR (CTCACCAAGCTCCTGGACTC and CAGGCAGAAGACATCTGAAAG), PSA (GCAGCATTGAACCAGAGGAG and AGAACTGGGGAGGCTTGAGT), HIP1 (CAACCCTGGCGAACAGTTCTA and TCCAAATGACCGAAGCTCG), HIP1R (CACGCAGCAGGAATTTTACGC and CCTCATACTTGCCCGTGTGAA), and β-actin (CACAGCTGAGAGGGAAATC and TCAGCAATGCCTGGGTAC).

Luciferase reporter assays

GAL4-based reporter assay. For transcriptional assays, HIP1 and its truncated versions were cloned into the PM2 vector fused to the GAL4 DNA-binding domain (aa positions 1–147). COS-7 cells grown in 6-well dishes were transiently transfected in triplicate with 0.3 μg of the GAL4-TK-luciferase reporter and with 1.2 μg of the different GAL4 fusion constructs using lipofectamine (Invitrogen). Cells were lysed after 48 h and analyzed by immunoblotting with anti-GAL4 antibodies (Santa Cruz Biotechnology, Inc.) to verify the levels of expression of the various GAL4 fusion proteins. Transactivation assays were performed only on sets of transfectants that showed comparable levels of expression of the various proteins. Luciferase activity was measured on identical amounts of total cellular lysates from the various transfectants using a commercial kit (Promega).

Androgen reporter assay. Cells were seeded into 24-well plates and grown in the presence of charcoal-stripped medium for at least 24 h before transfection with a PSA luciferase reporter construct (pPSALuc) and a β-Gal reporter. Reporter assays were undertaken as described previously (Gaughan et al., 2002). All experiments shown are the average of at least three independent experiments performed in triplicate ± SD.

Liposome sedimentation assay. Sedimentation assays were performed according to an established protocol (Peter et al., 2004). Recombinant protein was expressed and purified from BL21 DE3 cells. Liposomes consisting either of 40% phosphatidylcholine, 40% phosphatidylethanolamine,10% cholesterol, and 10% phoshatidylinositol (Avanti Polar Lipids, Inc.) or of Folch fraction1/total bovine brain lipids (Folch fraction 1; Sigma-Aldrich B1502) were resuspended at 1 mg/ml in 20 mM Hepes, pH 7.4, 150 mM NaCl, and 1 mM DTT and sized by extrusion. Supernatants and pellets were resuspended in an equal volume of sample buffer and subjected to SDS-PAGE and visualized by Coomassie stain.

ChIP. ChIP assays were performed as described previously (Gaughan et al., 2002). For immunoprecipitation, 2 μg of polyclonal AR and 2 μg monoclonal HIP1 antibodies were used as indicated. ReChIP analysis was performed as described previously (Reid et al., 2003). In brief, AR and HIP1 antibodies were added to chromatin extracts for 5 h followed by the addition of 60 μl of salmon sperm/protein A–Agarose (Upstate Biotechnology) to recover immunocomplexes. AR- and HIP1-containing complexes were eluted by 1-h incubation in reChIP buffer (0.5 mM DTT, 1% Triton X-100, 2 mM EDTA, 150 mM NaCl, and 20 mM Tris, pH 8.1) and subsequently reimmunoprecipitated by the addition of 2 μg of antibodies for AR, HIP1, or anti-VP16 for control, to an equal volume of eluted material. Recovery and preparation of DNA was performed as described previously (Gaughan et al., 2002). Semi-quantitative PCR was performed with 10 μl of DNA, BioTaq DNA polymerase, and α-[^{32}P]dATP, using the following primers: ARE IF, TCTGCCTTTGTCCCCTAGAT, and ARE IR, AACCTTCATTCCCCAGGACT, to amplify 235 bp of the proximal PSA promoter, encompassing the ARE I (Fig. 4 A); ARE IIIF, CCTCCCAGGTTCAAGTGATT, and ARE IIIR, GCCTGTAATCCCAGCACTTT, to amplify the distal ARE III; ARE XF, CTGTGCTTGGAGTTTACCTGA, and ARE XR, GCAGAGGTTGCAGTGAGCC, to amplify a non-ARE–containing portion of the PSA promoter. PCR products were resolved, dried, and then exposed to X-ray film for 2–12 h. ChIP data are representative of triplicate experiments performed using similar passage number LNCaP cells.

Online supplemental material

Fig. S1 shows coactivation of estrogen and glucocorticoid receptors by HIP1. HIP1 was cotransfected into COS7 cells with the estrogen or glucocorticoid receptors along with appropriate luciferase reporter constructs. Lysates were assayed for luciferase activity. Experiments were performed in triplicate and SDs are shown. Fig. S2 shows the effect of the HIP1 R1005E mutant on the nucleocytoplasmic distribution of the AR. LNCaP cells were transfected with Myc-tagged wtHIP1 or HIP1 R1005E and fractionated after androgen treatment. Nuclear and cytosolic fractions were resolved by SDS-PAGE and blotted for the AR and Myc illustrated with representative blots (Fig. S2 A). Fractions were also blotted for lamin B and clathrin as nuclear and cytosolic control proteins (Fig. S2 C). The degree of translocation of the AR and HIP1 was quantitated by densitometric analysis of the blots (Fig. S2 B). Experiments were performed five times and SDs are shown. Online supplemental material is available at http://www.jcb.org/cgi/content/full/jcb.200503106/DC1.

We thank B.A.J. Ponder and members of the Ross Laboratory for critical reading of the manuscript.

This work was supported by a Cancer Research UK Programme Grant (I.G. Mills), by the Association of International Cancer Research (L. Gaughan), and by the National Cancer Research Institute Prostate Research Collaborative (ProMPT).

Submitted: 21 March 2005
Accepted: 8 June 2005

References

Altschul, S.F., T.L. Madden, A.A. Schaffer, J. Zhang, Z. Zhang, W. Miller, and D.J. Lipman. 1997. Gapped BLAST and PSI-BLAST: a new generation of protein database search programs. *Nucleic Acids Res.* 25:3389–3402.

Barski, A., and B. Frenkel. 2004. ChIP Display: novel method for identification of genomic targets of transcription factors. *Nucleic Acids Res.* 32:e104.

Beitel, L.K., Y.A. Elhaji, R. Lumbroso, S.S. Wing, V. Panet-Raymond, B. Gottlieb, L. Pinsky, and M.A. Trifiro. 2002. Cloning and characterization of an androgen receptor N-terminal-interacting protein with ubiquitin-protein ligase activity. *J. Mol. Endocrinol.* 29:41–60.

Brady, M.E., D.M. Ozanne, L. Gaughan, I. Waite, S. Cook, D.E. Neal, and C.N. Robson. 1999. Tip60 is a nuclear hormone receptor coactivator. *J. Biol. Chem.* 274:17599–17604.

Burgdorf, S., P. Leister, and K.H. Scheidtmann. 2004. TSG101 interacts with apoptosis-antagonizing transcription factor and enhances androgen receptor-mediated transcription by promoting its monoubiquitination. *J. Biol.*

Chem. 279:17524–17534.

Chen, C.D., D.S. Welsbie, C. Tran, S.H. Baek, R. Chen, R. Vessella, M.G. Rosenfeld, and C.L. Sawyers. 2004. Molecular determinants of resistance to antiandrogen therapy. *Nat. Med.* 10:33–39.

Cokol, M., R. Nair, and B. Rost. 2000. Finding nuclear localization signals. *EMBO Rep.* 1:411–415.

Culig, Z. 2004. Androgen receptor cross-talk with cell signalling pathways. *Growth Factors.* 22:179–184.

Engqvist-Goldstein, A.E., M.M. Kessels, V.S. Chopra, M.R. Hayden, and D.G. Drubin. 1999. An actin-binding protein of the Sla2/Huntingtin interacting protein 1 family is a novel component of clathrin-coated pits and vesicles. *J. Cell Biol.* 147:1503–1518.

Ford, M.G., B.M. Pearse, M.K. Higgins, Y. Vallis, D.J. Owen, A. Gibson, C.R. Hopkins, P.R. Evans, and H.T. McMahon. 2001. Simultaneous binding of PtdIns(4,5)P2 and clathrin by AP180 in the nucleation of clathrin lattices on membranes. *Science.* 291:1051–1055.

Gaughan, L., M.E. Brady, S. Cook, D.E. Neal, and C.N. Robson. 2001. Tip60 is a co-activator specific for class I nuclear hormone receptors. *J. Biol. Chem.* 276:46841–46848.

Gaughan, L., I.R. Logan, S. Cook, D.E. Neal, and C.N. Robson. 2002. Tip60 and histone deacetylase 1 regulate androgen receptor activity through changes to the acetylation status of the receptor. *J. Biol. Chem.* 277:25904–25913.

Geli, M.I., and H. Riezman. 1998. Endocytic internalization in yeast and animal cells: similar and different. *J. Cell Sci.* 111:1031–1037.

Georget, V., B. Terouanne, J.C. Nicolas, and C. Sultan. 2002. Mechanism of antiandrogen action: key role of hsp90 in conformational change and transcriptional activity of the androgen receptor. *Biochemistry.* 41:11824–11831.

Hanstein, B., R. Eckner, J. DiRenzo, S. Halachmi, H. Liu, B. Searcy, R. Kurokawa, and M. Brown. 1996. p300 is a component of an estrogen receptor coactivator complex. *Proc. Natl. Acad. Sci. USA.* 93:11540–11545.

Hirst, J., S.E. Miller, M.J. Taylor, G.F. von Mollard, and M.S. Robinson. 2004. EpsinR is an adaptor for the SNARE protein Vti1b. *Mol. Biol. Cell.* 15:5593–5602.

Holtzman, D.A., S. Yang, and D.G. Drubin. 1993. Synthetic–lethal interactions identify two novel genes, *SLA1* and *SLA2*, that control membrane cytoskeleton assembly in *Saccharomyces cerevisiae*. *J. Cell Biol.* 122:635–644.

Hyman, J., H. Chen, P.P. Di Fiore, P. De Camilli, and A.T. Brunger. 2000. Epsin 1 undergoes nucleocytosolic shuttling and its eps15 interactor NH_2-terminal homology (ENTH) domain, structurally similar to *Armadillo* and HEAT repeats, interacts with the transcription factor promyelocytic leukemia Zn^2+ finger protein (PLZF). *J. Cell Biol.* 149:537–546.

Hyun, T.S., D.S. Rao, D. Saint-Dic, L.E. Michael, P.D. Kumar, S.V. Bradley, I.F. Mizukami, K.I. Oravecz-Wilson, and T.S. Ross. 2004. HIP1 and HIP1r stabilize receptor tyrosine kinases and bind 3-phosphoinositides via epsin N-terminal homology domains. *J. Biol. Chem.* 279:14294–14306.

Kalchman, M.A., H.B. Koide, K. McCutcheon, R.K. Graham, K. Nichol, K. Nishiyama, P. Kazemi-Esfarjani, F.C. Lynn, C. Wellington, M. Metzler, et al. 1997. HIP1, a human homologue of *S. cerevisiae* Sla2p, interacts with membrane-associated huntingtin in the brain. *Nat. Genet.* 16:44–53.

Kubler, E., and H. Riezman. 1993. Actin and fimbrin are required for the internalization step of endocytosis in yeast. *EMBO J.* 12:2855–2862.

Legendre-Guillemin, V., M. Metzler, M. Charbonneau, L. Gan, V. Chopra, J. Philie, M.R. Hayden, and P.S. McPherson. 2002. HIP1 and HIP12 display differential binding to F-actin, AP2, and clathrin. Identification of a novel interaction with clathrin light chain. *J. Biol. Chem.* 277:19897–19904.

Lu, M.L., M.C. Schneider, Y. Zheng, X. Zhang, and J.P. Richie. 2001. Caveolin-1 interacts with androgen receptor. A positive modulator of androgen receptor mediated transactivation. *J. Biol. Chem.* 276:13442–13451.

McCann, R.O., and S.W. Craig. 1997. The I/LWEQ module: a conserved sequence that signifies F-actin binding in functionally diverse proteins from yeast to mammals. *Proc. Natl. Acad. Sci. USA.* 94:5679–5684.

McCann, R.O., and S.W. Craig. 1999. Functional genomic analysis reveals the utility of the I/LWEQ module as a predictor of protein: actin interaction. *Biochem. Biophys. Res. Commun.* 266:135–140.

Metzler, M., V. Legendre-Guillemin, L. Gan, V. Chopra, A. Kwok, P.S. McPherson, and M.R. Hayden. 2001. HIP1 functions in clathrin-mediated endocytosis through binding to clathrin and adaptor protein 2. *J. Biol. Chem.* 276:39271–39276.

Miaczynska, M., S. Christoforidis, A. Giner, A. Shevchenko, S. Uttenweiler-Joseph, B. Habermann, M. Wilm, R.G. Parton, and M. Zerial. 2004. APPL proteins link Rab5 to nuclear signal transduction via an endosomal compartment. *Cell.* 116:445–456.

Mishra, S.K., N.R. Agostinelli, T.J. Brett, I. Mizukami, T.S. Ross, and L.M. Traub. 2001. Clathrin- and AP-2-binding sites in HIP1 uncover a general assembly role for endocytic accessory proteins. *J. Biol. Chem.* 276:46230–46236.

Munn, A.L., B.J. Stevenson, M.I. Geli, and H. Riezman. 1995. end5, end6, and end7: mutations that cause actin delocalization and block the internalization step of endocytosis in *Saccharomyces cerevisiae*. *Mol. Biol. Cell.* 6:1721–1742.

Ozanne, D.M., M.E. Brady, S. Cook, L. Gaughan, D.E. Neal, and C.N. Robson. 2000. Androgen receptor nuclear translocation is facilitated by the f-actin cross-linking protein filamin. *Mol. Endocrinol.* 14:1618–1626.

Peter, B.J., H.M. Kent, I.G. Mills, Y. Vallis, P.J. Butler, P.R. Evans, and H.T. McMahon. 2004. BAR domains as sensors of membrane curvature: the amphiphysin BAR structure. *Science.* 303:495–499.

Praefcke, G.J., M.G. Ford, E.M. Schmid, L.E. Olesen, J.L. Gallop, S.Y. Peak-Chew, Y. Vallis, M.M. Babu, I.G. Mills, and H.T. McMahon. 2004. Evolving nature of the AP2 alpha-appendage hub during clathrin-coated vesicle endocytosis. *EMBO J.* 23:4371–4383.

Rao, D.S., T.S. Hyun, P.D. Kumar, I.F. Mizukami, M.A. Rubin, P.C. Lucas, M.G. Sanda, and T.S. Ross. 2002. Huntingtin-interacting protein 1 is overexpressed in prostate and colon cancer and is critical for cellular survival. *J. Clin. Invest.* 110:351–360.

Reddy, P.H., M. Williams, and D.A. Tagle. 1999. Recent advances in understanding the pathogenesis of Huntington's disease. *Trends Neurosci.* 22:248–255.

Reid, G., M.R. Hubner, R. Metivier, H. Brand, S. Denger, D. Manu, J. Beaudouin, J. Ellenberg, and F. Gannon. 2003. Cyclic, proteasome-mediated turnover of unliganded and liganded ERalpha on responsive promoters is an integral feature of estrogen signaling. *Mol. Cell.* 11:695–707.

Sampson, E.R., S.Y. Yeh, H.C. Chang, M.Y. Tsai, X. Wang, H.J. Ting, and C. Chang. 2001. Identification and characterization of androgen receptor associated coregulators in prostate cancer cells. *J. Biol. Regul. Homeost. Agents.* 15:123–129.

Saporita, A.J., Q. Zhang, N. Navai, Z. Dincer, J. Hahn, X. Cai, and Z. Wang. 2003. Identification and characterization of a ligand-regulated nuclear export signal in androgen receptor. *J. Biol. Chem.* 278:41998–42005.

Schrantz, N., J. da Silva Correia, B. Fowler, Q. Ge, Z. Sun, and G.M. Bokoch. 2004. Mechanism of p21-activated kinase 6-mediated inhibition of androgen receptor signaling. *J. Biol. Chem.* 279:1922–1931.

Schreiber, E., P. Matthias, M.M. Muller, and W. Schaffner. 1989. Rapid detection of octamer binding proteins with 'mini-extracts', prepared from a small number of cells. *Nucleic Acids Res.* 17:6419.

Senetar, M.A., S.J. Foster, and R.O. McCann. 2004. Intrasteric inhibition mediates the interaction of the I/LWEQ module proteins Talin1,Talin2, Hip1, and Hip12 with actin. *Biochemistry.* 43:15418–15428.

Sun, Y., M. Kaksonen, D.T. Madden, R. Schekman, and D.G. Drubin. 2005. Interaction of Sla2p's ANTH domain with PtdIns(4,5)P2 is important for actin-dependent endocytic internalization. *Mol. Biol. Cell.* 16:717–730.

Tanner, T., F. Claessens, and A. Haelens. 2004. The hinge region of the androgen receptor plays a role in proteasome-mediated transcriptional activation. *Ann. NY Acad. Sci.* 1030:587–592.

Thomas, M., N. Dadgar, A. Aphale, J.M. Harrell, R. Kunkel, W.B. Pratt, and A.P. Lieberman. 2004. Androgen receptor acetylation site mutations cause trafficking defects, misfolding, and aggregation similar to expanded glutamine tracts. *J. Biol. Chem.* 279:8389–8395.

Tyagi, R.K., Y. Lavrovsky, S.C. Ahn, C.S. Song, B. Chatterjee, and A.K. Roy. 2000. Dynamics of intracellular movement and nucleocytoplasmic recycling of the ligand-activated androgen receptor in living cells. *Mol. Endocrinol.* 14:1162–1174.

Vecchi, M., S. Polo, V. Poupon, J.W. van de Loo, A. Benmerah, and P.P. Di Fiore. 2001. Nucleocytoplasmic shuttling of endocytic proteins. *J. Cell Biol.* 153:1511–1517.

Waelter, S., E. Scherzinger, R. Hasenbank, E. Nordhoff, R. Lurz, H. Goehler, C. Gauss, K. Sathasivam, G.P. Bates, H. Lehrach, and E.E. Wanker. 2001. The huntingtin interacting protein HIP1 is a clathrin and alpha-adaptin-binding protein involved in receptor-mediated endocytosis. *Hum. Mol. Genet.* 10:1807–1817.

Wang, J.C. 2005. Finding primary targets of transcriptional regulators. *Cell Cycle.* 4:356–358.

Wanker, E.E., C. Rovira, E. Scherzinger, R. Hasenbank, S. Walter, D. Tait, J. Colicelli, and H. Lehrach. 1997. HIP-I: a huntingtin interacting protein isolated by the yeast two-hybrid system. *Hum. Mol. Genet.* 6:487–495.

Wesp, A., L. Hicke, J. Palecek, R. Lombardi, T. Aust, A.L. Munn, and H. Riezman. 1997. End4p/Sla2p interacts with actin-associated proteins for endocytosis in *Saccharomyces cerevisiae*. *Mol. Biol. Cell.* 8:2291–2306.

Yang, S., M.J. Cope, and D.G. Drubin. 1999. Sla2p is associated with the yeast cortical actin cytoskeleton via redundant localization signals. *Mol. Biol. Cell.* 10:2265–2283.

Serum Antibodies to Huntingtin Interacting Protein-1: A New Blood Test for Prostate Cancer

Sarah V. Bradley,[1] Katherine I. Oravecz-Wilson,[1] Gaelle Bougeard,[1] Ikuko Mizukami,[1] Lina Li,[1] Anthony J. Munaco,[1] Arun Sreekumar,[2] Michael N. Corradetti,[1] Arul M. Chinnaiyan,[2,3] Martin G. Sanda,[3] and Theodora S. Ross[1]

Departments of [1]Internal Medicine, [2]Pathology, and [3]Urology, University of Michigan Medical School, Ann Arbor, Michigan

Abstract

Huntingtin-interacting protein 1 (HIP1) is frequently overexpressed in prostate cancer. HIP1 is a clathrin-binding protein involved in growth factor receptor trafficking that transforms fibroblasts by prolonging the half-life of growth factor receptors. In addition to human cancers, HIP1 is also overexpressed in prostate tumors from the transgenic adenocarcinoma of the mouse prostate (TRAMP) mouse model. Here we provide evidence that HIP1 plays an important role in mouse tumor development, as tumor formation in the TRAMP mice was impaired in the *Hip1*$^{null/null}$ background. In addition, we report that autoantibodies to HIP1 developed in the sera of TRAMP mice with prostate cancer as well as in the sera from human prostate cancer patients. This led to the development of an anti-HIP1 serum test in humans that had a similar sensitivity and specificity to the anti–α-methylacyl CoA racemase (AMACR) and prostate-specific antigen tests for prostate cancer and when combined with the anti-AMACR test yielded a specificity of 97%. These data suggest that HIP1 plays a functional role in tumorigenesis and that a positive HIP1 autoantibody test may be an important serum marker of prostate cancer. (Cancer Res 2005; 65(10): 4126-33)

Introduction

Currently, the prostate-specific antigen (PSA) blood test is widely relied upon for the early detection of prostate cancer. Despite the fact that this test was identified almost 20 years ago and standardized >10 years ago (1), the effect of this screening on mortality is not yet defined (2–4) and both its sensitivity (5, 6) and specificity (7) have limitations. Although there has been a stage migration with the use of the PSA test and therefore this test likely diminishes mortality from prostate cancer, the discovery of new biomarkers for early diagnosis and prognosis of prostate cancer may improve management of and survival from prostate cancer.

Recently, the identification of a test that identifies autoantibodies to the prostate tumor marker, α-methylacyl CoA racemase (AMACR) provided hope that use of cytoplasmic tumor markers in addition to secreted antigens could lead to blood screening tests (8). The proposed reason for the formation of autoantibodies is that upon turnover of tumor cells, tumor antigens are shed into the circulation at low levels inducing an immune response. Immunoreactivity to other cytoplasmic tumor antigens has been described in prostate cancer patients previously, but the formation of these autoantibodies did not show high sensitivities (9–11).

Because HIP1 is specifically up-regulated in prostate cancer relative to benign prostatic epithelia (12) and is a cytoplasmic protein, we hypothesized that HIP1 autoantibody formation could, like AMACR, yield a useful blood test for prostate cancer. In addition, because overexpression of HIP1 is associated with advanced prostate cancer (12) and HIP1 directly transforms fibroblasts (13), we hypothesized that HIP1 may be necessary for *in vivo* tumor cell survival or progression.

To experimentally evaluate these two questions in mice, we employed the transgenic adenocarcinoma of the mouse prostate (TRAMP) model (14) and *Hip1* mutant mice generated in our laboratory (15). TRAMP mice express SV40 T antigen under the control of the *probasin* promoter. This targets transgene expression to the epithelial cells of the prostate and leads to prostate cancer. Although many of the tumors in these mice are more representative of a neuroendocrine rather than epithelial cancer (16), the progression of these cancers in the TRAMP model is similar to human prostate cancer in that the prostates of these mice develop hyperplastic epithelia, *in situ* carcinoma, locally invasive cancers followed by metastases to the liver, lung, lymph nodes, and bone. In addition to providing evidence here that HIP1 may indeed be necessary for tumorigenesis in the TRAMP prostate, we have discovered that both TRAMP mice and men with prostate cancer produce autoantibodies to HIP1 more frequently than control individuals. Using both immunoblot and ELISA tests, described herein, we have found that the sensitivity and specificity of this novel prostate cancer blood test is similar to that of PSA, and when combined with AMACR, has the exciting potential to surpass the specificity of the PSA test.

Materials and Methods

Animals. The *Hip1*$^{null/null}$ mice (15) and TRAMP mice (14) were maintained on a C57BL/6;129svJ and C57BL/6 background, respectively. SV40 T antigen "homozygous" TRAMP male mice were intercrossed with *Hip1*$^{null/null}$ females to generate T antigen transgenic (TRAMP) mice that were heterozygous for the *Hip1* mutation (TRAMP/*Hip1*$^{null/+}$). The latter mice were intercrossed to make TRAMP littermates containing either wild type or knockout *Hip1* alleles. Mouse tail DNA was genotyped for the SV40 T antigen by PCR (14) or for the *Hip1* null allele by Southern (15, 17). Euthanized mice were subjected to complete necropsy as well as *Hip1*/SV40 T antigen genotype verification via repeat southern blot of tail tissue and Western blot of tumors for the presence or absence of HIP1 and T antigen proteins. Mouse care followed established institutional guidelines.

Evaluation of transgenic adenocarcinoma of the mouse prostate tissue. Sixteen TRAMP/*Hip1*$^{+/+}$ and eight TRAMP/*Hip1*$^{null/null}$ littermate mice were analyzed for tumor extent at 6.5 months of age. Prostate and

Note: S.V. Bradley and K.I. Oravecz-Wilson contributed equally to this work.
Requests for reprints: Theodora S. Ross, University of Michigan, 6322 CCGC, 1500 East Medical Center Drive, Ann Harbor, MI 48109-0942. Phone: 734-615-5509; E-mail: tsross@umich.edu.

Table 1. Clinical data for prostate cancer patients used in study

Characteristic	Value
Mean age (y) ± SD*	59.0 ± 8.0
Mean gland size (cm) ± SD†	1.6 ± 1.5
Mean gland weight (g) ± SD‡	53.6 ± 51.8
PSA§ (%)	
Mean ± SD (ng/mL)	7.5 ± 5.9
<4 ng/mL	23.3
4-10 ng/mL	55.5
>10 ng/mL	21.1
Biochemical recurrence	10.0
Gleason grade ≤ 6 (%)§	38.9
Gleason grade ≥ 7 (%)§	60.1

*Data were available for 91 patients only.
†Data available for 89 patients.
‡Data available for 97 patients.
§Data available for 90 patients.

tumor samples were fixed in 10% (v/v) buffered formalin, embedded in paraffin, serially sectioned and stained by H&E. The slides of prostatic tissue were evaluated for the presence of hyperplasia, adenoma, or invasive adenocarcinoma as described previously (18).

Acquisition of serum samples from transgenic adenocarcinoma of the mouse prostate mice. TRAMP mice and T antigen–negative control mice were initially bled between the ages of 2 and 4 months from the saphenous vein of the hind leg. Approximately 100 to 200 μL of blood was collected into Microvette CB 300 serum separation tubes (Starstadt, Nümbrecht, Germany) and 30- to 40-μL aliquots were stored at −20°C until analyzed.

Human patient cohort and samples. This study was approved by the University of Michigan Medical School Institutional Review Board. At the time of diagnosis and before prostatectomy, sera from 97 biopsy-proven clinically localized prostate cancer patients were collected and stored in the University of Michigan Prostate Specialized Programs of Research Excellence Tissue/Serum Bank from January 1995 to January 2003. The average age of the participants was 59 (range, 41-83). Table 1 summarizes the clinical data for the 97 prostate cancer patients. As controls, sera from 211 male subjects (average age, 61; range, 29-84; collected at the University of Michigan clinical pathology laboratories from May 2001 to May 2003) with no known history of cancer were used. All sera were stored in aliquots at −20°C.

Preparation of HIP1 antigen. A glutathione *S*-transferase-3′HIP1 (GST-3′HIP1) fusion construct was used to generate 3′HIP1 antigen. Briefly, GST was fused in frame to the COOH-terminal half of HIP1 amino acid sequence starting at the sole internal *Eco*RI site (nucleotide 1250) and ending at the native stop codon (nucleotide 3010; ref. 19). Expression of antigen was induced in bacteria with 0.1 mmol/L isopropyl-L-thio-B-D-galactopyranoside for 4 hours at 37°C, bacteria were sonicated and antigen initially fractionated from other bacterial proteins with glutathione-Sepharose. GST was then cleaved off of the partially pure protein with thrombin. The antigen was separated from free GST on a preparative 8% SDS-PAGE gel, electroeluted, dialyzed, and concentrated to obtain further purity.

Immunoblot analysis of anti-HIP1 antibodies in mouse or human serum. 3′HIP1 protein (10 μg for mouse sera and 20 μg for human sera) was separated on a 10% preparative gel, transferred to nitrocellulose, and blocked overnight at 4°C in TBST (mouse sera) or TBS (human sera) with 5% milk and 5% goat (mouse samples) or donkey (human samples) serum ("blocking solution"). A Miniblotter 28-dual unit system (Immunetics, Inc., Cambridge, MA) was used to make 25 incubation chambers for serum samples, diluted 1:50 in 1:10 blocking solution (human sera) or 1:15 in TBST/5% milk (mouse sera). Membranes were incubated with the serum samples for 2 hours at room temperature and washed with TBST. For blots of TRAMP sera, goat antimouse horseradish peroxidase (HRP)–conjugated secondary antibody (Sigma, St. Louis, MO) was used at 1:5,000 dilution in TBST/5% milk for 1 hour at room temperature. The blots were washed for 1 hour with TBST and HRP developed with enhanced chemiluminescence (ECL). For analysis of human sera, a donkey anti-human biotin conjugated secondary antibody (Jackson ImmunoResearch, West Grove, PA) was used at a 1:50,000 dilution in 1:10 "blocking solution" for 1 hour. After washing with TBST, HRP-conjugated streptavidin was incubated with the blots (1:25,000 dilution in 1:10 blocking solution) for 1 hour, and the blots were subjected to a final wash. Super-Signal ECL (Pierce, Rockford, IL) was used to develop the HRP for the human samples and generic ECL was used for mouse samples (20).

ELISA test for HIP1 autoantibodies. MaxiSorb immunoplates (Nalge Nunc International, Rochester, NY) were coated with 5 μg/mL of the 3′HIP1 antigen by incubating 50 μL per well overnight at 4°C. The plates were washed twice with TBST. Plates were blocked with 200 μL of 5% milk in TBST overnight at 4°C, washed twice with TBST, and stored at 4°C for a maximum of 2 weeks. Serum samples (50 μL per well) diluted 1:100 in blocking solution were assayed in duplicate and incubated with the antigen-coated plates at room temperature for 1 hour. The plates were washed five times with TBST and incubated with 1:10,000 goat anti-human IgG biotin–conjugated (Pierce) secondary antibody for 30 minutes. The plates were again washed five times with TBST and incubated with avidin-biotin complex reagent (Pierce) for 30 minutes and washed; 100 μL of the 1-Step Ultra TMB (Pierce) were incubated on the plates for 30 minutes for color development and quenched with 100 μL of H_2SO_4. Absorbance was measured at 450 to 550 nm using a VERSAmax microplate reader (Molecular Devices, Sunnyvale, CA).

Statistical analysis. All statistical analyses were done with Excel, Medcalc, or SPSS. To test for the difference in tumor incidence and histologic appearances the MedCalc program was used to perform correlative and χ^2 tests. To test for significant differences in HIP1 immune response between prostate cancer patients and control subjects, Pearson's χ^2 test as well as Student's two-sided t test were done using SPSS. ROC curve analysis was achieved using the MedCalc program.

Results

Diminished prostate tumor development in transgenic adenocarcinoma of the mouse prostate/*Hip1*$^{null/null}$ mice. To examine the *in vivo* necessity of HIP1 overexpression in prostate tumors, TRAMP mice (14) and *Hip1*$^{null/null}$ mice (15) were crossed to generate TRAMP mice deficient of HIP1 (TRAMP/*Hip1*$^{null/null}$ mice) as well as control littermates (TRAMP/*Hip1*$^{+/+}$ mice). This experiment was based on the previous observation that murine HIP1 is overexpressed in 50% of prostate tumors that develop in TRAMP mice (12) and that the loss of function mutation of *Hip1* does not alter the development or maintenance of normal prostate tissue nor does it affect hormone levels in mice including testosterone (15, 17). In an initial study of these mice, we noted that TRAMP mice deficient for HIP1 did not develop as many palpable tumors as their wild-type HIP1 expressing littermates (data not shown). To quantitate this observation, we initiated a second experiment where TRAMP littermates without HIP1 expression (TRAMP/*Hip1*$^{null/null}$) and their controls (TRAMP/*Hip1*$^{+/+}$) were sacrificed at 6.5 months of age. We chose to analyze mice at this age, as by 6 months of age, all TRAMP mice develop prostate tumors (18). As seen in Fig. 1*A*, the absence of HIP1 expression resulted in fewer grossly observed prostate tumors than littermate *Hip1* wild-type controls (2 of 8 TRAMP/*Hip1*$^{null/null}$ [25%] versus 13 of 16 TRAMP/*Hip1*$^{+/+}$ [81%], respectively; $P < 0.01$).

The diminished tumor frequency observed in the *Hip1*$^{null/null}$ mice could be due to a reduced rate of tumor initiation. Alternatively, HIP1 may be required for tumor growth or progression to invasive carcinoma. To begin to distinguish between these possibilities, the histologic characteristics of the prostates and their tumors from these mice was scored using a previously described grading system of prostatic lesions (18). Briefly, serial tissue sections were characterized for their most advanced lesions. For example, "hyperplasia" was scored when the epithelial cells of the acini were crowded and formed foci in cribiform or papillary patterns but still followed the outline of the acinus. "Adenoma" was scored when in some parts of the tissue the epithelial cells completely filled the lumen or distinct epithelial masses were found in the lumen of the acinus. "Invasive carcinoma" was scored when there was local invasion into and beyond the capsule of the acinus or there were distant metastases. The TRAMP mice with "adenomas" or "invasive carcinomas" also contained multiple foci of hyperplasia.

Using this scoring system, we found that development of invasive cancers was diminished in TRAMP/*Hip1*$^{null/null}$ mice. At 6.5 months of age, most of the TRAMP mice with normal *Hip1* had adenomas or invasive cancers (8 of 8 observed TRAMP/*Hip1*$^{+/+}$ [100%] versus 1 of 6 [17%] TRAMP/*Hip1*$^{null/null}$; Fig. 1*B*). In contrast, most of the TRAMP/*Hip1*$^{null/null}$ mice had only hyperplastic lesions (five of six, 84%). The differences in tumor incidence either by gross observation or by histology between control and TRAMP/*Hip1*$^{null/null}$ mice was significant ($P < 0.01$ and $P < 0.025$, Pearson's χ^2, respectively). These data suggest that there is a delay in the ability of prostatic lesions from *Hip1*$^{null/null}$ mice to progress from hyperplasia to adenomas and invasive carcinomas. Previously, we reported that 50% of TRAMP prostate tumors overexpressed HIP1 by Western blot analysis of tumors (12). In contrast, we find here that at least 75% of the TRAMP prostates required HIP1 expression for invasive tumor formation (Fig. 1*A*, *first column*). This suggests that the sensitivity to detect HIP1 overexpression by Western blot analysis of prostate tumors may be limited.

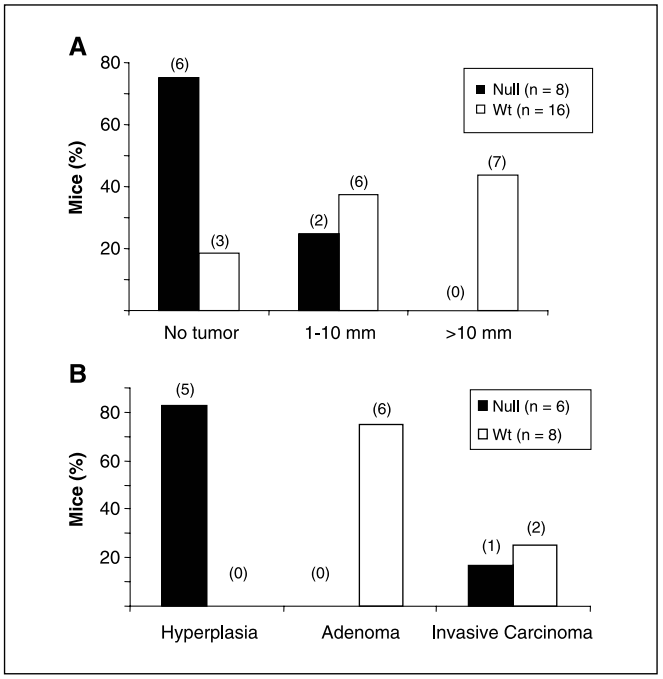

Figure 1. HIP1 deficiency impairs tumorigenesis in the TRAMP model of prostate cancer. *A,* grossly evident tumors were scored during necropsy of TRAMP/*Hip1*$^{+/+}$ ($n = 16$) and TRAMP/*Hip1*$^{null/null}$ ($n = 8$) littermate mice. Observations were recorded as either no obvious tumor, gross tumor of ~1 to 10 mm in diameter or large tumor measuring >10 mm. Most TRAMP/*Hip1*$^{null/null}$ mice had grossly normal prostates (6 of 8) compared to the TRAMP/*Hip1*$^{+/+}$ mice (3 of 16, 75% versus 18.8%, respectively). There were no tumors >10 mm in the absence of HIP1 compared with 7 of 16 in the presence of HIP1. Numbers of mice in each observation are bracketed above the columns. *B,* histologic analysis of prostate tissue from a second cohort of TRAMP mice at 6.5 months of age. Six prostate samples were derived from *Hip1* null prostates and eight prostates samples were derived from *Hip1* wild-type littermates. Serial sections of the prostates were prepared for H&E staining. These slides were scored for the presence of hyperplasia, adenoma, or invasive carcinoma within the prostate (18). Eighty-three percent (five of six) of the *Hip1*$^{null/null}$ mice had only hyperplasia in the prostate tissue. All of the TRAMP/*Hip1*$^{+/+}$ mice were found to have multiple foci of either adenoma (75%) or invasive carcinoma (25%), as expected.

Autoantibodies to HIP1 in transgenic adenocarcinoma of the mouse prostate mice. Because HIP1 was overexpressed in prostate tumors of both humans and mice (12), we attempted to measure HIP1 levels in mouse serum by Western blot analysis using anti-HIP1 polyclonal (UM323) and monoclonal (1B11) antibodies. Our goal was to determine if HIP1 antigen quantitation could be used as a novel serum biomarker of prostate cancer. As one might expect for a cytoplasmic protein, we were not able to detect the HIP1 antigen in sera (data not shown). Because of this limited sensitivity, we decided to test the hypothesis that a humoral immune response to overexpressed HIP1 marks prostate cancer presence. If such a response was detected, we hypothesized that it could be used as a potential blood test for prostate cancer detection and prognosis.

To begin to test this, recombinant HIP1 (19) was purified (Fig. 2*A*, *left*) and immunoblot with specific HIP1 monoclonal antibodies, 4B10 and 1B11, confirmed its identity (Fig. 2*A*, *right*). The lower of the two bands on the Western blot was variably seen in different preparations of the purified antigen and was likely the result of degradation during antigen preparation. In an initial pilot Western blot study of mouse sera and 3′ HIP1 antigen, we found that there was immune reactivity to the HIP1 antigen in sera from prostate tumor-bearing TRAMP/*Hip1*$^{+/+}$ mice but not control (T antigen negative) or TRAMP/*Hip1*$^{null/null}$ mice (data not shown). Serial serum samples from TRAMP mice and control mice were loaded in a miniblot apparatus (8) to determine the developmental time course and maintenance of autoantibodies to HIP1 in TRAMP mice (Fig. 2*B*). Remarkably, we found that there was an antibody response to HIP1 that varied in its time of onset (Fig. 2*B*) but was detected as early as 4 months of age in the TRAMP mice, all of which were expected to have developed prostatic lesions by 6.5 months of age. Twelve of the 22 (55%) TRAMP mice developed sustained immunity. In contrast, none of the 14 (0%) control (T antigen negative) littermates showed sustained presence of autoantibodies to HIP1.

Serum antibodies to HIP1 in human prostate cancer patients. In light of the presence of autoantibodies to HIP1 in prostate cancer-bearing TRAMP mice, we tested if there was an immune response to HIP1 in sera from human prostate cancer patients. Because one gel was only able to assay 25 distinct sera at a time and we had sera from 308 men available for testing, we used the same positive and negative HIP1 reactive sera on each blot as a reference point. This allowed us to quantitate and normalize signals between different blots. Results of one such screen using sera from prostate cancer patients and controls ($n = 23$ for each) are shown in Fig. 3*A*. Ultimately, the sera from

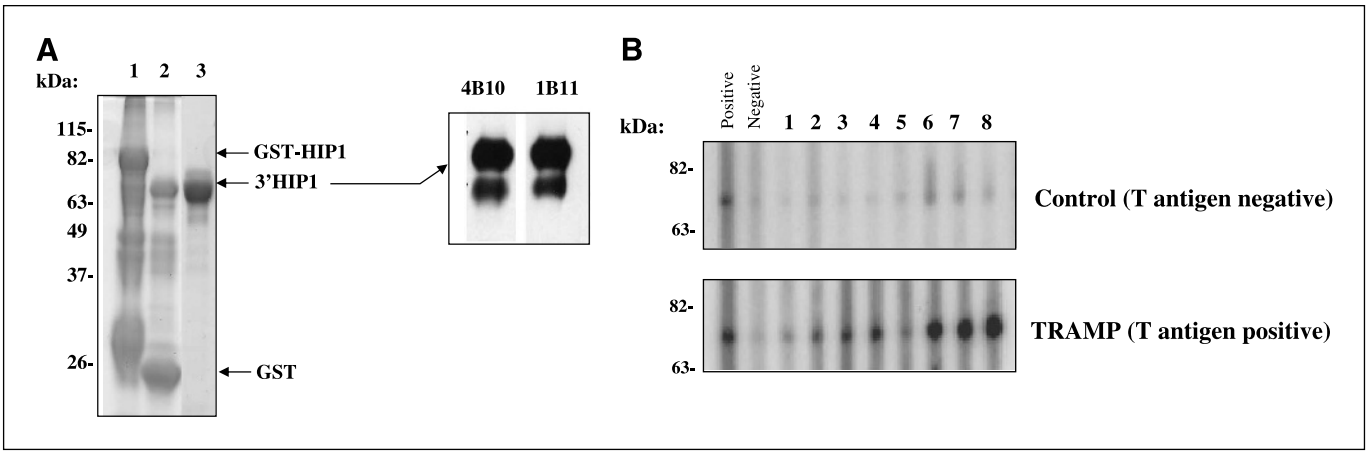

Figure 2. Humoral immune response to HIP1 in TRAMP mice. *A,* purification of recombinant 3′ HIP1 protein was achieved in three steps as described in the methods. *Lane 1,* contains 40 μg of protein from an IPTG-induced bacterial extract bound to and eluted with glutathione from glutathione Sepharose. *Lane 2,* partially purified thrombin-treated extract. Released GST (*bottom arrow*) and the HIP1 portion of the recombinant protein (*top arrow*) were visualized with Coomassie blue stain. *Lane 3,* 5 μg of the final "purified" recombinant 3′ HIP1 protein that was used for assays of a humoral response. This purified recombinant HIP1 was recognized by two different previously described (12) anti-HIP1 monoclonal antibodies (HIP1/4B10 and HIP1/1B11) as shown in the Western blot of 200 ng of antigen (*right*). *B,* antibodies to HIP1 in TRAMP mice. A group of 22 TRAMP and 14 T antigen negative control mice between the ages of 2 to 4 months, had blood samples drawn every 2 weeks and sera prepared to test for when and if a humoral response to HIP1 might develop. This representative blot shows a control, T antigen–negative mouse (*top*), and a TRAMP mouse (*bottom*). *Positive* and *Negative lanes,* reference positive (TRAMP/$Hip1^{+/+}$ mouse sera found to be positive in the original screen) and negative ($Hip1^{-/-}$ mouse sera) controls allowing for comparisons of HIP1 reactivity between immunoblots, respectively. Over 16 weeks beginning at age 2.5 months (*lanes 1-8*) serial serum analysis demonstrated that by 3 months of age a sustained immune response to HIP1 in the TRAMP mice occurred and increased significantly by 5 months of age. It should be noted that sera from T antigen–negative control mice would at times test positive but did not display sustained positive tests.

97 prostate cancer and 211 age-matched male control sera were screened by Western blot. The blots were analyzed by measuring the grayscale values of the reactive bands (Fig. 3*A*, *arrows*) and quantitated as a percent of the reference positive control (Fig. 3*B*). A positive score was assigned to bands with a value of ≥50% of the positive control, whereas those bands <50% of the positive control received a negative score. This cutoff was chosen because it yielded the highest values for specificity and sensitivity, as analyzed from ROC curves created from a randomly chosen subset of the prostate cancer and control subjects. All serum samples were validated for autoantibodies to HIP1 by this high-throughput immunoblot analysis. HIP1 antibodies were significantly more frequent in serum from prostate cancer patients compared with age-matched controls ($P < 0.001$ χ^2, likelihood ratio). Forty-five of 97 (46%) prostate cancer patient sera received a positive score compared with 58 of 211 (27%) of the age-matched control sera (Fig. 3*C*).

For confirmation of our Western blot results and the development of an additional clinical assay, an ELISA to monitor HIP1 immune response was developed. ELISA plates were coated with purified recombinant 3′ HIP1, and sera from patients with prostate cancer or age-matched controls were assayed. The measured absorbance was converted to values relative to negative reference controls and duplicate samples in each of two experiments ($n = 4$ replicates) were averaged. Figure 4*A* shows the average relative absorbencies for all of the prostate cancer patient sera and 81 of the control sera. A relative absorbance that was greater than the negative control (ELISA value, >1) was considered a positive score. The cutoff for this test was, like the high-throughput Western blot test, determined by using ROC curves on a subset of the patient sera and determining where the ELISA values yielded the highest specificity and sensitivity. All available serum samples were then tested for HIP1 antibodies by high-throughput ELISA. There were significantly more prostate cancer sera with positive scores (46% of sera from prostate cancer patients versus 27% of sera from age-matched controls; Fig. 4*B*). The ELISA test alone results in similar values for specificity and sensitivity as the Western blot analysis (Table 2). If both tests are required to be reactive for a positive test, only 24% of the prostate cancers are positive versus 12% of the controls. Although there is diminished sensitivity using the increased stringency (both tests necessarily reactive), it does raise the specificity to 88%. The observed decreased sensitivity with the combination of Western blot and ELISA tests is expected because the chance that both tests, which have distinct antigen presentations on either nitrocellulose membranes or plastic plates, would have accessible antigenic epitopes simultaneously in each patient is less likely than if only one were necessary. Hence, if only one of the two HIP1 reactivity tests is required for positivity, 69% of the prostate cancers are positive versus 44% of the controls (Table 2). It should be noted at this point that the control group did not undergo prostate biopsies or have close follow-up. Because of this limitation, the possibility of missed prostate cancer in the control group must be considered when evaluating this initial data. In addition, some of the "background" could be contributed by other occult malignancies such as melanoma, colon, or lung cancers.

Previously, we have found that using immunohistochemical analysis of HIP1 antigen in tissue sections, overexpression of HIP1 in prostate cancers predicted a poor outcome (12). It follows that the autoantibodies to HIP1 in prostate cancer patients might also contain prognostic information. In the current group of 97 prostate cancer patients, there were no statistically significant associations between HIP1 immune responses and linked clinical variables including initial PSA level, PSA recurrence, Gleason grade, tumor size, or stage.

In addition to assessing the relationship between linked clinical data and HIP1 autoantibody formation, we compared the HIP1 test

to other serum tests such as the PSA and AMACR tests. In the initial study of the AMACR humoral response, a specificity of 71.8% and sensitivity of 61.6% were found (8). The samples used for this current study of HIP1 humoral response were also tested for their humoral immune response to AMACR and similar values for AMACR specificity and sensitivity were found as previously reported (67% and 64%, respectively; Table 2). The ROC curves for HIP1 and AMACR yielded similar values for area under the curve (data not shown).

As well as comparison with the AMACR test, it follows that the HIP1 antibody test could complement the PSA test. However, the comparison of the HIP1 test to the PSA test in the group of patients (n = 90) and controls (n = 117) for which PSA data was available was problematic. This was due to the availability of only a limited supply of banked serum samples from control patients with PSA values of >4.0 ng/mL. This resulted in an expected but skewed specificity and sensitivity (75% and 77%, respectively) for the PSA test (positive, >4.0 ng/mL). The reported 45% specificity and 50% sensitivity for PSA in a previous group of sera that were tested for AMACR are closer to expected (8). Because of this limited supply, a subgroup of 68 prostate cancer sera and 29 age-matched control sera that had PSA values of >4 ng/mL was analyzed separately for HIP1 autoimmunity (Table 3). There was again a significant difference in the numbers of HIP1-positive samples from prostate cancer patients versus control individuals, as determined by ELISA or Western blot ($P \leq 0.025$ and $P \leq 0.01$, respectively). The most significant difference was seen when a positive score by either ELISA or Western blot was required, giving a specificity of 64% and a sensitivity of 88% ($P \leq 0.001$) in a group that would all be considered positive by the PSA test. In addition, a combination of AMACR and HIP1 tests increased specificity *dramatically* (97%) suggesting that the combination of these two tests could lead to better predictions of cancer if added to the PSA test. Although further analysis of additional patient and control populations with prospective follow-up, serial sampling (as shown for the TRAMP mice in Fig. 2*B*) and from multiple different institutions is essential, these results suggest that the combination of the HIP1 test with PSA and AMACR tests results has the potential to yield a highly specific diagnostic test for prostate cancer.

Discussion

Prostate cancer morbidity and mortality are due to its progression within the prostate as well as its metastatic spread beyond the prostate. Because of this, an understanding of the mechanism by which localized hyperplastic lesions progress to invasive and metastatic carcinomas is very important. In addition, obtaining blood tests that can provide for the earliest detection of prostate cancer will have important prognostic and therapeutic implications.

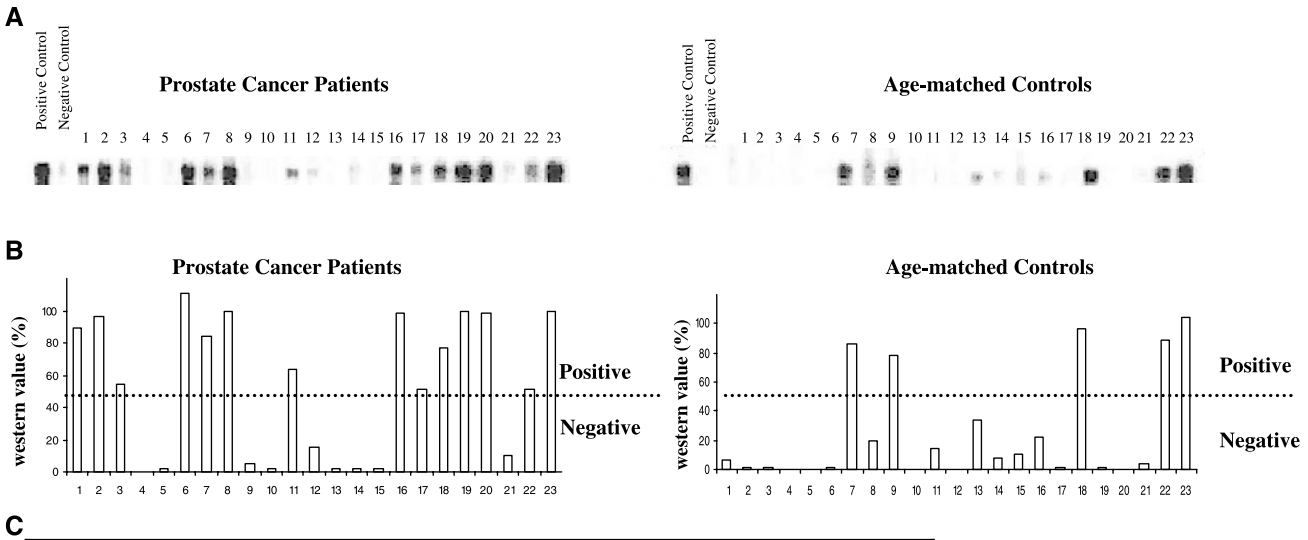

C

Scores	Prostate cancer patients (N=97)	Controls (N=211)
Positive	45*	58
Negative	52	153

* The frequency of a positive test in prostate cancer patients was statistically different than in control patients ($p \leq 0.001$, Specificity (73%), Sensitivity (46%))

Figure 3. Prostate cancer patients have a specific humoral response to HIP1 overexpression. *A,* representative immunoblot of 46 sera assayed for reactivity to recombinant HIP1. Twenty-three of the 97 biopsy-proven prostate cancer patients and 23 of the 211 control individuals. Equal aliquots of all of the 308 serum samples were analyzed by immunoblot in at least two independent experiments and contained reference positive and negative controls (*Positive* and *Negative lanes*, respectively). *B,* bands were scanned from the developed blots and converted to grayscale values using Adobe Photoshop. Normalized grayscale values were converted to percentage of the positive control (*Positive lane*). Samples with band intensity of ≥50% of the positive control were given a positive score (*above the dotted line*). A negative score was given to samples <50% of positive control (*below the dotted line*). *C,* distribution of the values between prostate cancer and the control individuals was significantly different ($P < 0.001$, Pearson's χ^2 test). Specificity of the test was 73% and calculated as those control samples with a negative test (153/153 + 58) and sensitivity was 46% and calculated as the percent of patient samples with a positive test (45/45 + 52).

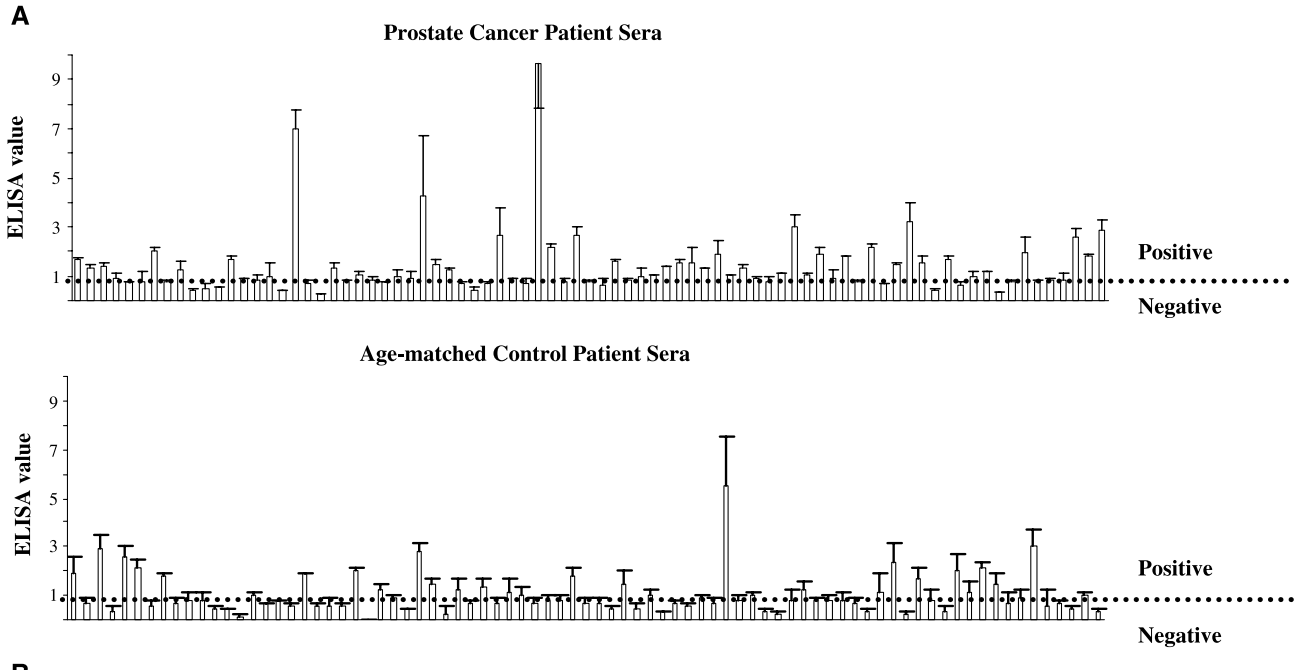

B

Scores	Prostate Cancer patients (N=81)	Controls (N=186)
Positive	37*	51
Negative	44	135

* The frequency of a positive test in prostate cancer patients was statistically different than in control patients ($p \leq 0.01$, Specificity (73%), Sensitivity (46%))

Figure 4. Detection of HIP1 humoral response in human prostate cancer patients by ELISA. *A,* average (four replicates) relative absorbances (ELISA values) and their standard deviations are shown for 81 prostate cancer patient and 186 control sera. A relative absorbance of >1.0 (*above the dotted line*) was considered positive. *B,* numbers of positive prostate cancer and age-matched control sera. The specificity of this test was 73% and the sensitivity was 46%. The difference between prostate cancer patients and controls was significant ($P < 0.01$, Pearson's χ^2).

Here we report *in vivo* genetic evidence for the necessity of the clathrin-binding protein, HIP1, in the prostatic hyperplasia-to-carcinoma transition. These experiments were initiated based on the fact that HIP1 expression is frequently elevated in human prostate cancer, and this overexpression predicts the progression of the disease in humans. In addition, because TRAMP mice have HIP1 up-regulated in their tumors (12), it was considered a relevant tumor model. We show that although all *Hip1*$^{null/null}$ mice developed prostatic hyperplastic lesions in response to expression of T antigen, the development of bona fide tumors was significantly diminished compared with TRAMP mice with normal levels of HIP1.

Although the absence of HIP1 leads to testicular degeneration, it should be noted that the prostate glands from *Hip1* knockout mice are normal histologically and serum testosterone levels are within normal limits (15, 17). This makes it unlikely that the effect of HIP1 deficiency on tumor development in this model is merely secondary to differences in the levels of testosterone or abnormalities in adult prostate epithelial cell maintenance. It should also be noted that the use of SV40 T antigen to induce prostate cancer is, in many ways, artificial in that T antigen does not seem to have a role in human prostate cancer. However, because HIP1 is overexpressed in TRAMP tumors, as it is in human tumors, and because T antigen does inhibit the human tumor suppressor gene products p53 and Rb, this model has significant validity for the purposes of initial studies of HIP1's *in vivo* role in cancer biology.

It will be important to better understand the mechanism of how HIP1 could participate in the development of prostate cancer in humans. Previous work has shown that the HIP1 family of proteins is involved in the modulation of a variety of receptors such as the glutamate receptor (21), the epidermal growth factor receptor (EGFR), platelet-derived growth factor β receptor (PDGFβR; ref. 22), and transferrin receptor (23). This modulation of receptors leads to an increased survival and transformation of cells when HIP1 is overexpressed (12, 13). Although a direct regulatory effect of HIP1 on clathrin trafficking in prostate cancer remains to be shown, HIP1 could modulate signals from the EGFR and PDGFβR in prostate cancer as these receptors are clearly regulated by the clathrin trafficking network and are altered in prostate cancer. Determination if HIP1 can modulate other types of receptors that are not regulated by clathrin-mediated endocytosis but are involved in prostate cancer, such as the steroid hormone receptors (e.g., androgen receptor), will be important future experiments.

In addition to testing for HIP1 necessity in prostatic carcinogenesis, the previous observation of HIP1 overexpression in tumors

of TRAMP mice (12) prompted us to test if HIP1 could be detected in the serum of these mice. As expected for a cytoplasmic protein, we found that the circulating HIP1 antigen levels are low and therefore difficult to detect. However, we did find that TRAMP mice developed early and sustained levels of antibodies against HIP1 when measuring longitudinal samples. Interestingly, the T antigen–negative control mice also had samples of sera that tested positive randomly. However, sustained presence of anti-HIP1 antibodies were never observed in the control mice.

This led us to test if a humoral response to HIP1 could occur in humans with prostate cancer. The goal would be to find a novel blood test to substitute for or to complement the PSA test. Indeed, the test we describe herein for autoantibodies to HIP1 in prostate cancer has a relatively high specificity and improves the specificity of the PSA and AMACR tests, making it an attractive serum marker. Because we were able to show a sustained humoral response in TRAMP mice, we predict that future studies that are designed for prospective serial testing of humans for HIP1 antibodies will show an increase in the anti-HIP1 test's sensitivity and specificity. Because prostate cancer is such a common cancer, markers with a greater specificity rather than sensitivity are needed to reduce unnecessary prostate biopsies or other invasive tests. For example, misdiagnosis with the PSA test may account for >30% of positive tests in a screened male population over the age of 55 (24), making reliance on the PSA test alone problematic. Finally, it is unlikely that any single marker for prostate cancer will have the desired high specificity and sensitivity, making it important to develop a collection of markers, which in combination could lead to accurate prostate cancer detection and prognosis.

Table 2. Comparison of diagnostic tests and their combinations for all prostate cancer and control samples

Test	Specificity (%)	Sensitivity (%)
HIP1 ELISA positive*	73	46
HIP1 western positive†	73	46
HIP1 ELISA + HIP1 Western positive‡	88	24
HIP1 ELISA or HIP1 Western positive†	56	69
AMACR positive†	67	64
AMACR positive + HIP1 ELISA or HIP1 Western positive†	86	50
PSA positive (≥4 ng/mL)†	75	77
PSA positive + HIP1 ELISA or HIP1 Western positive†	91	66

NOTE: There were a total of 97 prostate cancer and 211 control sera. Not all of these 308 sera, except for the HIP1 Western, were assayed for every test listed. HIP1 ELISA values were available from 81 of the prostate cancer patients and 186 controls. AMACR Western values were available for 77 prostate cancer patients and 126 controls. PSA values were available for 90 prostate cancer patients and 117 controls. The increased frequency of a positive test in prostate cancer patients compared with controls was statistically different in all cases.
*$P \leq 0.01$.
†$P \leq 0.001$.
‡$P \leq 0.025$.

Table 3. Comparison of diagnostic tests and their combinations for all prostate cancer and control samples with PSA values of ≥4 ng/mL

Test	Specificity (%)	Sensitivity (%)
HIP1 ELISA positive*	76	49
HIP1 Western positive†	82	54
HIP1 ELISA + HIP1 Western positive*	93	28
HIP1 ELISA or HIP1 Western positive‡	64	88
AMACR positive‡	83	64
AMACR positive + HIP1 ELISA or HIP1 Western positive‡	97	55

NOTE: There were 68 prostate cancer and 29 control sera that met the criterion of PSA of >4 ng/mL. Nine of the 68 prostate cancer patient sera were not available to test for HIP1 ELISA and AMACR Western. The increased frequency of a positive test in prostate cancer patients compared to controls was statistically different in all cases.
*$P \leq 0.025$.
†$P \leq 0.01$.
‡$P \leq 0.001$.

The increase in frequency of antibodies to HIP1 in prostate cancer compared with age-matched controls, together with the fact that we had previously found that HIP1 is overexpressed in many different epithelial cancers (12), will prompt us to investigate the potential for a specific humoral response in other cancers. This could also be a source of error in reducing the specificity of the HIP1 blood test for prostate cancer in our current control group, as the men could have had other occult or nonoccult malignancies. In fact, a specific humoral response to the HIP1-related protein, the only known mammalian relative of HIP1, has been reported to occur in colon cancer (25).

In conclusion, we have explored the role of HIP1 in *in vivo* tumorigenesis using the prostate cancer prone TRAMP mice and *Hip1* knockout mice. Our data indicate that HIP1 may be necessary for tumorigenesis and that both mice and men with prostate cancer have autoantibodies to HIP1 in their serum. These data provide groundwork for further investigation into the functional involvement of HIP1 in other cancers and as a specific marker (especially in combination with AMACR) for other cancers. These data also pave the way for further prospective, longitudinal, and multi-institutional studies of how to best use the HIP1 Western blot and ELISA tests for improved care of patients with prostate cancer.

Acknowledgments

Received 1/3/2005; revised 2/11/2005; accepted 2/18/2005.

Grant support: Komen Foundation predoctoral fellowship (S.V. Bradley), La Ligue Nationale contre le Cancer postdoctoral fellowship (G. Bougeard), NIH-R01 CA82363-01A1 (T.S. Ross), NIH-RO1 CA098730-02 (T.S. Ross), and NIH-R01 CA82419-01 (M.G. Sanda).

The costs of publication of this article were defrayed in part by the payment of page charges. This article must therefore be hereby marked *advertisement* in accordance with 18 U.S.C. Section 1734 solely to indicate this fact.

We thank Teresa Hyun, Sean Morrison, Anj Dlugosz, Peter Lucas, Grant Rowe, and Mark Day for critically reading this article and Dan Normolle, Jason Harwood, Paul Nolan, June Escara-Wilke, Jenny Loveridge, and Melissa Rogers for their assistance during the course of this study.

References

1. Catalona WJ, Smith DS, Ratliff TL, et al. Measurement of prostate-specific antigen in serum as a screening test for prostate cancer. N Engl J Med 1991;324:1156–61.
2. Etzioni R, Legler JM, Feuer EJ, Merrill RM, Cronin KA, Hankey BF. Cancer surveillance series: interpreting trends in prostate cancer. Part III. Quantifying the link between population prostate-specific antigen testing and recent declines in prostate cancer mortality. J Natl Cancer Inst 1999;91:1033–9.
3. Maattanen L, Auvinen A, Stenman UH, et al. European randomized study of prostate cancer screening: first-year results of the Finnish trial. Br J Cancer 1999;79: 1210–4.
4. Schroder FH, van der Maas P, Beemsterboer P, et al. Evaluation of the digital rectal examination as a screening test for prostate cancer. Rotterdam section of the European Randomized Study of Screening for Prostate Cancer. J Natl Cancer Inst 1998;90:1817–23.
5. Thompson IM, Pauler DK, Goodman PJ, et al. Prevalence of prostate cancer among men with a prostate-specific antigen level < or = 4.0 ng per milliliter. N Engl J Med 2004;350:2239–46.
6. Punglia RS, D'Amico AV, Catalona WJ, Roehl KA, Kuntz KM. Effect of verification bias on screening for prostate cancer by measurement of prostate-specific antigen. N Engl J Med 2003;349:335–42.
7. Catalona WJ. Management of cancer of the prostate. N Engl J Med 1994;331:996–1004.
8. Sreekumar A, Laxman B, Rhodes DR, et al. Humoral immune response to α-methylacyl-CoA racemase and prostate cancer. J Natl Cancer Inst 2004;96:834–43.
9. McNeel DG, Nguyen LD, Storer BE, Vessella R, Lange PH, Disis ML. Antibody immunity to prostate cancer associated antigens can be detected in the serum of patients with prostate cancer. J Urol 2000; 164:1825–9.
10. Mintz PJ, Kim J, Do KA, et al. Fingerprinting the circulating repertoire of antibodies from cancer patients. Nat Biotechnol 2003;21:57–63.
11. Nilsson BO, Carlsson L, Larsson A, Ronquist G. Autoantibodies to prostasomes as new markers for prostate cancer. Ups J Med Sci 2001;106:43–9.
12. Rao DS, Hyun TS, Kumar PD, et al. Huntingtin-interacting protein 1 is overexpressed in prostate and colon cancer and is critical for cellular survival. J Clin Invest 2002;110:351–60.
13. Rao DS, Bradley SV, Kumar PD, et al. Altered receptor trafficking in Huntingtin interacting protein 1-transformed cells. Cancer Cell 2003;3:471–82.
14. Greenberg NM, DeMayo F, Finegold MJ, et al. Prostate cancer in a transgenic mouse. Proc Natl Acad Sci U S A 1995;92:3439–43.
15. Oravecz-Wilson KI, Kiel MJ, Li L, et al. Huntingtin Interacting Protein 1 mutations lead to abnormal hematopoiesis, spinal defects and cataracts. Hum Mol Genet 2004;13:851–67.
16. Shappell SB, Thomas GV, Roberts RL, et al. Prostate pathology of genetically engineered mice: definitions and classification. The consensus report from the Bar Harbor meeting of the Mouse Models of Human Cancer Consortium Prostate Pathology Committee. Cancer Res 2004;64:2270–305.
17. Rao DS, Chang JC, Kumar PD, et al. Huntingtin interacting protein 1 is a clathrin coat binding protein required for differentiation of late spermatogenic progenitors. Mol Cell Biol 2001;21:7796–806.
18. Suttie A, Nyska A, Haseman JK, Moser GJ, Hackett TR, Goldsworthy TL. A grading scheme for the assessment of proliferative lesions of the mouse prostate in the TRAMP model. Toxicol Pathol 2003;31:31–8.
19. Saint-Dic D, Chang SC, Taylor GS, Provot MM, Ross TS. Regulation of the Src homology 2-containing inositol 5-phosphatase SHIP1 in HIP1/PDGFβ R-transformed cells. J Biol Chem 2001;276: 21192–8.
20. Kricka LJ. Chemiluminescent and bioluminescent techniques. Clin Chem 1991;37:1472–81.
21. Metzler M, Li B, Gan L, et al. Disruption of the endocytic protein HIP1 results in neurological deficits and decreased AMPA receptor trafficking. Embo J 2003;22:3254–66.
22. Hyun TS, Rao DS, Saint-Dic D, et al. HIP1 and HIP1r stabilize receptor tyrosine kinases and bind 3-phosphoinositides via epsin N-terminal homology domains. J Biol Chem 2004;279:14294–306.
23. Engqvist-Goldstein AE, Drubin DG. Actin assembly and endocytosis: from yeast to mammals. Annu Rev Cell Dev Biol 2003;19:287–332.
24. Draisma G, Boer R, Otto SJ, et al. Lead times and overdetection due to prostate-specific antigen screening: estimates from the European Randomized Study of Screening for Prostate Cancer. J Natl Cancer Inst 2003;95:868–78.
25. Scanlan MJ, Welt S, Gordon CM, et al. Cancer-related serological recognition of human colon cancer: identification of potential diagnostic and immunotherapeutic targets. Cancer Res 2002;62:4041–7.

THE JOURNAL OF BIOLOGICAL CHEMISTRY
Vol. 279, No. 14, Issue of April 2, pp. 14294–14306, 2004
Printed in U.S.A.

HIP1 and HIP1r Stabilize Receptor Tyrosine Kinases and Bind 3-Phosphoinositides via Epsin N-terminal Homology Domains*[S]

Received for publication, November 19, 2003, and in revised form, December 31, 2003
Published, JBC Papers in Press, January 19, 2004, DOI 10.1074/jbc.M312645200

Teresa S. Hyun‡§, Dinesh S. Rao‡, Djenann Saint-Dic‡, L. Evan Michael§¶, Priti D. Kumar‡, Sarah V. Bradley‡§, Ikuko F. Mizukami‡, Katherine I. Oravecz-Wilson‡, and Theodora S. Ross‡§‖

From the ‡Department of Internal Medicine, Division of Hematology/Oncology, §Graduate Program in Cellular and Molecular Biology, and the ¶Department of Dermatology, University of Michigan Medical School, Ann Arbor, Michigan 48109

Huntingtin-interacting protein 1-related (HIP1r) is the only known mammalian relative of huntingtin-interacting protein 1 (HIP1), a protein that transforms fibroblasts via undefined mechanisms. Here we demonstrate that both HIP1r and HIP1 bind inositol lipids via their epsin N-terminal homology (ENTH) domains. In contrast to other ENTH domain-containing proteins, lipid binding is preferential to the 3-phosphate-containing inositol lipids, phosphatidylinositol 3,4-bisphosphate and phosphatidylinositol 3,5-bisphosphate. Furthermore, the HIP1r ENTH domain, like that of HIP1, is necessary for lipid binding, and expression of an ENTH domain-deletion mutant, HIP1r/ΔE, induces apoptosis. Consistent with the ability of HIP1r and HIP1 to affect cell survival, full-length HIP1 and HIP1r stabilize pools of growth factor receptors by prolonging their half-life following ligand-induced endocytosis. Although HIP1r and HIP1 display only a partially overlapping pattern of protein interactions, these data suggest that both proteins share a functional homology by binding 3-phosphorylated inositol lipids and stabilizing receptor tyrosine kinases in a fashion that may contribute to their ability to alter cell growth and survival.

Huntingtin-interacting protein 1-related (HIP1r)[1] is a clathrin-binding protein that is the only known mammalian relative of huntingtin-interacting protein 1 (HIP1) (1), a protein that transforms fibroblasts via undefined mechanisms (2). HIP1 is also part of a t(5;7) chromosomal translocation that results in expression of an oncogenic HIP1/PDGFβR fusion protein that causes myelomonocytic leukemia (3). Furthermore, HIP1 is overexpressed in multiple primary epithelial tumors, and overexpression in prostate tumors predicts progression of prostate cancer (4). The transformation of fibroblasts by HIP1 is associated with altered levels of growth factor receptors (2).

The mechanism by which HIP1 overexpression alters growth factor receptor levels may be a result of its role in trafficking of growth factor receptors. HIP1 and HIP1r each contain a clathrin light chain-binding coiled-coil region (5), a leucine zipper, and a C-terminal TALIN homology domain. TALIN is a protein that binds actin and is involved in cell-substratum interactions (6). In addition, HIP1 and HIP1r contain epsin N-terminal homology (ENTH) domains. This domain in epsin and AP180 predominantly binds to phosphatidylinositol 4,5-bisphosphate ($PtdIns(4,5)P_2$) and is important in regulating clathrin-mediated endocytosis (7, 8). HIP1 and HIP1r both have a punctate immunolocalization and co-localize partially with clathrin, AP-2, and endocytosed transferrin (9–13).

Thus, structural and functional data suggest that HIP1 and HIP1r are involved in vesicle trafficking either at the plasma membrane, during sorting of vesicles, or at the *trans*-Golgi network. Unlike HIP1, HIP1r has lower affinity for clathrin, does not bind α-adaptin (5), does not bind huntingtin directly, and does bind actin via its TALIN homology domain (9). HIP1 homologues have been found in yeast (14) and *Caenorhabditis elegans* (15). Sla2p, the yeast homologue of HIP1 and HIP1r, is required for endocytosis, polarization of the cortical actin cytoskeleton, and growth (14).

We are interested in gaining a better understanding of what activities HIP1 and HIP1r might perform to affect tumorigenesis. Although the weight of evidence suggests that HIP proteins function in endocytosis, it is unclear how HIP1 and HIP1r might use clathrin-mediated trafficking to alter survival or growth of cells. One hypothesis suggested by our studies of HIP1 and transformation is that altered HIP1 expression may be a way to regulate growth factor receptor density and signaling and, as a result, affect cellular growth, death, and differentiation of cells (2). Along this line, one mechanism by which transformed cells escape the requirement for growth factors is to increase the activation of receptor tyrosine kinase signaling pathways (16, 17). Cells may compensate for decreased amounts of growth factors in the environment by elevating growth factor receptor levels. Another hypothesis derived from previous work studying ENTH domains (7, 8) is that the ENTH domains of HIP1 and HIP1r may be involved in regulating their roles in growth factor receptor endocytosis and thereby could be critical in their ability to promote cell growth or survival.

To test if there is a link between HIP expression, growth factor receptor signaling, and the role of the ENTH domains, we describe the generation of HIP1r constructs analogous to those generated previously for HIP1 (4). These mutants lack each of the HIP1/HIP1r shared domains, and their effects on

* This work was supported by University of Michigan Cancer Biology training grant (to T. S. H.), National Institutes of Health Grants RO1 CA82363-01A1 and RO1 CA 098730-02, and a Damon Runyon foundation grant (to T. S. R.). The costs of publication of this article were defrayed in part by the payment of page charges. This article must therefore be hereby marked "*advertisement*" in accordance with 18 U.S.C. Section 1734 solely to indicate this fact.

[S] The on-line version of this article (available at http://www.jbc.org) contains Figs. 1–4.

‖ To whom correspondence should be addressed. Tel.: 734-615-5509; E-mail: tsross@umich.edu.

[1] The abbreviations used are: HIP1r, huntingtin-interacting protein-1 related; HIP1, huntingtin-interacting protein-1; PDGFβR, platelet-derived growth factor-β receptor; ENTH, epsin N-terminal homology; PtdIns, phosphatidylinositol; EGF, epidermal growth factor; EGFR, EGF receptor; GFP, green fluorescent protein; GST, glutathione *S*-transferase; HA, hemagglutinin; FITC, fluorescein isothiocyanate; DAPI, 4,6-diamidino-2-phenylindole; PIP, phosphatidylinositol phosphate; IRES, internal ribosome entry site.

cell survival and growth factor receptor signaling were tested. Full-length HIP1r had no transient effects on cell survival, but expression of a mutant lacking the ENTH domain, HIP1r/ΔE, led to apoptosis when transfected into cells. In addition, the lipid binding characteristics mediated by the ENTH domains of both HIP1 and HIP1r were analyzed. To our surprise we found that, in contrast to other ENTH domain-containing proteins which bind PtdIns(4,5)P_2, HIP1 and HIP1r bound preferentially to 3-phosphoinositides. We also found that overexpression of HIP1 and HIP1r inhibited the degradation of ligand-stimulated growth factor receptors. Consistent with the results obtained using stable HIP1-transformed fibroblasts (2), transient transfection of either HIP1 or HIP1r into 293T cells stabilized pools of either EGFR or PDGFβR following ligand-induced endocytosis. In contrast, transfection of the HIP1 and HIP1r mutants lacking the ENTH domains did not stabilize growth factor receptors. By using a dynamin dominant negative mutant, rate-limiting activities of HIP1 and HIP1r were placed downstream of dynamin.

In light of these data, we propose that both HIP1r and HIP1 may stabilize growth factor receptor levels via altered intracellular trafficking. The finding that HIP proteins can function downstream of dynamin together with the fact that the inositol lipids that bind the HIP ENTH domains are concentrated on intracellular vesicular membranes suggest that the HIP proteins modulate the intracellular trafficking of receptors. This is in addition to a role described previously in clathrin vesicle formation at the plasma membrane. Our data suggest that the HIP proteins are either not rate-limiting in the kinetics of the internalization phase of endocytosis or under certain cellular conditions do not participate in the receptor uptake phase of the clathrin trafficking pathway.

MATERIALS AND METHODS

HIP1r Constructs—Full-length human HIP1r (NCBI accession number KIAA0655, amino acids 1–1069) was retrieved from a fetal cDNA library by PCR and cloned into the mammalian expression vectors pcDNA3 (pcDNA3-HIP1r) or pcDNA3.1-mycHis (pcDNA3.1-HIP1r) (Invitrogen). Deletion constructs were made with a combination of PCR and restriction digests using standard methods. For pcDNA3.1-HIP1r/TH, the TALIN homology region of HIP1r was generated by PCR and cloned into pcDNA3.1-mycHis by PCR. Primers 5′-ACC AGC AGG GAA TTC GGA ACA TGG AGG CCA GCC-3′ (underlined sequence denotes engineered EcoRI site) and 5′-GCT GGA CCC CTG GGG GAA GCT TTA GTT CAC GA-3′ (underlined sequence denotes engineered HindIII site) were used. PCR was performed with full-length HIP1r as template using the Expand High Fidelity PCR system (Roche Applied Science). PCR products and the pcDNA3.1 vector were digested with EcoRI and HindIII, ligated together, and confirmed by automated sequencing. Human HIP1r contains a BamHI restriction site at base pair position 2513 (Fig. 1*A*). pcDNA3-HIP1r was digested with EcoRI and BamHI to release the 5′ portion of HIP1r and inserted into EcoRI and BamHI digested pcDNA3.1-HIP1r/TH to generate pcDNA3.1-HIP1r. pcDNA3-HIP1r has an EcoRI site in the multicloning site and an internal BamHI in the HIP1r insert. The EcoRI- and BamHI-digested fragment was inserted into the EcoRI and BamHI sites in the pcDNA3.1 vector to generate pcDNA3.1-HIP1r/ΔTH. To generate pcDNA3.1-HIP1r/ΔE, pGEX-HIP1r/ΔE (see below) was digested with EcoRI and BamHI. This fragment was ligated into the EcoRI- and BamHI-digested portion of pcDNA3.1-HIP1r (containing the vector and the 3′ end of HIP1r). To generate pcDNA3.1-HIP1r/ΔEΔT, the EcoRI-BamHI fragment from pGEX-HIP1r/ΔE was ligated into EcoRI- and BamHI-digested pcDNA3.1. Human HIP1r contains three internal KspI restriction sites (Fig. 1*A*). To generate pcDNA3.1-HIP1r/Δ153, pcDNA3.1-HIP1r was digested with KspI and the 5′ and 3′ ends ligated together to produce a construct whose product lacks amino acids 153–632 of HIP1r.

pGEX-HIP1r was prepared by ligation of an EcoRI-XhoI fragment from the pcDNA3-HIP1r construct, containing human FL-HIP1r, into EcoRI- + XhoI-digested pGEX-4T3 (Amersham Biosciences).

To create pGEX-HIP1r/ΔE, pGEX-4T-3 was digested first with SmaI. A plasmid containing the HIP1r coding sequences (designated pKIAA0655 and kindly provided by the Kazusa DNA Research Institute) was then digested with HindIII and BamHI to release a 1.9-kb sequence that encoded nucleotides 610–2513. This fragment was blunted with Klenow and then ligated with the SmaI-digested pGEX-4T-3. The latter plasmid, pGEX/HIP1r/nt610–2513, was digested with XhoI, filled in with Klenow, and then digested with SalI. The vector sequences plus the 5′ HIP1r sequences starting at bp 610 (up to the SalI site) were ligated with a 1.1-kb SalI-SspI fragment (HIP1r bp 2500–3541) also derived from pKIAA0655. The resultant construct pGEX/HIP1r/ΔE was confirmed at its junctions by automated sequencing.

To create pGEX-HIP1r/ENTH, a PCR product encompassing the first 450 bp of human HIP1r with engineered XhoI and NotI restriction sites at the 5′ and 3′ ends, respectively, was generated. The PCR product and the pGEX-4T3 vector were digested with XhoI and NotI and ligated together. Constructs were confirmed by automated sequencing. For construction of PGEX-HIP1r/LZ, a 323-bp PCR product encompassing bp 1437–1760 of human HIP1r was generated with engineered EcoRI and XhoI restriction sites at the 5′ and 3′ ends, respectively. The digested PCR product was cloned into EcoRI- and XhoI-digested pGEX-4T3 and confirmed by sequencing. pGEX HIP1r constructs were transfected into BL21 bacteria, and proteins were isolated by bacterial GST fusion protein purification using a glutathione-Sepharose 4B column (Amersham Biosciences) according to the manufacturer's instructions. Following purification, the protein samples were dialyzed against phosphate-buffered saline and concentrated. When used to make antibodies, the GST portion was cleaved off with thrombin.

pcDNA3.1(−)/dynamin1-K44A-HA was the kind gift of Dr. Sandra Schmid (University of California, San Diego). pcDNA3.1(+)/IRES-GFP was the kind gift of Dr. Kathleen Collins (University of Michigan). Mutant dynamin1 was subcloned into the IRES-GFP vector utilizing BamHI sites flanking the entire insert. Full-length HIP1 and HIP1/ΔE were subcloned into the pcDNA3.1(+)/IRES-GFP vector from the pcDNA3 constructs described previously (4).

HIP1r Antibodies—The polyclonal anti-HIP1r antibody UM 359 was generated using pGEX-HIP1r/ΔE as the antigen (Cocalico Biologicals, Inc., Reamstown, PA). pGEX-HIP1r/TH was used as the antigen for polyclonal antibody UM 374. The monoclonal antibodies 1E1, 1E5, and 1C5 were made by the University of Michigan Hybridoma Core Facility using pGEX-HIP1r/TH or pGEX-HIP1r/LZ as the antigen. All antibodies were screened by enzyme-linked immunosorbent assay, immunofluorescence, and Western blot.

Immunoprecipitation and Western Blotting—293T cells in 100-mm dishes were transfected with 2.5 μg of the various HIP1 or HIP1r constructs using 90 μl of Superfect transfection reagent (Invitrogen) according to manufacturer's directions. Cells were harvested 48 h later and resuspended in lysis buffer containing 1% Triton X-100 and protease inhibitors. Protein concentrations were determined using the Bradford reagent (Bio-Rad). For immunoprecipitations, 2–3.5 mg of protein were mixed with 20 μl of the polyclonal HIP1r antibody UM359 and incubated at 4 °C overnight. Fifty microliters of protein G-Sepharose beads (50% slurry) were added, and the mixture was rotated at room temperature for 30 min. Beads were pelleted, washed 3–6 times in lysis buffer, and resuspended in SDS-PAGE loading buffer. One-tenth of the supernatants and the entire pellet from the immunoprecipitations were run on SDS-PAGE gels. Samples were run on 6–8% SDS-PAGE gels and transferred to nitrocellulose. Membranes were blocked in 5% milk/TBST and incubated at 4 °C overnight with anti-clathrin (TD.1, 1:200), anti-adaptin γ (BD Transduction Laboratories, clone 88, 1:1000), or anti-adaptin α (Sigma, clone 100/2, 1:500), and signals were detected using ECL. Membranes were then overblotted with the HIP1r antibodies 1E1 + 1E5 (1:20 dilution of tissue culture supernatant) or UM359 (1:2000 dilution of serum).

Lipid Binding—PIP arrays were obtained from Echelon. Lipid binding was done following the manufacturer's protocol by using 12.5 μg of isolated protein in TBST at 4 °C overnight. HIP1r mutants were detected using a mixture of the monoclonal 1E1 and 1C5 antibodies at 1:5000 in TBST. Anti-mouse secondary antibodies (Amersham Biosciences) were used at 1:5000 in TBST, 3% fatty acid-free bovine serum albumin. Liposomes contained 40% phosphatidylethanolamine, 40% phosphatidylcholine, 10% phosphatidylserine, and 10% of one of the following: phosphatidylinositol (PtdIns), phosphatidic acid, PtdIns(3)P, PtdIns(4)P, PtdIns(5)P, PtdIns(3,4)P_2, PtdIns(3,5)P_2, PtdIns(4,5)P_2, or PtdIns(3,4,5)P_3. The mixture was resuspended in 1:1 chloroform/methanol containing 0.1% HCl, dried under nitrogen, and resuspended to a final concentration of 0.5 mg/ml in 50 mM Hepes (pH 7.2), 100 mM NaCl, and 0.5 mM EDTA. Resuspended lipids were sonicated in a bath sonicator (45 °C) until a clear suspension was formed. Liposomes were collected by centrifugation at 16,000 × *g* for 10 min and resuspended in ice-cold cytosol buffer (0.2 M sucrose, 25 mM Hepes (pH 7.0), 125 mM

potassium acetate, 2.5 mM magnesium acetate, 1 mM dithiothreitol, protease inhibitors, and 0.1 mg/ml bovine serum albumin) at 2 mg/ml of total lipid. 100 μg of liposomes were mixed with isolated protein at 4 °C for 1 h and precipitated for 5 min at 16,000 $\times$ *g*. Pellets and one-fifth of the supernatants were run on 7% SDS-PAGE gels. Gels were transferred to nitrocellulose and analyzed by Western blotting for HIP1 or HIP1r.

Time Course of HIP1r Construct Expression—293T cells in 100-mm plates were transfected with 2.5 μg of the various pcDNA3.1-HIP1r constructs using Superfect transfection reagent. Cells were collected into lysis buffer at 1, 2, 4, and 7 days post-transfection. Fifty μg of protein was run on 10 or 15% SDS-PAGE gels and transferred to nitrocellulose. Membranes were blotted with anti-HIP1r polyclonal antibody (UM 359, 1:5000) and signals detected by ECL.

Apoptosis Assays—COS 7 cells were transfected with pcDNA3.1-HIP1r, pcDNA3.1-HIP1r/ΔE, or pcDNA3-HIP1/ΔE and fixed with 3% formaldehyde at 24 and 48 h post-transfection. Cells were permeabilized with 0.1% Triton X-100 and blocked with 1% milk for 20 min, followed by staining with DAPI and anti-HIP1 monoclonal antibody 4B10 or anti-HIP1r monoclonal antibody 1C5. Bound antibodies were visualized with anti-mouse IgG-FITC (Vector Laboratories). Cells expressing the HIP constructs were scored for apoptosis by nuclear morphology. At least 100 cells were counted for each sample, and transfections were performed in triplicate.

Growth Factor Transfection and Stimulation—For the EGFR stabilization experiments, 293T cells were grown to 50–60% confluency in 100-mm dishes and transfected with 5 μg of pRK5-EGFR (kindly provided by the molecular signaling group at the Ludwig Institute for Cancer Research) and 5 μg of either the various pcDNA3.1-HIP1r constructs or pcDNA3-HIP1 using Superfect transfection reagent. One day later, cells were starved for 20–24 h, treated with cycloheximide (100 μg/ml) for 30 min, and stimulated with EGF (100 ng/ml) in the presence of cycloheximide. Samples were collected at 0, 1, 2, and 4 h after stimulation. Fifteen micrograms of protein were run on 6% SDS-PAGE gels and transferred to nitrocellulose. Membranes were blotted with anti-phospho-EGFR (Cell Signaling, Tyr-845, 1:5000), anti-EGFR (Cell Signaling, 1:2000), anti-HIP1r (1C5 or UM374, 1:2000), or anti-HIP1 (4B10, 1:2000) and signals detected by SuperSignal West Pico Chemiluminescent Substrate (Pierce). Experiments with dominant negative caspase 9 also included 5 μg of pcDNA3-DNC9 (gift of Dr. Gabriel Nunez) or vector in the transfection. Dominant negative caspase 9 was detected using anti-caspase 9 antibody (Cayman Chemical Co., 1:1000). For PDGFβR experiments, 5 μg of SRα-PDGFβR (18) were transfected with either vector, pcDNA3.1-HIP1r, pcDNA3.1-HIP1r/ΔE, pcDNA3-HIP1, or pcDNA3-HIP1/ΔE. Cells were starved, stimulated, and harvested as described. PDGFβR expression was detected using polyclonal anti-PDGFβR antibody (BD Pharmingen, 1:1000).

Immunofluorescence—COS 7 cells were plated onto coverslips and transfected with pRK5-EGFR and either vector, pcDNA3.1-mycHis/HIP1, pcDNA3.1-HA/HIP1r, or pcDNA3.1-HA/DynaK44A using Superfect. The cells were starved the next day for 20 h, treated for 30 min with cycloheximide (Sigma; 100 μg/ml) at 37 °C, and stimulated with EGF (100 ng/ml) for 0 or 30 min. For each time point, cells were fixed with 3% formaldehyde, permeabilized with Triton X-100, and blocked with 5% milk/PBST. The primary antibodies used were anti-EGFR polyclonal antibody (Cell Signaling), anti-Myc monoclonal antibody (Cell Signaling), anti-HA monoclonal antibody (Babco), and anti-EEA1 antibody (Cell Signaling). FITC anti-rabbit and Texas Red anti-mouse (Vector Laboratories) were the secondary antibodies used. Images were obtained with a Zeiss confocal microscope.

For localization of HIP1 and HIP1r, COS 7 cells were plated onto coverslips, transfected with pcDNA3-HIP1 and pcDNA3.1-HIP1r, and fixed with 3% formaldehyde at 24 h post-transfection. Cells were permeabilized with 0.1% Triton X-100 and blocked with 1% milk for 20 min, followed by staining with anti-HIP1 monoclonal antibody 4B10 and anti-HIP1r polyclonal antibody UM359. Bound antibodies were visualized with anti-mouse IgG-FITC or anti-rabbit IgG-Texas Red (Vector Laboratories). Cells were analyzed with a Zeiss confocal microscope and the images processed using Adobe Photoshop software.

Flow Cytometry—For analysis of endocytic uptake of endogenous EGFR, HeLa cells were plated 2 days prior to transfection into 6-well dishes at an approximate density of 2×10^5 cells/well. By the time of transfection, cells were 60–80% confluent. The constructs, pcDNA3.1(+)/IRES-GFP, pcDNA3.1(+)/IRES-GFP/HIP1, pcDNA3.1(+)/IRES-GFP/HIP1/ΔE, and pcDNA3.1(+)/IRES-GFP/dynamin1-K44A were transfected into HeLa cells (2 μg/well of a 6-well dish). Following transfection, cells were grown in medium containing 10% fetal bovine serum for 24 h and then starved in serum-free medium for an addition 20 h. Cells were then stimulated with EGF for the times indicated, trypsinized, washed twice with ice-cold phosphate-buffered saline containing 1% fetal bovine serum, and incubated with anti-EGFR antibody conjugated to phycoerythrin (Pharmingen) for 60 min with gentle rocking at 4 °C. Following staining, cells were washed three times with ice-cold phosphate-buffered saline and were subjected to flow cytometric analysis on a BD Biosciences FACS Elite within 4 h after staining, with measurement of fluorescence intensity in the green and red wavelengths (for GFP positivity and phycoerythrin-conjugated anti-EGFR, respectively). Distinct populations of GFP-positive and negative cells were analyzed for mean fluorescence intensity. For graphical analysis, the fraction of fluorescence remaining after stimulation was plotted as a percentage of initial fluorescence against time. For analysis of transferrin uptake, 293T cells were transfected with the same constructs as above, and following starvation, cells were incubated with Alexa-Fluor-633-labeled transferrin as described previously (2).

RESULTS

HIP1r Mutants and Antibody Characterization—In order to define the relevance of the various protein domains in the activity of HIP1r, deletion mutants lacking these domains were generated (Fig. 1*A*). In addition, monoclonal and polyclonal antibodies were raised against HIP1r using various HIP1r-GST fusion proteins as antigens (see "Materials and Methods"). The monoclonal antibodies HIP1r/1C5 and HIP1r/1E1 resulted from use of the HIP1r TALIN homology region as the antigen, and both antibodies recognized all of the deletion mutants (Fig. 1*A*) except those that did not contain the TALIN homology region (HIP1r/ΔT and HIP1r/ΔEΔT) (Fig. 1*B*). The polyclonal anti-HIP1r antibody UM359, which was generated against a ΔE-HIP1r-GST fusion protein, immunoprecipitated all of the HIP1r mutants (see the Supplemental Material Fig. 1*a*, *lower panel*). The monoclonal antibody HIP1r/1E5 was generated from a region of HIP1r that contained the coiled-coil domain and, as expected, did recognize HIP1r/ΔT. This is shown by the fact that all of the HIP1r mutants were recognized by Western blot using a mix of the monoclonal antibodies 1E1 and 1E5 (Supplemental Material Fig. 1*a*, *bottom panel*).

Prior to using the HIP1r constructs (Fig. 1*A*), they were tested for expression levels and for association with endocytic proteins that had been published previously (5, 9–13) to interact with HIP1 and HIP1r. 293T cells were transfected with the various HIP1 (4) and HIP1r constructs, immunoprecipitated with the polyclonal anti-HIP1 antibody UM323 or the polyclonal anti-HIP1r antibody UM359, and immunoblotted for various endogenous endocytic proteins. As has been reported previously, we found that HIP1r (Supplemental Material Fig. 1*A*, *lane 2*) and HIP1 (Supplemental Material Fig. 1*b*, *lane 2*) associated with clathrin. The HIP1 mutants HIP1/ΔT and HIP1/ΔE and the HIP1r mutants HIP1r/ΔTH, HIP1r/ΔE, and HIP1r/ΔEΔT were able to associate with clathrin equally well compared with full-length HIP1 and HIP1r (Supplemental Material Fig. 1*b*, *lanes 3* and *5*; Fig. 1*a*, *lanes 5–7*). This provides evidence that the mutants we have created are folding properly in the cell. In addition, these data confirm the previous work showing that the LMD motif and coiled-coil regions of HIP1 are necessary for association with clathrin (Supplemental Material Fig. 1*b*, *lanes 4* and *6*) (11).

Next, we tested whether HIP1 and HIP1r associate with AP-1, an endocytic protein complex localized primarily to the *trans*-Golgi network and late endosomes. Immunoprecipitation and Western blotting for γ-adaptin, the large subunit of the AP-1 tetrameric complex, showed that neither HIP1 nor HIP1r associated with AP-1 (data not shown). We also confirmed that although HIP1 associates with α-adaptin, the large subunit of the adaptor protein AP-2, HIP1r did not (data not shown) (5, 9–13). This is consistent with the differences in domain structure between HIP1, which contains a consensus binding se-

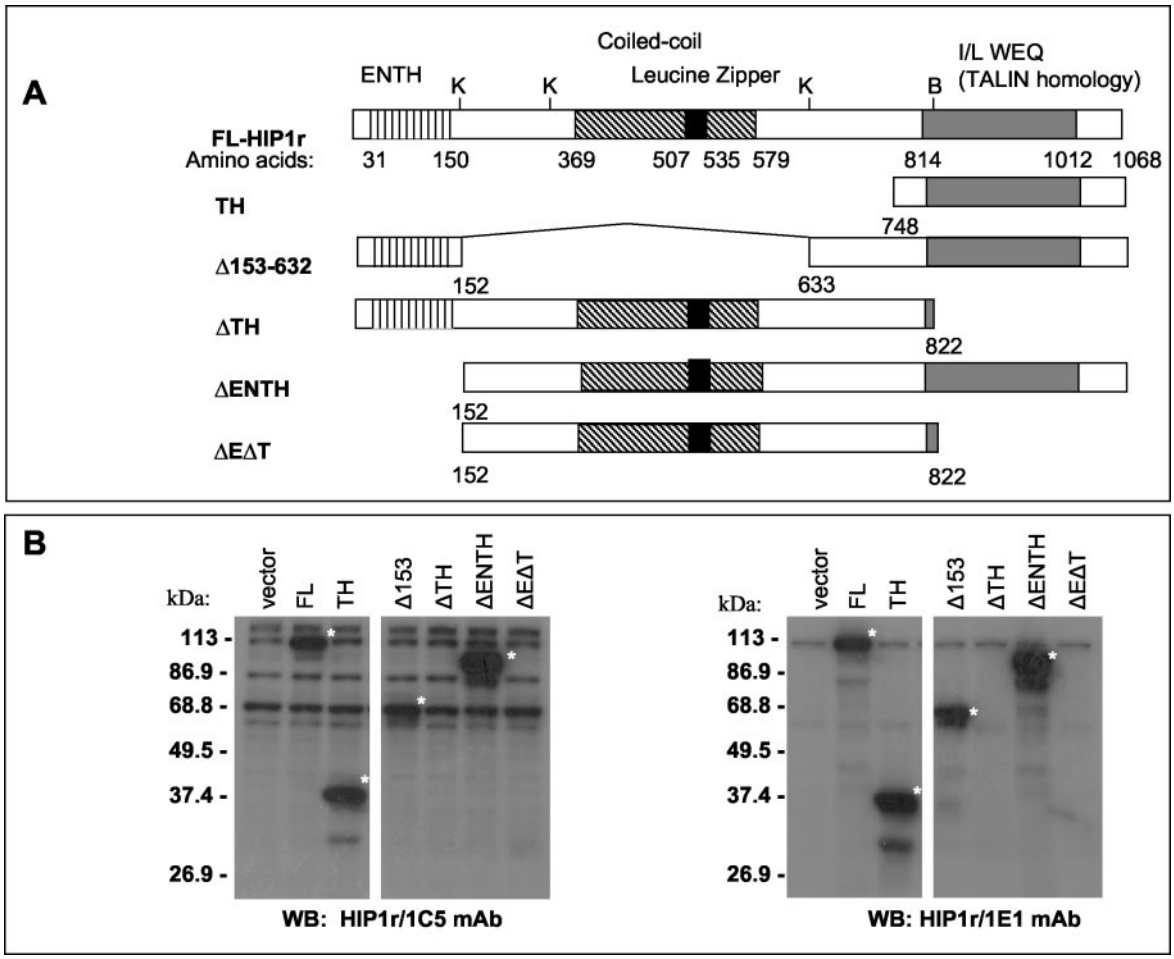

FIG. 1. **HIP1r mutants and antibody characterization.** *A*, the human HIP1r protein has an epsin N-terminal homology (*ENTH*) domain, a central coiled-coil domain containing a leucine zipper, and a C-terminal TALIN homology domain. These domains were deleted to produce the constructs pcDNA3.1-HIP1r/TH, pcDNA3.1-HIP1r/Δ153, pcDNA3.1-HIP1r/ΔTH, pcDNA3.1-HIP1r/ΔE, and pcDNA3.1-HIP1r/ΔEΔT. Restriction sites for KspI (*K*) and BamHI (*B*) are marked. *B*, polyclonal and monoclonal antibodies were raised against purified HIP1r fragments. Western blots (*WB*) using monoclonal antibodies 1C5 and 1E1, which recognize the TALIN homology region, are shown. *Asterisks* denote the location of HIP1r mutants.

quence for AP-2 (the DPF motif), and HIP1r, which lacks this motif (Fig. 1*A*).

Most interesting, the HIP1/ΔE mutant that lacks the putative inositol lipid-binding domain did not reproducibly associate with AP-2 (data not shown) but did associate with clathrin (Supplemental Material Fig. 1*b, lane 3*). We have found previously that expression of this mutant, but not the full-length HIP1, induces cell death in 293T (4) and BT549 breast cancer cells (2). One reason that HIP1/ΔE may not have associated with AP-2 is that it was concentrated in a relatively AP-2-deficient perinuclear area of the cell by confocal immunofluorescence (Supplemental Material Fig. 2*b*). In comparison, when full-length HIP1 was overexpressed in the same cells, it was more widely distributed in the cytoplasm in a punctate pattern (Supplemental Material Fig. 2*a*). The HIP1r/ΔE mutant also showed a similar and more perinuclear subcellular localization compared with full-length HIP1r (compare Supplemental Material Fig. 2, *c* and *d*). Although HIP1r co-localized partially with HIP1, it consistently showed an additional localization to the more peripheral ruffled plasma membrane (Supplemental Material Fig. 2*c*, *white arrow,* and *g*). This HIP1r location to the actin containing membrane ruffles confirms the HIP1r subcellular localization described previously (15).

HIP1 and HIP1r Bind Preferentially to 3-Phosphate Containing Inositol Lipids via Their ENTH Domains—The ENTH domain is found in several proteins implicated in endocytosis including Epsin 1 and AP180/CALM (7, 8), CLINT ((19) also known as enthoprotin (20) or EpsinR (21)), as well as the HIP family. The Epsin 1 and AP180/CALM ENTH domains are documented lipid-binding motifs that have been shown to bind predominantly to PtdIns(4,5)P_2 and PtdIns(3,4,5)P_3 (7, 8). Recently, the ENTH domains from several proteins including those of the HIP family have also been found to bind tubulin (22). In contrast, the lipid binding specificity of the HIP family of ENTH domains has not been studied. It should be noted that Mishra *et al.* (13) did find that phosphoinositides were a necessary component of the liposomes for HIP1 binding. However, the preparation of inositol lipids was not purified, and therefore conclusions about lipid specificity were not made in that study.

One obvious hypothesis derived from the different subcellular localization of the ΔE mutants (Supplemental Material Fig. 2, *b* and *d*) is that important protein or lipid binding activities of the ENTH domain are not present in the deletion mutants. These binding activities would anchor HIP proteins to the particular subcellular location of those proteins or lipids. In addition, it is well established that inositol lipids are used by the cell to generate diversity in the destinations of protein cargo during trafficking (23). To begin to explore if a lipid binding activity of the HIP family is important in their cellular function/location, we assayed the lipid binding specificity of the HIP1 and HIP1r ENTH domains by using a variety of techniques. First, myc-His-tagged HIP1 and HIP1/ΔE were overex-

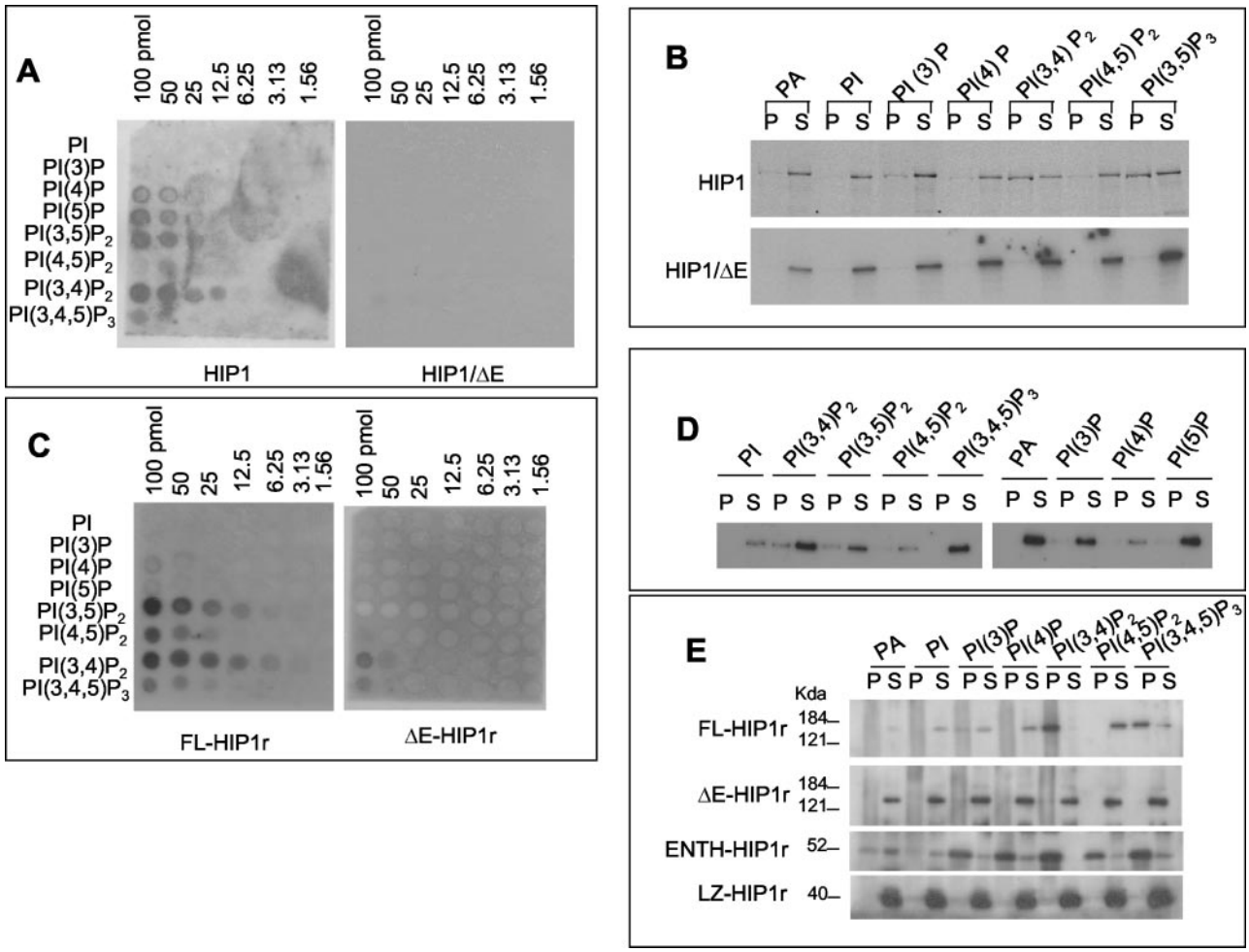

FIG. 2. **Lipid binding characteristics of HIP1 and HIP1r.** *A*, specificity and relative affinity of PtdIns lipid binding by HIP1. Purified HIP1-myc-His and HIP1/ΔE-myc-His were bound to PIP arrays containing from 1.56 to 100 pmol of each lipid series. Proteins were detected using anti-Myc antibody. *B*, liposome binding assays with full-length HIP1 and HIP1/ΔE performed with liposomes containing 10% of the indicated lipid series (see "Materials and Methods"). Pelleted liposomal-bound (*P*) and supernatant (*S*) fractions are shown. *C*, HIP1r-GST binds preferentially to PI3,5-P_2 and PI3,4-P_2 on PIP arrays. FL-HIP1r-GST and ΔE-HIP1r-GST were used for binding to PIP arrays. Proteins were detected using a mix of monoclonal 1E1 and 1C5 HIP1r antibodies. Control blots using antibody alone showed no signal (not shown). *D*, liposome binding assays using full-length HIP1r performed with liposomes containing 10% of the indicated lipid series. *E,* the ENTH domain is critical for HIP1r lipid binding. Various HIP1r mutant proteins fused to GST were mixed with liposomes containing 10% of the indicated lipid species. Liposomes were pelleted, and the pellets and supernatants were run on 7% acrylamide gels. Proteins were detected by Western blot.

pressed and purified from 293T extracts by nickel column chromatography. PIP arrays were used to assess initially the binding of these purified proteins to PtdIns lipids. Most surprising, the highest affinity of binding for HIP1 was to PtdIns(3,4)P_2 and PtdIns(3,5)P_2 (Fig. 2*A, left panel*). As expected, HIP1/ΔE did not bind these lipids (Fig. 2*A, right panel*). We also looked at the lipid binding of ^{35}S-labeled proteins that were synthesized using reticulocyte lysates. The *in vitro* translated proteins were incubated with liposomes containing a variety of phosphatidylinositol lipids. Pelleted liposomes and supernatants were run on SDS-PAGE gels and analyzed by autoradiography. HIP1 bound to liposomes containing PtdIns (3)P, PtdIns(3,4)P_2, and PtdIns(3,5)P_2 but did not bind to PtdIns(4,5)P_2 (Fig. 2*B, top panel*). As predicted, the HIP1/ΔE protein was unable to bind any of the inositol lipid-containing liposomes (Fig. 2*B, bottom panel*).

Because we unexpectedly found that the myc-His tag was not recognized by anti-His or anti-Myc antibodies or the nickel column when attached to the HIP1r C terminus (despite repeated sequence confirmation of the constructs), it was necessary to generate a series of HIP1r deletion mutants fused to GST to characterize the lipid binding properties of HIP1r (see "Materials and Methods"). First, purified FL-HIP1r-GST and ΔE-HIP1r-GST fusion proteins were used to test binding to PIP arrays. Like HIP1, full-length HIP1r bound preferentially to PtdIns(3,4)P_2 and PtdIns(3,5)P_2 using the PIP arrays (Fig. 2*C, left panel*), and significant binding was abolished in the mutant lacking the ENTH domain (Fig. 2*C, right panel*). HIP1r-GST also exhibited some lower affinity binding to PtdIns(4,5)P_2 and PtdIns(3,4,5)P_3 (Fig. 2*C, left panel*). HIP1r-GST fusion proteins were also subjected to liposome pelleting assays. Consistent with the PIP array results, full-length HIP1r bound preferentially to PtdIns(3,4)P_2 and PtdIns(3,5)P_2-containing liposomes (Fig. 2*D*). We also observed less reproducible binding in some cases to other 3-phosphorylated inositol lipids, namely PtdIns(3)P and PtdIns(3,4,5)P_3 (Fig. 2, *D* and *E*, and data not shown). The ENTH domain was necessary for binding, as the ΔE-HIP1r and LZ-HIP1r mutants failed to bind any of the lipids tested (Fig. 2*E*). The HIP1r-GST mutant containing only the ENTH domain (ENTH-HIP1r) also pelleted with liposomes but was less specific and bound to PtdIns(3)P, PtdIns(4)P, PtdIns(3,4)P_2, PtdIns(4,5)P_2, and PtdIns(3,4,5)P_3, as well as phosphatidic acid (Fig. 2*E*). The latter data suggest that sequences not present in the ENTH mutant are necessary for conferring preferential binding to 3-phosphorylated inositol lipids.

The differences in lipid binding reported here compared with previous mammalian ENTH domain-containing proteins suggest that HIP1 and HIP1r may participate in a distinct part of the pathway of clathrin trafficking different from the other ENTH domain-containing proteins. Another possibility is that the binding of the HIP proteins to inositol lipids has a completely different function that remains to be determined. However, we think this interaction is significant as several proteins know to co-localize with endosomal membranes also bind to 3-phosphate-containing bisphosphoinositides (24, 25). For example, the yeast protein Ent3p has been shown recently to have a PtdIns(3,5)P_2-binding ENTH domain that mediates its role in intracellular multivesicular body protein sorting (26).

In addition, we have found that PtdIns 3-kinase was activated in cells that overexpressed HIP1 but that phospholipase C-γ, in contrast, was not activated (2). This together with our 3-phosphoinositide binding data suggested the hypothesis that HIP1 binding to 3-phosphorylated inositol lipids may contribute to Akt activation by these lipids. If this hypothesis were true, a dominant negative HIP1 that lacked lipid binding might lead to Akt inhibition and subsequent apoptosis as Akt activation is a cell survival signal. On the other hand, constitutively activated Akt would be expected to bypass this dominant negative HIP1-induced apoptosis as it would be expected to be downstream of HIP1. Indeed, we have found that constitutively active Akt (Myr-Akt), but not oncogenic Ras-V12, is able to rescue dominant negative HIP1/ΔE-mediated apoptosis (Supplemental Material Fig. 3). The latter data, albeit indirect, suggests that 3-phosphoinositides may indeed be important in the fundamental cellular functions of the HIP family.

The HIP1r Mutant Lacking the ENTH Domain Induces Cell Death—We have shown previously (4) that HIP1 is overexpressed in several cancers, especially prostate and colon cancer. In addition, it has been shown that specific antibodies against HIP1r are produced in patients with colon cancer, suggesting that HIP1r is also overexpressed in colon cancers (27). Furthermore, expression of the ENTH deletion mutant of HIP1, but not full-length HIP1, induces cell death in a dominant interfering manner (4). The discrepancies between our data that suggest HIP1 has a cellular survival function and the data of Hackam *et al.* (44) and Gervais *et al.* (30) that suggest HIP1 is primarily pro-apoptotic are not yet understood. We speculate that the cellular environment may influence whether or not the full-length HIP proteins have pro-apoptotic *versus* survival functions. By removal of the ENTH domain, potential pro-apoptotic domains (such as the pseudo-DED domain described by Gervais *et al.* (30)) may be unveiled.

To begin to test which domains of HIP1r were important to its function, we expressed the HIP1r deletion mutants in 293T cells. A time course of protein expression after transient transfection of HIP1r deletion mutants showed that HIP1r/ΔE and HIP1r/ΔEΔT were not as stable as other HIP1r mutants (Fig. 3*A*). This result parallels our previous finding that the HIP1/ΔE mutant was not as stable as other HIP1 mutants and induced apoptosis. In contrast, expression of full-length HIP1r and most of the deletion mutants remained stable for at least 7 days post-transfection (Fig. 3*A*). We have also overexpressed the ENTH domain of HIP1 in cells, and it did not induce apoptosis (Ref. 4 and data not shown).

In contrast to full-length HIP1 and HIP1r (Supplemental Material Fig. 2, *a* and *c*), many cells transfected with HIP1r/ΔE or HIP1/ΔE and visualized by immunofluorescence 48 h post-transfection were condensed and blebbing, characteristic of apoptotic cells. In order to quantitate the apoptosis caused by the HIP1r/ΔE mutant and to compare this mutant with the HIP1/ΔE mutant, cells were transfected in triplicate with HIP1r/ΔE, full-length HIP1r, or HIP1/ΔE, stained with anti-HIP1r or anti-HIP1 antibodies, and then assayed for apoptosis by scoring apoptotic nuclear morphology. DAPI-stained nuclei of transfected cells were scored as apoptotic if they possessed condensed or fragmented nuclei. Whereas full-length HIP1r-transfected cells had a minimal percentage of apoptosis, cells transfected with HIP1/ΔE and HIP1r/ΔE consistently exhibited increased incidence of cellular apoptosis 48 h post-transfection (Fig. 3*B*). Most interesting, compared with HIP1/ΔE, HIP1r/ΔE did not show significant apoptosis at 24 h post-transfection. This was also confirmed with terminal dUTP nick-end labeling analysis in an independent experiment (data not shown). These results, together with our previous data documenting a dominant interfering function of HIP1/ΔE (4), imply that HIP1r, like HIP1, may have a role in cellular survival. The difference in time course also suggests that HIP1 and HIP1r may have functions in the cell that are distinct from each other in addition to those that are overlapping.

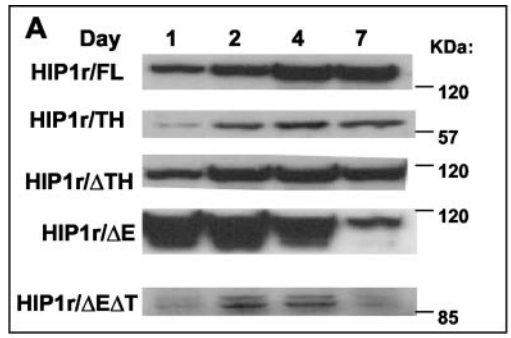

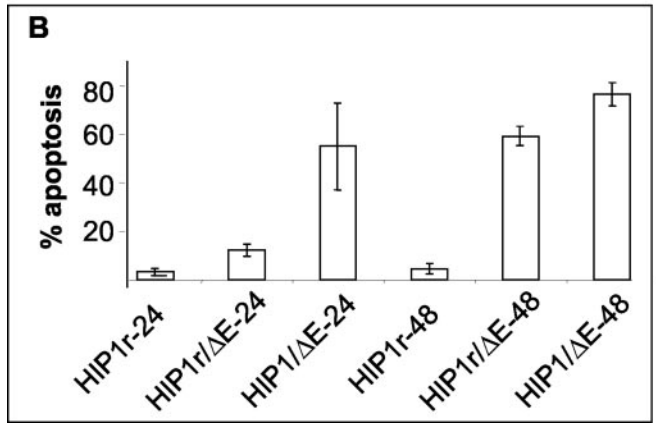

FIG. 3. **Expression of an HIP1r mutant lacking the ENTH domain causes apoptosis.** *A*, HIP1r mutants were transfected into 293T cells, and extracts were analyzed by Western blot at days 1, 2, 4, and 7 post-transfection. *B*, quantitation of apoptosis caused by HIP1r/ΔE compared with HIP1/ΔE. Transfected cells (stained with HIP1r/1C5 antibody or HIP1/4B10 antibody as described under "Materials and Methods") were scored at either 24 or 48 h post-transfection as apoptotic if DAPI-stained nuclear condensation or fragmentation was present. Experiments were performed three times. *Error bars* represent the mean ± S.D.

The HIP Family Stabilizes Growth Factor Receptors—The activities of HIP1 and HIP1r that might lead to the survival of cells and contribute to tumorigenesis remain to be defined. Recently, we have found that HIP1 is overexpressed in multiple epithelial tumors, and stable overexpression of HIP1 in NIH3T3 fibroblasts causes transformation. In HIP1-overexpressing cells, this process may be mediated in part by elevated levels of epidermal growth factor receptor (EGFR) and the resultant activation of mitogenic signaling pathways (2). In

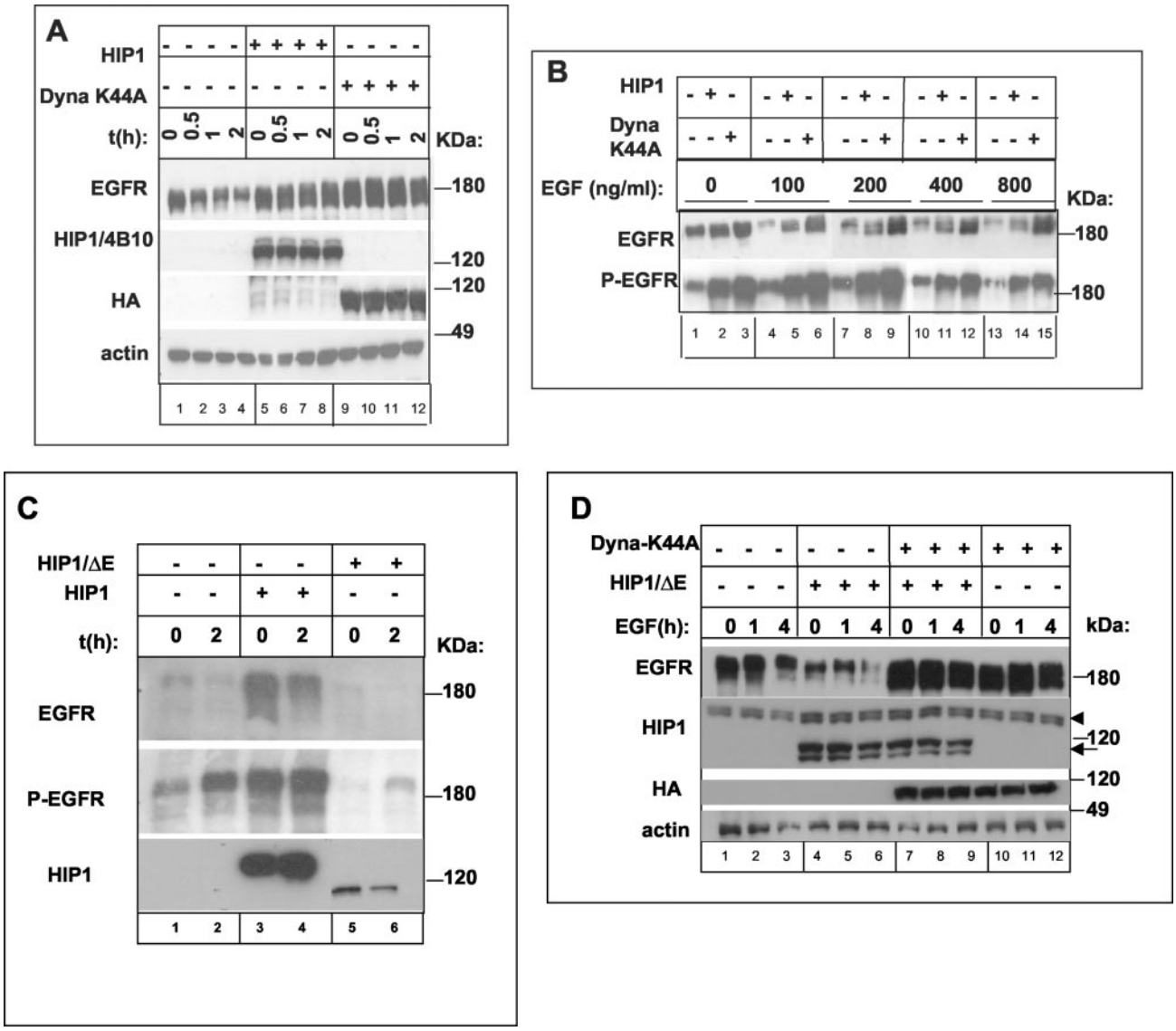

FIG. 4. **HIP1 expression stabilizes receptor tyrosine kinases during post-stimulation endocytosis and degradation.** *A*, levels of EGFR are stabilized by the overexpression of HIP1 and the dynamin1-K44A mutant. 20 μg of protein were loaded on SDS-PAGE gels and analyzed for EGFR expression following stimulation with 100 ng/ml EGF. Actin levels were used as a loading control. *B*, comparison of EGFR levels and EGFR phosphorylation after stimulation with various amounts of EGF for 60 min. Gels were loaded with 20 μg of protein extracts from cells transfected with EGFR and the indicated construct. *C*, comparison of EGFR levels and EGFR phosphorylation in cells transfected with EGFR and full-length HIP1 or HIP1/ΔE, starved for 48 h, and stimulated with 100 ng/ml EGF for 0 or 2 h. 50 μg of protein was loaded on SDS-PAGE gels and analyzed. *D*, the dynamin1-K44A mutant overcomes EGFR destabilization caused by HIP1/ΔE. 293T cells were co-transfected with EGFR, dynamin1-K44A (*Dyna-K44A*), and HIP1/ΔE as indicated and stimulated with EGF. 20 μg of protein were loaded on SDS-PAGE gels and analyzed by Western blot.

order to determine whether the elevated levels of EGFR in the transformed cells was a direct result of HIP1 overexpression or a more secondary effect of transformation, we have begun to evaluate the effect of transient HIP1 and HIP1r overexpression on growth factor receptor stability after ligand stimulation. Briefly, to allow for sufficient sensitivity of detection and semi-quantitation of growth factor receptor half-life, 293T cells were co-transfected with EGFR or PDGFβR and the various full-length or mutant HIP constructs. The transfected cells were then stimulated with ligand and analyzed for the rate of receptor tyrosine kinase degradation. In order to validate our assay, we utilized the well characterized GTPase-deficient dynamin1 dominant negative mutant dynamin1-K44A (28). Dynamin is critical for release of invaginated clathrin-coated pits from the plasma membrane to form clathrin-coated vesicles (29). The dynamin1-K44A construct exerts a dominant interfering effect on endogenous dynamin, resulting in the loss of normal dynamin function. The net effect of expression of this mutant in cells is to prevent ligand-induced endocytosis and degradation of growth factor receptors and thereby increase surface levels of the receptor (28).

Following transfection of the constructs and starvation in serum-free medium, transfected cells were stimulated with EGF for various lengths of time. It is noteworthy that we found it necessary to include cycloheximide in the assay to inhibit the confounding rapid translation of new EGFR. If cycloheximide was not included, there were no reproducible differences detected in EGFR half-life in any of the cells transfected with EGFR and vector, full-length or mutant HIP constructs. This indicates that the HIP-mediated EGFR stabilization described below was via post-translational mechanisms (data not shown). As expected, in the presence of cycloheximide we were able to show that the EGFR was degraded in vector-transfected cells following EGF stimulation with an approximate half-life of 30

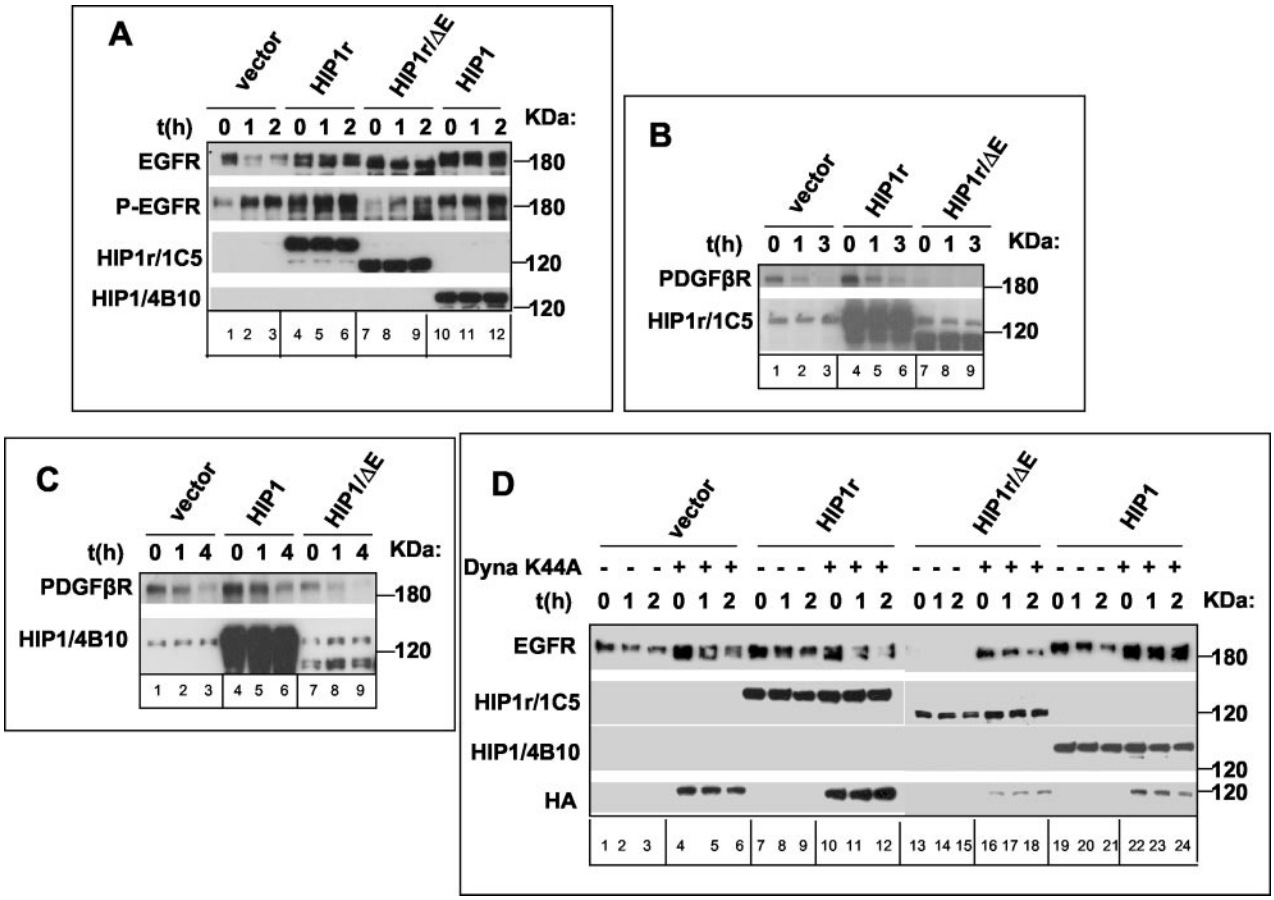

FIG. 5. **HIP1r-transfected cells have increased levels of growth factor receptors.** *A,* HIP1r stabilizes total and Tyr-845-phosphorylated EGFR, whereas HIP1r/ΔE reduces levels of activated EGFR. 293T cells were transfected with EGF and either vector (*lanes 1–3*), HIP1r (*lanes 4–6*), HIP1r/ΔE (*lanes 7–9*), or HIP1 (*lanes 10–12*). Samples were taken 0, 1, and 2 h after starvation and stimulation with human EGF and subject to Western blot analysis. *B,* comparison of PDGFβR levels following stimulation with PDGF-ββ. 293T cells were transfected with vector, HIP1r or HIP1r/ΔE, along with 5 μg of pSRα-PDGFβR. Cells were harvested 0, 1, and 3–4 h after starvation and stimulation with PDGF-ββ and subjected to Western blot analysis. *C,* same experiment as *B* except that HIP1 and HIP1/ΔE were assayed. *D,* down-regulation of EGFR by HIP1r/ΔE can be partially overcome by dynamin1-K44A. Cells were co-transfected with EGFR, dynamin1-K44A (*Dyna K44A*), and either HIP1r, HIP1r/ΔE, or HIP1 and stimulated with EGF. 15 μg of protein were loaded on SDS-PAGE gels and analyzed by Western blot.

min (Fig. 4*A*, *lanes 1–4*). In contrast, there was a dramatic prolongation of the EGFR half-life to greater than 2 h in HIP1-transfected cells following stimulation. This is shown by steady levels of the EGFR at all time points in the presence of HIP1 (Fig. 4*A*, *lanes 5–8*). A similar effect where the EGFR half-life was prolonged beyond the last time point in our assay was seen in dynamin1-K44A-transfected cells (Fig. 4*A*, *lanes 9–12*), whereas transfection of a wild type dynamin construct caused higher levels of EGFR degradation (data not shown).

It should also be noted that the Western blots presented are a portion of those actually analyzed. It was necessary for us to evaluate different exposures or to run varying amounts of each of our extracts to achieve blots where the semi-quantitation of EGFR in the extracts from the various transfection conditions were in a range of ECL signal that was linear. This allowed us to conclude that the half-life of the EGFR was prolonged in the HIP and dynamin1-K44A-transfected cells. In addition, this effect was apparent across different concentrations of EGF, with HIP1- or dynamin1-K44A-expressing cells consistently showing not only higher levels of EGFR at 60 min post-stimulation but also greater EGFR tyrosine phosphorylation (Fig. 4*B*). Lower doses of EGF (25–50 ng/ml) in this assay did not effectively stimulate degradation of the EGFR in response to ligand in the vector-transfected cells and, as a result, were not used.

It should also be noted that the levels of the HIPs and the dynamin mutant did not vary during the time course of each experiment. This allowed us to quantitate the growth factor half-lives without having to quantitate ratios of growth factor levels and modifier proteins. It also allowed us to conclude that the half-lives of the HIPs and dynamin mutant were much longer than 4 h, as the presence of cycloheximide did not lead to detectable changes in their levels in the presence or absence of growth factor receptor stimulation.

Co-expression of full-length HIP1r produced analogous results, with stabilization of the EGFR to a half-life of greater than 2 h and higher levels of EGFR phosphorylation after stimulation compared with vector-transfected controls (Fig. 5*A*, compare *lanes 4–6* to *lanes 1–3*). It is also significant that the starting levels of EGFR prior to EGF stimulation were frequently increased in the HIP or dynamin dominant negative transfected cells. This is likely due to a continual effect of HIPs and the dynamin1-K44A mutant on the turnover of EGFR. As expected, this difference in starting amounts of EGFR was not observed in the absence of cycloheximide.

To determine whether HIP1r and HIP1 were able to alter the stability of other receptors whose endocytosis is mediated by clathrin and its cofactors, we assayed the effect of HIP1r and HIP1 on the degradation of the PDGFβR after stimulation with its ligand, PDGF-ββ. Following stimulation, overexpression of HIP1r or HIP1 led to diminished degradation of the PDGFβR, albeit to a lesser extent than that seen for the EGFR (Fig. 5*B*, compare *lanes 4–6* to *lanes 1–3*; Fig. 5*C*, compare *lanes 4–6* to *lanes 1–3*). The approximate half-life of the PDGFβR was pro-

longed from 1 to 3 h in the presence of full-length HIPs. The similar but distinct effects seen with the EGFR and PDGFβR when either HIP1 or HIP1r was overexpressed indicate not only a general role for the HIP1 family in post-stimulation regulation of receptor tyrosine degradation but also a possible selectivity of the HIP family in its activity of receptor stabilization.

Mutants Lacking the ENTH Domain Do Not Stabilize EGFRs—We and others (4, 10, 30) have previously gathered data that indicate HIP1 has an effect on cellular survival. It is possible that altered HIP1r expression also affects the survival of cells. We hypothesize that the pro-survival functions of HIP1 and HIP1r may be dependent upon their ability to stabilize and thereby up-regulate growth factor receptor tyrosine kinases through their role in clathrin trafficking. Conversely, the withdrawal of growth factor receptor stimulation has been noted to be sufficient to cause apoptosis (31). These facts led to the hypothesis that the pro-apoptotic effects of interfering with HIP1 or HIP1r function might result from the disruption of receptor tyrosine kinase trafficking.

To address this hypothesis, we co-transfected the HIP1/ΔE construct along with EGFR and analyzed its effect on EGFR half-life. We have provided evidence previously (4) that the HIP1/ΔE protein functions as a dominant interfering mutant. HIP1/ΔE did not have the same stabilizing effect as full-length HIP1; indeed, EGFR degradation following stimulation appeared to be accelerated in cells expressing HIP1/ΔE (Fig. 4*D*, *lanes 4–6* compared with *lanes 1–3*). Phosphorylation of the EGFR was also diminished after ligand stimulation compared with vector-transfected control (Fig. 4*C*, *lanes 5* and *6* compared with *lanes 1* and *2*).

Similar but distinct results were observed upon transfection of HIP1r/ΔE. Western blots of total EGFR show at least two species of EGFR of slightly different molecular weights. Levels of the upper phosphorylated or monoubiquitinated EGFR band were diminished at every time point in the HIP1r/ΔE-transfected samples compared with vector-transfected cells (Fig. 5*A*, compare *lanes 7–9* to *lanes 1–3*). This activated EGFR isoform was not stable in the HIP1r/ΔE-expressing cells (Fig. 5*A*, *lanes 7–9*) but was in the HIP1r-transfected cells (Fig. 5*A*, *lanes 4–6*). Immunoblot analysis for phosphorylated EGFR confirmed that activated EGFR levels were, like in the HIP1/ΔE-expressing cells, reduced in the HIP1r/ΔE-expressing cells (Fig. 5*A*, *lanes 7–9* compared with *lanes 1–3*).

Next, we analyzed the effects of the other HIP1r mutants on EGFR expression and ligand-stimulated activation. Like full-length HIP1r, the HIP1r/ΔTH mutant stabilized total EGFR levels and also showed increased tyrosine phosphorylation of the EGFR compared with vector-transfected cells (data not shown). Like HIP1r/ΔE, HIP1r/ΔEΔT-transfected cells lacked the higher molecular weight EGFR species seen in vector- or HIP1r-transfected cells and showed reduced tyrosine phosphorylation of the receptor (data not shown). These results suggest that the ENTH domain is necessary for effective maintenance of EGF signal duration, likely via stabilization of the receptor in early pH neutral endocytic vesicles. It is interesting to note again that the HIP1/ΔE-containing cells contain predominantly the slower migrating, phosphorylated EGFR band (Fig. 4*D*, *lanes 4–6*), whereas the HIP1r/ΔE-containing cells contain more of the faster migrating EGFR band (Fig. 5*A*, *lanes 7–9*). This suggests that the different patterns of EGFR banding, as seen in the HIP1/ΔE compared with the HIP1r/ΔE-transfected cells, may reflect subtle differences in the ways HIP1 and HIP1r affect total levels of EGFR *versus* total levels of tyrosine-phosphorylated EGFR.

Previously, we have shown that HIP1/ΔE-mediated apoptosis could be rescued by a dominant negative caspase 9 but not a dominant negative caspase 8, suggesting that HIP1/ΔE induced caspase 9-dependent apoptosis (4). To determine whether the same effect could be seen in terms of receptor stabilization, EGF stimulation assays were performed with co-transfection of EGFR, HIP1/ΔE, and either vector or dominant negative caspase 9. Dominant negative caspase 9 did not alter the effect of HIP1/ΔE on EGFR, although this construct does correct the cell death induced by HIP1/ΔE (data not shown and see Ref. 4). These results indicate that the effect of HIP1/ΔE or HIP1r/ΔE on EGFR levels in our assays is not simply due to increased apoptosis of cells that express transfected EGFR and the ΔE mutants. Moreover, it suggests that caspase 9-dependent apoptosis mediated by the ΔE mutants may be a downstream effect of receptor down-regulation and that the apoptosis can be corrected without a correction of the receptor abnormality.

Because previous studies have indicated that HIP1 and HIP1r have activities at the plasma membrane, it is possible that they are rate-limiting in these functions. Overexpression of HIP1 or HIP1r could inhibit the initial stages of clathrin-coated vesicle formation, similar to the dynamin1-K44A mutant (29). This mechanism would favor retention of growth factor receptors at the plasma membrane and allow continued activation of signaling pathways. To begin to test at which step of endocytosis the ΔE mutants might act predominantly, cells were transfected with EGFR and the ΔE mutants with or without dynamin1-K44A. Dynamin1-K44A was able to overcome the diminished levels of EGFR in cells expressing HIP1/ΔE and exhibited EGFR levels comparable with transfection with dynamin1-K44A alone (Fig. 4*D,* compare *lanes 7–9* to *lanes 10–12*). In contrast, the ability of dynamin1-K44A to overcome the effects of HIP1r/ΔE was not nearly as robust. Co-transfection of dynamin1-K44A with HIP1r/ΔE did cause some increase in EGFR levels, but only in the EGFR species of lower molecular weight and not to the extent seen with HIP1/ΔE (Fig. 5*D*, compare *lanes 16–18* with *lanes 13–15*). Based on this finding, HIP1 and HIP1r may have different but partially overlapping mechanisms of growth factor stabilization. These results suggest HIP1 acts in a rate-limiting way downstream of the initial stages of clathrin-vesicle formation to promote receptor tyrosine kinase stabilization. HIP1r may also act in the endocytic pathway after clathrin-vesicle formation, as the dynamin1-K44A was able to partially overcome HIP1r/ΔE-mediated down-regulation of EGFR. However, the data suggest that HIP1r may have some rate-limiting functions that are upstream of HIP1. This would be consistent with its localization to peripheral membrane ruffles (15).

Finally, we tested whether the ΔE mutants of HIP1 and HIP1r caused a more widespread down-regulation of receptor tyrosine kinase levels by assaying their effects on PDGFβR after starvation and stimulation with PDGF-ββ. Similar to EGFR, cells expressing HIP1r/ΔE and HIP1/ΔE exhibited diminished levels of PDGFβR at each time point after ligand stimulation compared with vector-transfected cells (Fig. 5*B*, compare *lanes 7–9* to *lanes 1–3*; Fig. 5*C*, compare *lanes 7–9* to *lanes 1–3*). However, the extent of receptor down-regulation was less pronounced in cells expressing HIP1/ΔE compared with HIP1r/ΔE-expressing cells.

Inhibition of Receptor Tyrosine Kinase Degradation by the HIP Family Occurs Post-endocytosis—Ligand-mediated degradation of receptor tyrosine kinases occurs via endocytosis of clathrin-coated pits to progressively form clathrin-coated vesicles, endosomes, and lysosomes via vesicle trafficking (32). Thus, there are numerous steps of trafficking at which HIP1 and HIP1r might act to inhibit the degradation of receptor

tyrosine kinases. In order to begin to understand at which stages of endocytosis HIP1 and HIP1r might act, immunofluorescent analysis of EGFR-containing vesicles in cells transfected with EGFR and either vector, HIP1, HIP1r, or dynamin1-K44A was performed. This assay was derived from a recently published assay of transforming growth factor-β receptor endocytosis (33). Vesicles containing EGFR were visualized after ligand stimulation by staining with anti-EGFR antibody. Prior to stimulation, EGFR was localized to the plasma membrane as denoted by the absence of vesicular structures in the cytoplasm (Fig. 6*A*, *1st three left-hand panels*). After 30 min of stimulation, cells expressing EGFR alone demonstrated the formation of vesicular structures containing EGFR (Fig. 6*A, three right-hand panels, top row*). Similarly, HIP1- or HIP1r-overexpressing cells also had EGFR-positive vesicular structures after ligand stimulation, indicating endocytic uptake in the HIP-transfected cells (Fig. 6*A*, *three right-hand panels, 2nd* and *3rd rows*). In cells transfected with EGFR and either vector or HIP1, EGFR-containing vesicular structures also co-localized with the early endosomal antigen EEA-1 as expected (Fig. 6*B, top* and *middle rows; columns 3* and *6*). In contrast, in cells transfected with the positive control dynamin1-K44A and EGFR, EGFR-containing vesicular structures did not form, and EGFR remained on the surface rather than being internalized (Fig. 6*A*, *three right-hand panels, bottom row*). There was also no co-localization of EGFR with EEA-1 (Fig. 6*B, bottom row, column 6*). This is consistent with prior results that indicated the dynamin1-K44A dominant negative mutant functions to inhibit clathrin-coated vesicle release from the plasma membrane (29). If HIPs had functioned in a rate-limiting fashion during clathrin vesicle formation, we would have expected the HIP-transfected cells to not form EGFR-positive vesicles in a manner similar to that observed with the dynamin1-K44A-positive control.

We also attempted to assay the effects of the ΔE mutants of HIP1 and HIP1r on EGFR endocytosis by using this assay. However, due to the enhanced degradation of the EGFR in the presence of the ΔE mutants, the sensitivity of this assay for the EGFR was not high enough to make solid observations. Because of this, we devised a more sensitive flow cytometry assay that quantitated the surface EGFR in transfected cells. In this assay we quantitated by flow cytometry the relative amounts of cell-surface EGFR following EGF stimulation in HIP1- or HIP1/ΔE-transfected HeLa cells, which contain significant quantities of endogenous EGFR (28). In this assay HeLa cells were transfected with pcDNA3-IRES-GFP constructs containing nothing (*i.e.* vector alone), HIP1, dynamin1-K44A or HIP1/ΔE cDNAs cloned in front of the IRES-GFP cassette. These constructs express GFP in addition to the protein of interest, allowing us to restrict flow cytometric analysis of EGFR to only those cells that were GFP-positive (transfected cells). Following stimulation with EGF, live, non-permeabilized cells were stained with an anti-EGFR antibody conjugated to phycoerythrin, and relative fluorescence of GFP-positive cells was measured by flow cytometry. Similar to the effect seen by the immunofluorescence assay of EGFR uptake, there was no effect of HIP1 or HIP1/ΔE on endocytic clearance of surface EGFR (Fig. 6*C*). On the other hand, dynamin1-K44A promoted retention of the EGFR on the cell surface at all time points indicated. In addition, even though HIP1/ΔE failed to have an effect on surface levels of the EGFR post-EGF stimulation, it did cause apoptosis in HeLa cells (Supplemental Material Fig. 4). Thus, this provides further evidence that a main effect of HIP1 and HIP1/ΔE on EGFR degradation likely occurs subsequent to the uptake phase of ligand-stimulated receptor tyrosine kinase endocytosis.

Because endocytosis of EGFR results primarily in degradation, whereas the endocytosis of transferrin receptor results primarily in recycling of the receptor, we examined the effect of HIP1 or HIP1/ΔE on uptake of fluorescently labeled transferrin. It has been shown previously that full-length HIPs do not affect the uptake of transferrin (12, 15). The effect of the HIP1/ΔE mutant has not yet been tested in transferrin accumulation. To test this, the same IRES-GFP constructs were used as those used in the assay of endogenous EGFR uptake in HeLa cells. Similar to the effects seen for the EGFR, transferrin uptake was unaffected in HIP1 or HIP1/ΔE-transfected cells but was inhibited in dynamin1-K44A (positive control)-transfected cells (Fig. 6*D*). Thus, there was no effect of transient overexpression of HIP1 or its ENTH deletion mutant on the uptake phase of either degradative or recycling endocytic pathways.

These results with the dynamin dominant negative, together with the lack of growth factor receptor stabilization in cells co-transfected with the ENTH domain deletion mutants, suggest that the HIP family does not function to inhibit growth factor receptor degradation, in a rate-limiting fashion, by inhibiting the internalization phase of endocytosis. Because the HIP-stabilized EGFR is also activated, we suggest that, in addition to a non-rate-limiting function at the cell surface, the HIP family also inhibits the conversion of the early endocytic vesicles to later inactivating acidic endosomes or lysosomes (Fig. 7). This is consistent with the fact that HIP1 and HIP1r localization in the cell is not only at the plasma membrane but also found in intracellular vesicles (10). The more membranous localization of HIP1r is consistent with the inability of dynamin1-K44A to fully overcome HIP1r/ΔE-mediated EGFR down-regulation. Finally, the 3-phosphorylated bisphosphoinositide binding properties of HIP1 and HIP1r (Fig. 2) are also consistent with HIP1 and HIP1r playing a role in intracellular trafficking as these lipids are concentrated in intracellular membranes (34).

DISCUSSION

Our findings demonstrate a unique binding preference of HIP1 and HIP1r via their ENTH domains for 3-phosphorylated bisphosphoinositides. This binding is likely necessary for proper functioning of HIP proteins. This is suggested by our observation that mutants lacking the ENTH domains are mislocalized in the cell and induce apoptosis. We reported previously that full-length HIP1 promotes growth and transformation of fibroblasts. A potential direct mechanism for this transformation is described here, where we show by using cycloheximide that both HIP1 and HIP1r stabilize activated receptor tyrosine kinases by inhibiting protein degradative pathways post-ligand stimulation. Consistent with this, the pro-apoptotic mutants, HIP1/ΔE and HIP1r/ΔE, do not stabilize growth factor receptors.

These results are of interest in light of data demonstrating a causative role for HIP1 in oncogenesis as well as the recent finding that HIP1 deficiency alters the levels of intracellular AMPA receptors in cultured central nervous system neurons (35). In addition, the HIP1 portion of the HIP1/PDGFβR fusion protein, independent of its dimerizing activity, is necessary for its transforming activity (18). We suggest that HIP1 and HIP1r act in a rate-limiting fashion downstream of receptor uptake to inhibit trafficking of receptor tyrosine kinases to the lysosome for subsequent degradation.

It is interesting to speculate that HIP1 and HIP1r, by binding inositol lipid determinants of clathrin-coated vesicles, early endosomes, and recycling endosomes via their ENTH domains, may cause the endocytic machinery to favor continued signaling either by stabilizing the early endosome or by stimulating growth

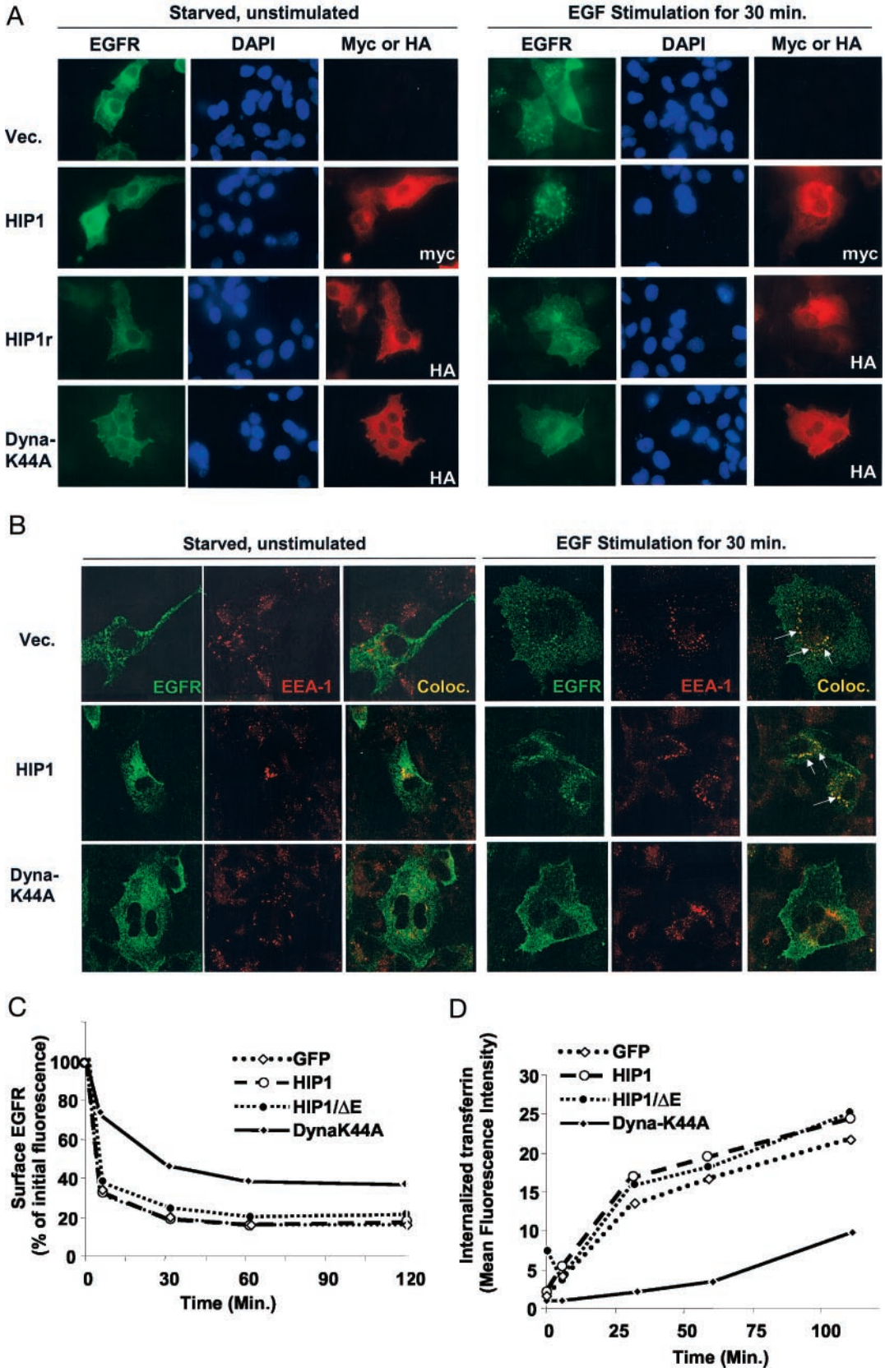

FIG. 6. **HIP1 and HIP1r and the HIP1/ΔE mutant do not alter EGFR uptake.** *A*, COS 7 cells were transfected with EGFR and either vector (*Vec*), HIP1, HIP1r, or dynamin1-K44A. Cells were starved and stimulated with EGF for 30 min before fixation for confocal microscopic analysis. Staining for EGFR (*green*) shows the presence of EGFR in vesicles at 30 min after stimulation in vector-, HIP1-, or HIP1r-transfected cells (*1st, 2nd,* and *3rd row*), but not in dynamin1-K44A-transfected cells (*bottom row*). *B*, the EGFR vesicles (*green*) seen at 30 min in vector- or HIP1-transfected cells co-localize (*Coloc*) with the endosomal marker, EEA1 (*red*). *C*, internalization of endogenous EGFR following stimulation with EGF in HIP1, HIP1/ΔE, and dynamin1-K44A-transfected HeLa cells. Following transfection, cells were starved and stimulated with 100 ng/ml EGF. Shown are the relative amounts of surface EGFR (*i.e.* EGFR fluorescence at indicated time/EGFR fluorescence prior to stimulation), expressed as a percentage, as measured by mean phycoerythrin fluorescence in 10^4 GFP-positive cells by flow cytometry. Mean EGFR fluorescence

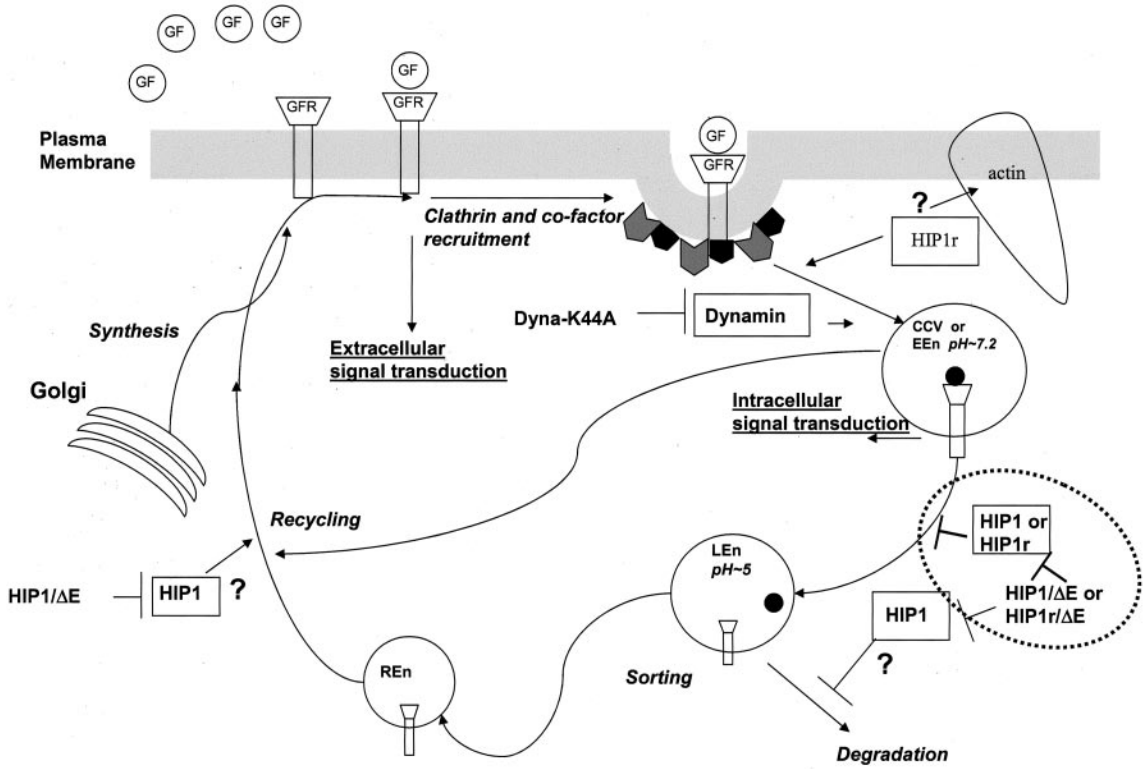

FIG. 7. **A proposed model of HIP function in trafficking and signal transduction.** Binding of ligand to the growth factor receptor leads to intracellular signal transduction events and concurrent recruitment of clathrin and co-factors to the bound complex. Uptake of ligand-bound growth factor receptors occurs via a clathrin and dynamin-dependent mechanism. Once pinching off the plasma membrane generates clathrin-coated vesicles (*CCV*), bound ligand-receptor complexes continue to signal. HIPs may stabilize this vesicle or the uncoated early endosome (*EEn*) by inhibiting the conversion to the more acidic late endosome (*LEn*) and favoring sorting to the recycling endosome (*REn*). In this report we provide evidence that suggests HIPs inhibit the conversion of early signaling neutral pH vesicles to later non-signaling acidic compartments (*dotted line*). We also show that HIP1 is not rate-limiting for the uptake phase of endocytosis.

factor receptor recycling to the cell surface (Fig. 7). This would be in lieu of growth factor receptor degradation by trafficking to the lysosome. We also speculate that this depends on the lipid components of the various intracellular compartments. Thus, HIP location could be regulated in part by the inositol lipid phosphorylation state, and may act in more than one step of trafficking to decrease the degradation of growth factor receptors and increase signal duration following receptor-ligand uptake. This in turn could lead to dysregulated growth of cells, with suppression of various cell cycle checkpoints, accumulation of mutations, and oncogenic transformation.

These results are also important because HIP1 and HIP1r are the first mammalian ENTH domain-containing proteins that bind preferentially to 3,4- and 3,5-phosphorylated inositol lipids. Previously identified ENTH domains, including those of AP180 and Epsin 1, have been shown to bind primarily PtdIns(4,5)P_2 and PtdIns(3,4,5)P_3 (7, 8). Both of the latter lipid moieties are enriched at the plasma membrane, whereas it has been suggested that PtdIns(3,4)P_2 and PtdIns(3,5)P_2 are localized to intracellular vesicles, predominantly those in the perinuclear sorting area (36). Localization of HIP1 and HIP1r via their ENTH lipid binding domains to intracellular vesicles would be consistent with their having an additional role in EGFR degradation post-internalization. Recent evidence points toward different functions for the ENTH domain of Epsin 1 *versus* that of AP180. The epsin ENTH domain has been shown to promote tubulation of lipid micelles, implying that the structure of the domain causes curvature of membranes (37). Thus, its function is consistent with a role in the internalization phase of endocytosis. The ENTH domain of AP180, also referred to as an ANTH domain, does not promote the curvature of the membrane. HIP1 and HIP1r ENTH domains appear to be more similar by sequence comparison to the AP180 ANTH domain than to the ENTH domain of epsin.

It is also worth noting at this point that the precise activities of HIP1 and HIP1r in endocytosis and trafficking remain to be elucidated. Although HIP1r and HIP1 have similar domain structures, their interacting partners and subcellular locales are somewhat different. Most important, they do have similar lipid binding specificities and similar inhibitory effects on ligand-stimulated receptor tyrosine kinase degradation, showing that there is overlap in their functions.

Another example of a putative endocytic protein that may have similar functions to HIP1 and HIP1r is Eps15 and its relative Eps15R. Eps15 co-localizes with HIP1 (10), and its overexpression alters growth of NIH3T3 cells by enhancing their ability to grow at low density (38). Eps15 is monoubiquitinated in response to EGF and is a major substrate for the EGFR tyrosine kinase (39). However, like HIP1 and HIP1r, its activity in trafficking is not well defined. Testing whether Eps15 or mutants of Eps15 have activity in the EGFR stabilization assay described here will be of use.

in untransfected cells (*i.e.* GFP-negative cells in each well containing the different transfectants) was identical to the vector-transfected cells. This experiment was repeated twice with identical results. *D*, internalization of Alexa-fluor-633-transferrin in 293T cells transfected with HIP1, HIP1/ΔE, and dynamin1-K44A. Shown are the mean fluorescence intensities for 10^4 GFP-positive cells measured by flow cytometry, following the indicated times of transferrin incubation with the cells. Mean fluorescence intensity was not significantly different in untransfected cells *versus* vector-transfected cells.

There is growing evidence that intracellular sorting of endocytic vesicles plays a major role in regulating receptor stability. Other proteins that have an effect on growth factor receptor trafficking following the internalization phase of endocytosis include Hrs, Rab5, and Cbl (40–43). The regulation of these proteins and their potential dysregulation in states of increased growth such as cancer warrants further study.

In summary, the results in this report provide evidence for a link between HIP1 or HIP1r expression, lipid binding, cellular survival, and growth factor receptor stability and signaling. The activities of the HIP family members are mediated in part by their ENTH domains. The evidence provided here that interfering with HIP1 or HIP1r function down-regulates growth factor receptor tyrosine kinase levels should be of great interest to those studying endocytosis, signaling, and cancer. Finally, the inhibition of HIP1 or HIP1r activity in tumors could concomitantly interfere with the function of multiple growth factor receptors, providing a multipronged approach to therapy.

Acknowledgments—We thank Sandra Schmid for the generous supply of dynamin and dynamin mutant constructs. We also thank members of the Ross laboratory, Sean Morrison, Andrzej Dlugosz, Steve Weiss, and Greg Taylor, for critical review of this manuscript.

REFERENCES

1. Seki, N., Muramatsu, M., Sugano, S., Suzuki, Y., Nakagawara, A., Ohhira, M., Hayashi, A., Hori, T., and Saito, T. (1998) *J. Hum. Genet.* **43,** 268–271
2. Rao, D. S., Bradley, S. V., Kumar, P. D., Hyun, T. S., Saint-Dic, D., Oravecz-Wilson, K., Kleer, C. G., and Ross, T. S. (2003) *Cancer Cell* **3,** 471–482
3. Ross, T. S., Bernard, O. A., Berger, R., and Gilliland, D. G. (1998) *Blood* **91,** 4419–4426
4. Rao, D. S., Hyun, T. S., Kumar, P. D., Mizukami, I. F., Rubin, M. A., Lucas, P. C., Sanda, M. G., and Ross, T. S. (2002) *J. Clin. Investig.* **110,** 351–360
5. Legendre-Guillemin, V., Metzler, M., Charbonneau, M., Gan, L., Chopra, V., Philie, J., Hayden, M. R., and McPherson, P. S. (2002) *J. Biol. Chem.* **277,** 19897–19904
6. Rees, D. J., Ades, S. E., Singer, S. J., and Hynes, R. O. (1990) *Nature* **347,** 685–689
7. Itoh, T., Koshiba, S., Kigawa, T., Kikuchi, A., Yokoyama, S., and Takenawa, T. (2001) *Science* **291,** 1047–1051
8. Ford, M. G., Pearse, B. M., Higgins, M. K., Vallis, Y., Owen, D. J., Gibson, A., Hopkins, C. R., Evans, P. R., and McMahon, H. T. (2001) *Science* **291,** 1051–1055
9. Engqvist-Goldstein, A. E., Warren, R. A., Kessels, M. M., Keen, J. H., Heuser, J., and Drubin, D. G. (2001) *J. Cell Biol.* **154,** 1209–1223
10. Rao, D. S., Chang, J. C., Kumar, P. D., Mizukami, I., Smithson, G. M., Bradley, S. V., Parlow, A. F., and Ross, T. S. (2001) *Mol. Cell. Biol.* **21,** 7796–7806
11. Waelter, S., Scherzinger, E., Hasenbank, R., Nordhoff, E., Lurz, R., Goehler, H., Gauss, C., Sathasivam, K., Bates, G. P., Lehrach, H., and Wanker, E. E. (2001) *Hum. Mol. Genet.* **10,** 1807–1817
12. Metzler, M., Legendre-Guillemin, V., Gan, L., Chopra, V., Kwok, A., McPherson, P. S., and Hayden, M. R. (2001) *J. Biol. Chem.* **276,** 39271–39276
13. Mishra, S. K., Agostinelli, N. R., Brett, T. J., Mizukami, I., Ross, T. S., and Traub, L. M. (2001) *J. Biol. Chem.* **276,** 46230–46236
14. Holtzman, D. A., Yang, S., and Drubin, D. G. (1993) *J. Cell Biol.* **122,** 635–644
15. Engqvist-Goldstein, A. E., Kessels, M. M., Chopra, V. S., Hayden, M. R., and Drubin, D. G. (1999) *J. Cell Biol.* **147,** 1503–1518
16. Di Fiore, P. P., Pierce, J. H., Kraus, M. H., Segatto, O., King, C. R., and Aaronson, S. A. (1987) *Science* **237,** 178–182
17. Di Fiore, P. P., Pierce, J. H., Fleming, T. P., Hazan, R., Ullrich, A., King, C. R., Schlessinger, J., and Aaronson, S. A. (1987) *Cell* **51,** 1063–1070
18. Ross, T. S., and Gilliland, D. G. (1999) *J. Biol. Chem.* **274,** 22328–22336
19. Kalthoff, C., Groos, S., Kohl, R., Mahrhold, S., and Ungewickell, E. J. (2002) *Mol. Biol. Cell* **13,** 4060–4073
20. Wasiak, S., Legendre-Guillemin, V., Puertollano, R., Blondeau, F., Girard, M., de Heuvel, E., Boismenu, D., Bell, A. W., Bonifacino, J. S., and McPherson, P. S. (2002) *J. Cell Biol.* **158,** 855–862
21. Hirst, J., Motley, A., Harasaki, K., Peak Chew, S. Y., and Robinson, M. S. (2003) *Mol. Biol. Cell* **14,** 625–641
22. Hussain, N. K., Yamabhai, M., Bhakar, A. L., Metzler, M., Ferguson, S. S., Hayden, M. R., McPherson, P. S., and Kay, B. K. (2003) *J. Biol. Chem.* **278,** 28823–28830
23. Sato, T. K., Overduin, M., and Emr, S. D. (2001) *Science* **294,** 1881–1885
24. Gillooly, D. J., Morrow, I. C., Lindsay, M., Gould, R., Bryant, N. J., Gaullier, J. M., Parton, R. G., and Stenmark, H. (2000) *EMBO J.* **19,** 4577–4588
25. Corvera, S. (2001) *Traffic* **2,** 859–866
26. Friant, S., Pecheur, E. I., Eugster, A., Michel, F., Lefkir, Y., Nourrisson, D., and Letourneur, F. (2003) *Dev. Cell* **5,** 499–511
27. Scanlan, M. J., Welt, S., Gordon, C. M., Chen, Y. T., Gure, A. O., Stockert, E., Jungbluth, A. A., Ritter, G., Jager, D., Jager, E., Knuth, A., and Old, L. J. (2002) *Cancer Res.* **62,** 4041–4047
28. Vieira, A. V., Lamaze, C., and Schmid, S. L. (1996) *Science* **274,** 2086–2089
29. Damke, H., Baba, T., Warnock, D. E., and Schmid, S. L. (1994) *J. Cell Biol.* **127,** 915–934
30. Gervais, F. G., Singaraja, R., Xanthoudakis, S., Gutekunst, C. A., Leavitt, B. R., Metzler, M., Hackam, A. S., Tam, J., Vaillancourt, J. P., Houtzager, V., Rasper, D. M., Roy, S., Hayden, M. R., and Nicholson, D. W. (2002) *Nat. Cell Biol.* **4,** 95–105
31. Kari, C., Chan, T. O., Rocha deq Uadros, M., and Rodeck, U. (2003) *Cancer Res.* **63,** 1–5
32. Conner, S. D., and Schmid, S. L. (2003) *Nature* **422,** 37–44
33. Hayes, S., Chawla, A., and Corvera, S. (2002) *J. Cell Biol.* **158,** 1239–1249
34. Itoh, T., and Takenawa, T. (2002) *Cell. Signal.* **14,** 733–743
35. Metzler, M., Li, B., Gan, L., Georgiou, J., Gutekunst, C. A., Wang, Y., Torre, E., Devon, R. S., Oh, R., Legendre-Guillemin, V., Rich, M., Alvarez, C., Gertsenstein, M., McPherson, P. S., Nagy, A., Wang, Y. T., Roder, J. C., Raymond, L. A., and Hayden, M. R. (2003) *EMBO J.* **22,** 3254–3266
36. Lemmon, M. A. (2003) *Traffic* **4,** 201–213
37. Ford, M. G., Mills, I. G., Peter, B. J., Vallis, Y., Praefcke, G. J., Evans, P. R., and McMahon, H. T. (2002) *Nature* **419,** 361–366
38. Fazioli, F., Minichiello, L., Matoskova, B., Wong, W. T., and Di Fiore, P. P. (1993) *Mol. Cell. Biol.* **13,** 5814–5828
39. Klapisz, E., Sorokina, I., Lemeer, S., Pijnenburg, M., Verkleij, A. J., and van Bergen en Henegouwen, P. M. (2002) *J. Biol. Chem.* **277,** 30746–30753
40. Raiborg, C., Bache, K. G., Gillooly, D. J., Madshus, I. H., Stang, E., and Stenmark, H. (2002) *Nat. Cell Biol.* **4,** 394–398
41. Raiborg, C., Bache, K. G., Mehlum, A., Stang, E., and Stenmark, H. (2001) *EMBO J.* **20,** 5008–5021
42. Levkowitz, G., Waterman, H., Zamir, E., Kam, Z., Oved, S., Langdon, W. Y., Beguinot, L., Geiger, B., and Yarden, Y. (1998) *Genes Dev.* **12,** 3663–3674
43. Chen, X., and Wang, Z. (2001) *EMBO Rep.* **2,** 842–849
44. Hackam, A. S., Yassa, A. S., Singaraja, R., Metzler, M., Gutekunst, C. A., Gan, L., Warby, S., Wellington, C. L., Vaillancourt, J., Chen, N., Gervais, F. G., Raymond, L., Nicholson, D. W., and Hayden, M. R. (2000) *J. Biol. Chem.* **275,** 41299–41308

Review TRENDS in Molecular Medicine Vol.10 No.4 April 2004

HIP1: trafficking roles and regulation of tumorigenesis

Teresa S. Hyun and Theodora S. Ross

Department of Internal Medicine and Graduate Program in Cellular and Molecular Biology, University of Michigan Medical School, Ann Arbor, MI 48109, USA

During recent years, alterations in proteins of the endocytic pathway have been associated with tumors. Disrupted regulation of the endocytic pathway is a relatively unstudied mechanism of tumorigenesis, which can concomitantly disrupt several different signaling pathways to affect growth, differentiation and survival. Several endocytic proteins have been identified, either as part of tumor-associated translocations or to have the ability to transform cells. Here, we summarize the information known about huntingtin interacting protein 1 (HIP1), an endocytic protein with transforming properties that is involved in a cancer-causing translocation and which is overexpressed in a variety of human cancers. We describe the known normal functions of HIP1 in endocytosis and receptor trafficking, the evidence for its role as an oncoprotein and how HIP1 might be altered to promote tumorigenesis.

Cells become cancerous owing to abnormalities in the normal mechanisms that exist to control their growth, differentiation and lifespan. Pathways that regulate cell division, DNA repair, apoptosis, aging and migration are obvious targets for tumorigenic mutations, and oncogenes and tumor suppressor genes have been found to participate in these processes. In recent years, alterations in proteins involved in the endocytic pathway have been found to be associated with tumors. This has lead to the hypothesis that altered regulation of endocytosis is one way to disrupt several different signaling pathways, leading to the initiation of, and progression to, cancer [1]. Here, we review the functions of huntingtin interacting protein 1 (HIP1) in endocytosis and receptor trafficking, and how alterations to this role might lead to tumorigenesis.

HIP1 was first cloned in 1997 owing to its interaction with huntingtin (htt), the protein whose gene is mutated in Huntington's disease [2,3]. The mutated htt has an expanded N-terminal polyglutamine tract and a decreased affinity for HIP1, suggesting that this diminished interaction might play a role in the pathophysiology of Huntington's disease [3]. The yeast homologue of HIP1, Sla2p, was discovered in 1993 as a protein necessary for normal cell growth, morphology and cytoskeletal properties [4]. Sla2p also has confirmed roles in endocytosis and actin dynamics [5]. The only other mammalian member of the HIP1 family, huntingtin interacting protein 1-related (HIP1r), was cloned in 1998 from its sequence similarity to HIP1 [6]. The first clue that HIP1 might have a role in tumorigenesis came in 1998, when a mutant fusion protein of HIP1 and the PDGFβ receptor was discovered as the cause of a chronic myelomonocytic leukemia [7]. Subsequently, HIP1 overexpression was found in several primary epithelial tumors including breast, ovarian, prostate, lung and colon, and its expression negatively correlated with survival in men with prostate cancers [8]. Further studies demonstrated that HIP1 can transform fibroblasts and alter signaling via growth factor receptors [9].

The HIP1 family in endocytosis

Current evidence points to a role for HIP1, HIP1r and Sla2p in clathrin-mediated vesicular trafficking. However, their precise roles are unknown. HIP1 is a 120-kDa protein that partially co-localizes, co-sediments and co-purifies with clathrin-coated vesicles [10–12]. The HIP1 family of proteins contains several conserved domains that could be important for their functions; these include the AP180 N-terminal homology domain (ANTH), a central coiled-coil region and a C-terminal talin homology domain. The coiled-coil domain of HIP1 contains a leucine-zipper motif and mediates heterodimerization with HIP1r [13]. HIP1r, but not HIP1, co-localizes with actin through its talin homology domain, and binds to F-actin *in vitro* [14,15]. Although HIP1 has a talin homology domain, it does not bind to F-actin under the same conditions [13]. This lack of actin binding explains their differential localization: HIP1r is concentrated at membrane ruffles and HIP1 is not. Both HIP1 and HIP1r have a punctate cytoplasmic distribution. In addition, immunofluorescence shows intense staining in the peri-nuclear region [16]. HIP1, but not HIP1r, contains consensus binding sites for the endocytic adaptor protein AP2 (DPF motif) and the clathrin heavy chain (LMDMD clathrin-box motif), and associates directly with these proteins [10–12,17]. In mice with deleted *Hip1*, recruitment of HIP1-binding endocytic proteins, including HIP1r and AP2, to liposomes from brain lysates is diminished [18]. In addition, the central helical domains of both HIP1 and HIP1r are able to bind directly to the clathrin light chain and stimulate clathrin assembly *in vitro* [13,15].

These data demonstrate that the HIP1 family has a role in clathrin-mediated endocytosis. The interaction of HIP1

Corresponding author: Theodora S. Ross (tsross@umich.edu).

 1471-4914/$ - see front matter doi:10.1016/j.molmed.2004.02.003

with AP2 suggests that it is involved in receptor uptake at the plasma membrane. The interaction of HIP1r with actin suggests that it links cytoskeletal and endocytic processes. HIP1 and HIP1r might play a role similar to Sla2p, which has recently been shown to be necessary for the productive interaction of the actin cytoskeleton with the endocytic machinery, to allow membrane invagination [19].

In addition to the interaction with clathrin and induction of clathrin lattices, the HIP1 family contains an ANTH domain that implicates them in endocytosis. The ENTH/ANTH (epsin N-terminal homology) domain family has been found in several proteins, all with roles in clathrin-mediated vesicle trafficking [20]. These proteins include epsin, enthoprotin/Clint/epsin-related protein [21–23], AP180 and CALM (clathrin assembly lymphoid myeloid leukemia), as well as the HIP1 family of proteins. The ENTH/ANTH domains are phosphoinositide binding domains with varied specificity. In AP180 and epsin, the ENTH/ANTH domains bind phosphatidylinositol-4,5-bisphosphate [PtdIns(4,5)P_2] and phosphatidylinositol-3,4,5-triphosphate [PtdIns(3,4,5)P_2] [24,25]. The lipid-binding activity of epsin is required for its role in the endocytosis of epidermal growth factor (EGF). Expression of an epsin-deletion mutant lacking the ENTH domain, or a point mutant abolishing the binding of epsin to PtdIns(4,5)P_2, inhibits EGF internalization [24]. The ANTH domain group of proteins, which includes AP180, as well as HIP1, HIP1r and Sla2p, were only recently classified separately from proteins containing the closely related ENTH domain [20,24–26]. Although both ENTH- and ANTH-containing proteins bind lipids, only ENTH domains have the ability to induce curvature of the plasma membrane [26,27].

It was recently discovered that HIP1 and HIP1r have different lipid specificities for epsin and AP180 than was previously described. The HIP1 proteins bind preferentially to PtdIns(3,4)P_2 and PtdIns(3,5)P_2 as opposed to PtdIns(4,5)P_2 [16]. PtdIns(3,4)P_2 and PtdIns(3,5)P_2 are enriched in early endosomes, whereas PtdIns(4,5)P_2 is predominantly a plasma membrane inositol lipid [28]. This lipid specificity suggests that HIP1 and HIP1r have additional endocytic roles downstream of the clathrin-mediated invagination step of receptor endocytosis (Figure 1). Consistent with the hypothesis that this lipid-binding specificity of the HIP1 family implicates it in intracellular membrane trafficking, the yeast protein Ent3p has also been shown to have a PtdIns(3,5)P_2-binding ENTH domain that mediates its role in protein sorting from the intracellular mutivesicular body [29]. Although Ent3p has an ENTH domain (and the HIP1 family an ANTH domain), their related lipid specificity suggests a similar subcellular localization. Further work is required to understand how HIP1 binding to PtdIns(3,4)P_2 and PtdIns(3,5)P_2, clathrin, HIP1r, AP2 and htt are coordinated to mediate the different locations and functions of HIP1 in the many phases of clathrin-mediated trafficking.

HIP1 and HIP1r in cellular survival

There are conflicting data in the literature concerning the influence of HIP1 on cellular survival. Originally, it was reported that HIP1 functions as a pro-apoptotic protein, because overexpression of HIP1 induced apoptosis in transfected NT2 and HEK 293T cells. The mechanism of cell death was unclear, but both the caspase 8-independent intrinsic and the caspase 8-dependent extrinsic death-receptor final pathways have been implicated [30,31]. The latter has been shown to be mediated by a HIP1 protein-binding partner, designated HIPPI (HIP1 protein interactor) [31]. By contrast, Rao *et al.* reported that overexpression of full-length HIP1 or HIP1r does not induce apoptosis, whereas transfection of mutants lacking the ANTH domain leads to induction of apoptosis in multiple cell types, including HEK 293T cells [8,9]. Apoptosis mediated by the ANTH deletion mutant of HIP1 was inhibited by a dominant-negative caspase-9, suggesting that the final apoptotic pathway targeted was the intrinsic mitochondrial pathway [8]. Alternative splicing of the *HIP1* gene yielding two splice variants that have differing 5′ sequences has been reported [32] and could explain the discrepancy in the reported pro- and anti-apoptotic effects of HIP1. Mutation of murine *Hip1 in vivo* leads to testicular degeneration due to apoptosis of postmeiotic spermatids (where HIP1 is normally expressed [17]), suggesting a primary role for full-length HIP1 in the survival of some cell types. Finally, because HIP1 can transform fibroblasts and is overexpressed in multiple cancers, there are many neoplastic cell types where the putative pro-apoptotic activity of HIP1 is not realized [8,9].

Regulation of receptors by HIP1 and HIP1r

In spite of an accumulated body of work implicating the HIP1 family in endocytosis, a detailed understanding of HIP1 and HIP1r activities in these processes is lacking. Several studies have elucidated the importance of receptor sorting by endocytic mechanisms for signaling through membrane receptors [33,34]. Recent data suggest that HIP1 can influence levels of various growth factor receptors following ligand stimulation. In addition, confocal microscopy and glutathione S-transferase (GST) pull-down experiments have shown that HIP1 exists in complex with the AMPA (α-amino-3-hydroxy-5-methyl-4-isoxazolepropionic acid) receptor [35]. Primary neurons from mice with targeted mutation of *Hip1* have altered surface:intracellular ratios of the AMPA receptor following ligand stimulation, suggesting a blocking of internalization, but have normal transferrin receptor trafficking [35]. In other studies, overexpression of HIP1 in cell culture stabilized levels of the EGF receptor after EGF stimulation [9,16], and resulted in increased phosphorylation of downstream effectors [9]. In this case, receptor stabilization was not due to a block in internalization, because HIP1-overexpressing cells showed normal movement of EGF receptor to early endosomes, post-stimulation [16]. Increased levels of other receptors have also been observed, including fibroblast growth factor (FGF) receptor and the platelet derived growth factor (PDGF)-β receptor, in cells overexpressing HIP1 [9,16]. HIP1r has some similar effects to HIP1, stabilizing EGF receptor and PDGFβ receptor and increasing EGF receptor phosphorylation following ligand stimulation. One possibility for

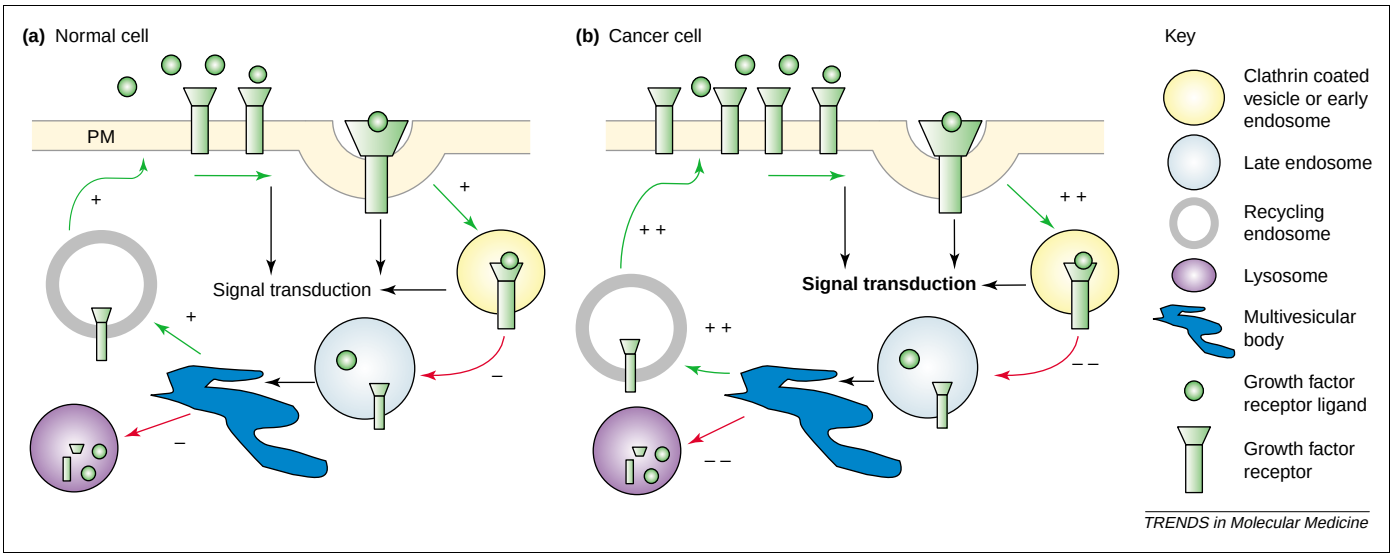

Figure 1. Putative roles of huntingtin interacting protein 1 (HIP1) in receptor trafficking and tumorigenesis. **(a)** Functions of HIP1 in a normal cell. Binding of growth factor (green) to its receptor results in endocytosis of the ligand–receptor complex. Accessory endocytic proteins, including HIP1, mediate the formation of clathrin-coated pits from the plasma membrane that has phosphatidylinositol (PtdIns)-4,5-P_2 and PtdIns-3,4,5-P_3 as its main inositol lipids. These pits then convert to clathrin-coated vesicles and early endosomes (yellow) that have PtdIns-3,4-P_2 and PtdIns-3,5-P_2 enriched in their membranes owing to activities of PtdIns polyphosphate 5- and 4-phosphatases, respectively. Receptor-mediated signal transduction occurs from the plasma membrane, the clathrin-coated pit and the early endosome owing to sustained ligand binding at neutral pH. HIP1 might also be involved in the conversion of the early endosome to the late endosome (light blue). Additional hypothetical roles for HIP1 include a role in sorting receptors at the multivesicular body (dark blue) for degradation to the lysosome (purple) or for recycling back to the plasma membrane. **(b)** HIP1 in cancer. Overexpression of HIP1 in tumors could increase one or several of its putative rate-limiting functions in endocytosis and vesicle trafficking, leading to an amplification of signal transduction from growth factor receptors, rather than termination via receptor degradation. Alternatively, HIP1 overexpression might mediate tumorigenesis by altering the activities of currently undefined fundamental cellular pathways. Abbreviations: PM, plasma membrane; +, possible positive regulation by HIP1; −, possible negative regulation by HIP1.

these variable results is that HIP1 and HIP1r act differentially on a broad range of receptors to affect their internalization, recycling, degradation or signaling following ligand stimulation (Figure 1).

Altered regulation of HIP1 and HIP1r in cancers

The first clue suggesting that altered regulation of HIP1 family members could be associated with cancers was the discovery of a translocation between the genes encoding HIP1 and PDGFβ receptor, resulting in the expression of a HIP1–PDGFβ receptor fusion protein in chronic myelomonocytic leukemia [7]. Furthermore, stable expression of this fusion protein in the IL-3-dependent murine Ba/F3 hematopoietic cell line resulted in a transformation to IL-3-independent growth [7]. HIP1 sequences, independent of those that dimerize the fusion protein, were necessary for this transforming ability. This was shown by the fact that a deletion mutant of the HIP1–PDGFβ receptor fusion protein containing only the talin homology region of HIP1 failed to cause IL-3-independent growth in Ba/F3 cells, despite retaining its properties of constitutive oligomerization and tyrosine phosphorylation [36].

Further studies showed that the expression of HIP1 itself is altered in several types of cancer. Analysis, by western blot, of 60 cancer cell lines showed that 50 of the 53 lines that were derived from solid tumors (breast, colon, kidney, lung, melanoma, ovarian and prostate) had high levels of HIP1 protein. This pattern was confirmed by analysis of HIP1 expression using immunohistochemical staining of primary human cancer tissue microarrays, which demonstrated moderate–high staining of HIP1 in most of these types of cancer [8]. Because HIP1 was undetected in normal colon and prostate epithelium, whereas the corresponding tumors had high levels, these tumors were studied in more detail. Staining of 25 colon cancers showed that 48% of well differentiated tumors had moderate or high HIP1 staining, whereas adjacent normal epithelium did not. Similarly, staining of prostate tissue microarrays, containing tissue samples ranging from normal prostate epithelium to metastatic prostate cancer from 128 patients, demonstrated the absence of HIP1 staining in normal epithelium and an increasing percentage of HIP1-positive samples as the severity of the neoplasia increased from PIN (prostatic intra-epithelial neoplasia) to hormone-refractory metastatic prostate cancer [8]. These findings suggested that expression of HIP1 is a late event in prostate cancer progression. Strikingly, analysis of linked clinical data for 114 patients with prostate-confined cancer revealed that those with HIP1-negative tumors did not relapse after radical prostatectomy, whereas 28% with HIP1-positive tumors did [8]. For breast tumors, analysis of a primary human breast tumor tissue microarray showed elevated levels of HIP1 expression in atypical ductal hyperplasia, ductal carcinoma *in situ* and invasive breast cancer compared with low expression in normal or fibrocystic breast tissue [9]. In contrast to the results with prostate cancer prognosis and HIP1 expression, clinical outcomes independent of the estrogen receptor, progesterone receptor and Her2 status of breast tumors were not predicted by HIP1 staining.

Another study suggests that HIP1r is also altered in cancers. Screening of sera from 74 patients with colon cancer and 75 unaffected donors for reactivity to immunogenic tumor antigens produced five serum samples from patients with colon cancer that had antibody reactivity to

HIP1r [37]. There was no immunoreactivity to HIP1r in any of the unaffected donors. It remains possible that these antibodies, reported to be specific against HIP1r, were cross-reactive with HIP1r (i.e. the primary tumor antigen was HIP1).

Further analysis of the effects of HIP1 overexpression on cells led to the surprising discovery that HIP1 can transform fibroblasts [9]. Stable overexpression of HIP1 under the control of a long terminal repeat (LTR) or cytomegalovirus (CMV) promoter produced cell lines that had higher growth rates and saturation densities compared with control cell lines. They also had the ability to proliferate in 0.1% serum; this reduction in the requirement for growth factors was hypothesized to be related to receptor tyrosine kinase signaling pathway activation, because the HIP1-overexpressing cell lines displayed elevated levels of both total and phosphorylated EGF receptor, as well as activation of the downstream effector phosphatidlyinositide 3-kinase and mitogen activated protein kinase (MAPK) pathways. Furthermore, HIP1-overexpressing cell lines formed colonies in a soft agar assay, foci when plated at low density and tumors in nude mice, confirming that HIP1 has oncogenic activity in fibroblasts. HIP1 might cause transformation of cells by prolonging activation and signaling of various growth factor receptors. It is possible that the effect of HIP1 on receptors occurs after the internalization step of endocytosis, because no defect in this step was observed when HIP1 was transiently overexpressed [16]. Whether this mechanism in cancer pathogenesis is an amplification of one of the normal functions of HIP1 in vesicle trafficking remains to be determined.

Unknown roles of HIP1

In spite of our knowledge of the structural, biochemical and cell biological properties of the HIP1 family, their roles *in vivo* remain unclear. Various mutant alleles of *Hip1* in mice result in complex phenotypes that are not easily explained by our current knowledge of HIP1 function. Although HIP1 is normally expressed in the brain, the *Hip1* mutant mice do not have discernable central nervous system (CNS) abnormalities [17,18,38], but do have testicular degeneration [17]. *Hip1* mutant mice also demonstrate kypholordosis, which results in tremor and an abnormal gait. No abnormalities have yet been found in analysis of the skeleton, peripheral nerves, and muscle function, but reduced binding of HIP1-interacting endocytic proteins, including AP-2, clathrin, Htt and HIP1r, to liposomal membranes from *Hip1*-knockout mice was observed [18]. How this might cause the kypholordosis and tremor is still unclear, but Metzler *et al.* have suggested that, by default, this hunchback phenotype is secondary to CNS defects in AMPA receptor signaling *in vivo* [18]. A new *Hip1* mutant mouse also exhibits kypholordosis and, in addition, has abnormalities in the frequency of some hematopoietic progenitors, microophthalmia and cataracts [38]. These complex phenotypic characteristics suggest that HIP1 is important for the normal development or maintenance of several tissues, but further studies are required to determine which activities of HIP1 are important for these *in vivo* processes.

Other endocytic proteins involved in tumorigenesis

In addition to HIP1, other endocytic proteins have been implicated in cancer, suggesting a general mechanism in which perturbation of endocytosis and/or vesicle trafficking can affect survival, proliferation and migration of cells [1]. The best example is disabled-2 (*Dab2*), which was originally identified as a tumor suppressor gene in ovarian carcinomas [39,40]. Subsequent studies found that Dab2 binds the LDL-receptor family, AP2, clathrin and phosphoinositides [41], and acts to negatively regulate the canonical Wnt signaling pathway [42]. Dab2 is particularly interesting, as it is the only other known endocytic protein that, like HIP1, has altered levels in human tumors.

Other endocytic proteins that transform cells and have a putative, but undocumented, role in human cancers include intersectin, Eps15 and Hrs. Intersectin is an endocytic accessory protein that can bind Eps15, epsin and dynamin. Overexpression of intersectin regulates mitogenic signaling pathways, activating the Elk-1 transcription factor and causing transformation of rodent fibroblasts [43]. The endocytic protein Eps15 can directly alter mitogenic signaling pathways, and its overexpression in NIH/3T3 cells also results in transformation [44]. The hepatocyte growth factor-regulated tyrosine kinase substrate Hrs interacts with the neurofibromatosis-2 tumor suppressor [45], and functions to sort ubiquitinated membrane receptors in the multivesicular body to the degradative pathway, and prevent recycling to the cell surface [46]. A remaining question for all of these examples is whether their altered regulation is crucial to the pathophysiology of human cancer.

Finally, similar to HIP1, other genes encoding endocytic proteins are involved in genetic translocations that cause leukemias, making them candidates for the formation of other cancers. For example, the PDGFβ receptor is also part of a translocation with Rabaptin-5, a regulatory component of early endosomes; the resulting fusion protein, similar to HIP1–PDGFβ receptor, causes chronic myelomonocytic leukemia and can transform Ba/F3 cells to IL-3-independent growth [47]. In addition, CALM, an ANTH-containing endocytic protein homologous to AP180, was originally identified from a translocation common in acute lymphoblastic leukemia [48]. An MLL–CALM (mixed-lineage leukemia) translocation was also recently identified in an infant patient with aggressive acute myelogenous leukemia, suggesting that altered regulation of CALM functions contributes to leukemogenesis [49].

Concluding remarks

Current evidence assigns a role for HIP1 in the endocytic pathway, by virtue of its ANTH domain, interaction with other endocytic proteins and subcellular localization. The specific nature of the role of HIP1 in endocytosis and vesicle trafficking is less clear, but data suggest that HIP1 functions in the early steps of clathrin-coated pit formation and, possibly, progression from early to late endosomes (Figure 1a). HIP1 might function at other steps of vesicle

trafficking, such as the sorting of late endosomes to either degradative lysosomes or recycling endosomes. Alteration of HIP1 functions, by overexpression of the normal protein or translocations involving the HIP1 gene, might lead to the amplification of signal transduction cascades mediated by growth factor receptors that are normally regulated by endocytosis (Figure 1b). Several questions remain to be answered in this model concerning HIP1 function in both normal and cancer cells. The regulation of HIP1 expression and the mechanism by which it is increased in tumors is largely unknown at present. The specific role of other accessory endocytic proteins in tumorigenesis also needs to be clarified. Finally, the role of HIP1 interaction with Htt, HIPPI or other yet to be discovered HIP1 partners in tumorigenesis is unknown. The interaction with Htt might prove to be important in cancer pathophysiology. An intriguing epidemiological report shows that patients with Huntington's disease have a lower incidence of cancer compared to their healthy relatives [50].

Concurrent amplification of many signaling cascades through the modification of endocytic pathways could affect several processes important in the progression to cancer, including survival, proliferation and migration. Therefore, manipulation of receptor-mediated signaling pathways via alterations in endocytic proteins, such as HIP1, is a novel mechanism for tumorigenesis that involves a fundamental cellular pathway. A better understanding of this mechanism might lead to novel drug targets and treatments.

Acknowledgements

We thank Katherine I. Oravecz-Wilson, Gaelle Bougeard-Denoyelle, Dinesh S. Rao, Lina Li, Ikuko Mizukami, Sarah V. Bradley, Paul Nolan, Hanshi Sun and Anthony Munaco for critical review of this article. This work was supported by a University of Michigan Cancer Biology training grant (T.S.H.), the NIH/NCI and Damon Runyon foundation (T.S.R.).

References

1 Floyd, S. and De Camilli, P. (1998) Endocytosis proteins and cancer: a potential link? *Trends Cell Biol.* 8, 299–301
2 Wanker, E.E. *et al.* (1997) HIP-I: a huntingtin interacting protein isolated by the yeast two-hybrid system. *Hum. Mol. Genet.* 6, 487–495
3 Kalchman, M.A. *et al.* (1997) HIP1, a human homologue of *S. cerevisiae* Sla2p, interacts with membrane-associated huntingtin in the brain. *Nat. Genet.* 16, 44–53
4 Holtzman, D.A. *et al.* (1993) Synthetic-lethal interactions identify two novel genes, *SLA1* and *SLA2*, that control membrane cytoskeleton assembly in *Saccharomyces cerevisiae*. *J. Cell Biol.* 122, 635–644
5 Wesp, A. *et al.* (1997) End4p/Sla2p interacts with actin-associated proteins for endocytosis in *Saccharomyces cerevisiae*. *Mol. Biol. Cell* 8, 2291–2306
6 Seki, N. *et al.* (1998) Cloning, expression analysis, and chromosomal localization of HIP1R, an isolog of huntingtin interacting protein (HIP1). *J. Hum. Genet.* 43, 268–271
7 Ross, T.S. *et al.* (1998) Fusion of Huntingtin interacting protein 1 to platelet-derived growth factor β receptor (PDGFβR) in chronic myelomonocytic leukemia with t(5;7)(q33;q11.2). *Blood* 91, 4419–4426
8 Rao, D.S. *et al.* (2002) Huntingtin-interacting protein 1 is overexpressed in prostate and colon cancer and is critical for cellular survival. *J. Clin. Invest.* 110, 351–360
9 Rao, D.S. *et al.* (2003) Altered receptor trafficking in Huntingtin interacting protein 1-transformed cells. *Cancer Cell* 3, 471–482
10 Mishra, S.K. *et al.* (2001) Clathrin- and AP-2-binding sites in HIP1 uncover a general assembly role for endocytic accessory proteins. *J. Biol. Chem.* 276, 46230–46236
11 Metzler, M. *et al.* (2001) HIP1 functions in clathrin-mediated endocytosis through binding to clathrin and adaptor protein 2. *J. Biol. Chem.* 276, 39271–39276
12 Waelter, S. *et al.* (2001) The huntingtin interacting protein HIP1 is a clathrin and α-adaptin-binding protein involved in receptor-mediated endocytosis. *Hum. Mol. Genet.* 10, 1807–1817
13 Legendre-Guillemin, V. *et al.* (2002) HIP1 and HIP12 display differential binding to F-actin, AP2, and clathrin. Identification of a novel interaction with clathrin light chain. *J. Biol. Chem.* 277, 19897–19904
14 Engqvist-Goldstein, A.E. *et al.* (1999) An actin-binding protein of the Sla2/Huntingtin interacting protein 1 family is a novel component of clathrin-coated pits and vesicles. *J. Cell Biol.* 147, 1503–1518
15 Engqvist-Goldstein, A.E. *et al.* (2001) The actin-binding protein Hip1R associates with clathrin during early stages of endocytosis and promotes clathrin assembly in vitro. *J. Cell Biol.* 154, 1209–1223
16 Hyun, T.S. *et al.* (2004) HIP1 and HIP1r stabilize receptor tyrosine kinases and bind 3-phosphoinositides via ENTH domains. *J. Biol. Chem.* doi: 10.1074/jbc.M312645200 (www.jbc.org)
17 Rao, D.S. *et al.* (2001) Huntingtin interacting protein 1 is a clathrin coat binding protein required for differentiation of late spermatogenic progenitors. *Mol. Cell. Biol.* 21, 7796–7806
18 Metzler, M. *et al.* (2003) Disruption of the endocytic protein HIP1 results in neurological deficits and decreased AMPA receptor trafficking. *EMBO J.* 22, 3254–3266
19 Kaksonen, M. *et al.* (2003) A pathway for association of receptors, adaptors, and actin during endocytic internalization. *Cell* 115, 475–487
20 Legendre-Guillemin, V. *et al.* (2004) ENTH/ANTH proteins and clathrin-mediated membrane budding. *J. Cell Sci.* 117, 9–18
21 Kalthoff, C. *et al.* (2002) Clint: a novel clathrin-binding ENTH-domain protein at the Golgi. *Mol. Biol. Cell* 13, 4060–4073
22 Wasiak, S. *et al.* (2002) Enthoprotin: a novel clathrin-associated protein identified through subcellular proteomics. *J. Cell Biol.* 158, 855–862
23 Hirst, J. *et al.* (2003) EpsinR: an ENTH domain-containing protein that interacts with AP-1. *Mol. Biol. Cell* 14, 625–641
24 Itoh, T. *et al.* (2001) Role of the ENTH domain in phosphatidylinositol-4,5-bisphosphate binding and endocytosis. *Science* 291, 1047–1051
25 Ford, M.G. *et al.* (2001) Simultaneous binding of PtdIns(4,5)P2 and clathrin by AP180 in the nucleation of clathrin lattices on membranes. *Science* 291, 1051–1055
26 Ford, M.G. *et al.* (2002) Curvature of clathrin-coated pits driven by epsin. *Nature* 419, 361–366
27 Stahelin, R.V. *et al.* (2003) Contrasting membrane interaction mechanisms of AP180 N-terminal homology (ANTH) and epsin N-terminal homology (ENTH) domains. *J. Biol. Chem.* 278, 28993–28999
28 Lemmon, M.A. (2003) Phosphoinositide recognition domains. *Traffic* 4, 201–213
29 Friant, S. *et al.* (2003) Ent3p is a PtdIns(3,5)P2 effector required for protein sorting to the multivesicular body. *Dev. Cell* 5, 499–511
30 Hackam, A.S. *et al.* (2000) Huntingtin interacting protein 1 induces apoptosis via a novel caspase-dependent death effector domain. *J. Biol. Chem.* 275, 41299–41308
31 Gervais, F.G. *et al.* (2002) Recruitment and activation of caspase-8 by the Huntingtin-interacting protein Hip-1 and a novel partner Hippi. *Nat. Cell Biol.* 4, 95–105
32 Chopra, V.S. *et al.* (2000) HIP12 is a non-proapoptotic member of a gene family including HIP1, an interacting protein with huntingtin. *Mamm. Genome* 11, 1006–1015
33 Di Fiore, P.P. and De Camilli, P. (2001) Endocytosis and signaling. an inseparable partnership. *Cell* 106, 1–4
34 Clague, M.J. and Urbe, S. (2001) The interface of receptor trafficking and signalling. *J. Cell Sci.* 114, 3075–3081
35 Metzler, M. *et al.* (2003) Disruption of the endocytic protein HIP1 results in neurological deficits and decreased AMPA receptor trafficking. *EMBO J.* 22, 3254–3266
36 Ross, T.S. and Gilliland, D.G. (1999) Transforming properties of the Huntingtin interacting protein 1/platelet-derived growth factor β receptor fusion protein. *J. Biol. Chem.* 274, 22328–22336

37 Scanlan, M.J. *et al.* (2002) Cancer-related serological recognition of human colon cancer: identification of potential diagnostic and immunotherapeutic targets. *Cancer Res.* 62, 4041–4047
38 Oravecz-Wilson K.I. *et al.* (2004) Huntingtin interacting protein 1 mutations lead to abnormal hematopoiesis, spinal defects and cataracts. *Hum. Mol. Gen.* (in press)
39 Mok, S.C. *et al.* (1998) DOC-2, a candidate tumor suppressor gene in human epithelial ovarian cancer. *Oncogene* 16, 2381–2387
40 Mok, S.C. *et al.* (1994) Molecular cloning of differentially expressed genes in human epithelial ovarian cancer. *Gynecol. Oncol.* 52, 247–252
41 Mishra, S.K. *et al.* (2002) Disabled-2 exhibits the properties of a cargo-selective endocytic clathrin adaptor. *EMBO J.* 21, 4915–4926
42 Hocevar, B.A. *et al.* (2001) The adaptor molecule disabled-2 links the transforming growth factor β receptors to the Smad pathway. *EMBO J.* 20, 2789–2801
43 Adams, A. *et al.* (2000) Intersectin, an adaptor protein involved in clathrin-mediated endocytosis, activates mitogenic signaling pathways. *J. Biol. Chem.* 275, 27414–27420
44 Fazioli, F. *et al.* (1993) eps15, a novel tyrosine kinase substrate, exhibits transforming activity. *Mol. Cell. Biol.* 13, 5814–5828
45 Scoles, D.R. *et al.* (2000) The neurofibromatosis 2 tumor suppressor protein interacts with hepatocyte growth factor-regulated tyrosine kinase substrate. *Hum. Mol. Genet.* 9, 1567–1574
46 Raiborg, C. *et al.* (2002) Hrs sorts ubiquitinated proteins into clathrin-coated microdomains of early endosomes. *Nat. Cell Biol.* 4, 394–398
47 Magnusson, M.K. *et al.* (2001) Rabaptin-5 is a novel fusion partner to platelet-derived growth factor β receptor in chronic myelomonocytic leukemia. *Blood* 98, 2518–2525
48 Dreyling, M.H. *et al.* (1996) The t(10;11)(p13;q14) in the U937 cell line results in the fusion of the AF10 gene and CALM, encoding a new member of the AP-3 clathrin assembly protein family. *Proc. Natl. Acad. Sci. U. S. A.* 93, 4804–4809
49 Wechsler, D.S. *et al.* (2003) A novel chromosomal inversion at 11q23 in infant acute myeloid leukemia fuses MLL to CALM, a gene that encodes a clathrin assembly protein. *Genes Chromosomes Cancer* 36, 26–36
50 Sorensen, S.A. *et al.* (1999) Significantly lower incidence of cancer among patients with Huntington disease: an apoptotic effect of an expanded polyglutamine tract? *Cancer* 86, 1342–1346